Formation of Non-equilibrium Phases in the Alloy Systems with Positive Heat of Mixing by Mechanical Alloying

1992

KEISUKE UENISHI

Formation of Non-equilibrium Phases in the Alloy Systems with Positive Heat of Mixing by Mechanical Alloying

1992

KEISUKE UENISHI

ACKNOWLEDGEMENTS

The author wishes to express his sincere gratitude to Professor P.H.Shingu, Kyoto University for his supervision throughout this study. He is also grateful to Dr.K.N.Ishihara, Mr.S.Fujimoto, Kyoto University, Professor K.F.Kobayashi and Dr.S.Nasu, Osaka University for their useful advice in accomplishing this work.

The author is indebted to all the members of Prof. Shingu's research group, especially Drs.S.R.Nishitani, B.Huang, Messrs. J.Kuyama, S.Sasakawa, N.Inoue, H.Saito, K.Yamamoto, K.Hori, H.Hatano and T.Yamamoto for their general guidance and support in this study.

The author thanks to Mr.T.Tanaka, Osaka Sangyo University for all of the experimental assistance, to Messrs.Y.Hayashi and S.Kashiwai, Industrial Research Institute of Hyogo Prefecture for TEM observation and chemical analysis and to S.Imaoka, Osaka University for Mössbauer measurement.

CHAPTER 1 General introduction ---------- 1

1.1 Non-equilibrium phases ---------- 1

1.2 Mechanical alloying ---------- 2

1.3 Trends of the recent studies on MA and the purpose of this thesis ---------- 3

References ---------- 11

CHAPTER 2 Formation of super-saturated solid solution in the Ag-Cu system ---------- 16

2.1 Introduction ---------- 16

2.2 Experimental ---------- 18

2.2.1 Mechanical alloying ---------- 18

2.2.2 Chemical analysis ---------- 18

2.2.3 Structure observation ---------- 20

2.2.4 X-ray diffraction analysis ---------- 20

2.2.5 Thermal analysis ---------- 21

2.2.6 Electrical resistivity ---------- 21

2.3 Results and discussion ---------- 22

2.3.1 Chemical composition of mechanically alloyed powders ---------- 22

2.3.2 Structural evolution by MA ---------- 24

2.3.3 Formation of super-saturated solid solution -- 27

2.3.4 Thermal stability of super-saturated solid solution ---------- 33

2.4 Conclusion ---------- 42

References ---------- 43

CHAPTER3 Mechanical alloying in the Fe-Cu system------ 44

3.1 Introduction ---------- 44

3.2 Experimental ---------- 44

3.3 Results and discussion ---------- 47

3.4 Conclusion ---------- 66

References ---------- 67

CHAPTER 4 Non-equilibrium phases formation in the Fe-Ag-Cu system ---------- 68

4.1 Introduction ---------- 68

4.2 Experimental ---------- 69

4.3 Results and discussion ---------- 69

4.4 Conclusion ---------- 84

References ---------- 85

CHAPTER 5 Formation of non-equilibrium phases by repeated rolling ---------- 86

5.1 Introduction ---------- 86

5.2 Experimental ---------- 86

5.3 Results and discussion ---------- 88

5.3.1 Structural evolution ---------- 88

5.3.2 Non-equilibrium phase formation ---------- 90

5.4 Conclusion ---------- 96

References---------- 98

CHAPTER 6 Thermodynamical analysis ---------- 99

6.1 Introduction ---------- 99

6.2 Results and discussion ---------- 99

6.3 Conclusion ---------- 109

References---------- 110

CHAPTER 7 Summary ---------- 111

Chapter 1

General introduction

1.1 Non-equilibrium materials

With remarkable industrial progress, request for new materials has come to be varied and advanced one. However, it is not always easy to find the conventionally cast alloys with excellent properties enough to meet the request. As the result, new alloys such as non-equilibrium alloys or composite materials have come to be designed and synthesized. The non-equilibrium or metastable alloys are not thermodynamically stable compared with equilibrium alloys. But, there are conditions on which non-equilibrium alloys are on a stable state. Thus, on such conditions, non-equilibrium alloys can be used like equilibrium alloys and amorphous or diamond, which are non-equilibrium alloys have been actually put to practical use. Non-equilibrium alloys can be readily synthesized by quenching from a high temperature equilibrium solid state. This was the basis of conventional metallurgical process to prepare super-saturated solid solutions and martensite materials. Turnbull established such non-equilibrium alloy forming process as "Energize and Quench" process and the development of non-equilibrium phases started.

There have been extensive works on the formation of non-equilibrium alloys by quenching from a high temperature liquid or vapor state. First, Duwez actually demonstrated that some metal alloys were rapidly quenched from liquid to be

amorphous[1].

The process used to prepare non-equilibrium phases was the quenching process from energized state, liquid or vapor, but recently it has been found these non-equilibrium phases can be synthesized by solid state reaction. Yeh et al.[2] reported the formation of amorphous $Zr_3RhH_{5.5}$ by the dissolution of hydrogen gas in crystalline Zr_3Rh. Herd et al.[3] produced an amorphous by annealing amorphous Si and crystalline Rh bilayer. The preparation of amorphous alloy from crystalline alloy was reported by Schwarz et al[4]. They prepared the crystalline Au and La multilayer and obtained amorphous by annealing it below the crystallization temperature.

The above introduced process to produce non-equilibrium materials is complex, expensive and hard for mass production, so these newly developed materials without any specific functions have shown little practical use. In 1983, a new simple technique for the preparation of non-equilibrium materials at low temperature (around room temperature) was discovered by Koch et al[5]. This technique is a mechanical alloying (MA) of elemental crystalline powders.

1.2 Mechanical Alloying

Mechanical alloying (MA), which was first introduced by Benjamin at INCO in 1970[6], is a high energy ball milling process to produce composite powders with controlled and extremely fine microstructures. The fundamental processes of MA are repeated welding, fracturing and rewelding of a mixture of powder particles by ball-powder-ball collisions. By using this

MA process, Benjamin first succeeded to produce oxide dispersion strengthened(ODS) Ni-base superalloy[7]. Afterwards, alloy preparation in other systems, such as preparation of iron-based[8] and aluminum-based[9] ODS superalloy were reported. Thus, those developed ODS alloys such as the INCONEL alloy MA 6000[10] have been made practicable as materials with high strength at high temperature like turbine blading materials.

The advantages of MA are not restricted to produce such complex ODS alloys. MA is a means to produce composite metal powders, too. Especially, it is effective to produce alloys which are difficult or impossible to produce by conventional melting or casting process. Finely dispersed homogeneous alloy powders were successfully obtained in liquid immiscible Cu-Pb system, in solid immiscible Cu-Fe, and in Nb-Sn with very different melting points[11] by using this MA, solid state processing.

Koch et al.[5] reported the formation of an amorphous phase for Ni-Nb alloy system by mechanical alloying of elemental Ni and Nb powders in 1983. This MA process is significantly different from the MA process to used produce ODS alloy. The former is a process to solve the materials while the latter is a process that only mix them.

1.3 Trends of the recent studies on MA and the purpose of this thesis

Since the first report on solid state amorphization by Koch, MA has attracted researchers' attentions as a new method to

prepare non-equilibrium alloys. Fig.1.1 shows the number of the papers on MA reported in the corresponding year. Besides, the papers on solid state reaction are darkened in the histogram. It is clearly recognized from this figure that researches on MA have remarkably increased since Koch's report. These solid state amorphization phenomena were intensely examined mainly in transition metal(TM)-TM system. Table 1.1 is the list of amorphous forming binary alloy system by MA. From these results, amorphous forming system was confirmed to be extended by MA. For example, Schultz et al.[19] reported the formation of new amorphous in Al-Ti system that is difficult by rapid quenching. In addition to the extension of amorphous forming system, the forming composition range was also confirmed to be extended by MA. Weeber et al.[56] reported the extension of amorphous forming range in Ni-Zr, and Schultz et al.[57] reported the interesting results that amorphous was formed in a quite different composition range from that in case of rapid quenching. Simultaneously, many reports have introduced the mechanism of this solid state amorphization. Schwarz defined that solid state amorphization involve the fast diffusion of one component and the driving force is a large negative heat of mixing of alloy[47], which is evident from the heat of mixing value[12] shown in Table 1.1. Namely, as shown in Fig.1.2, the free energy of the liquid (amorphous, state 2) is lower than that of the mixture of pure crystalline components (state 1) and in this mean this solid state amorphization may be said to be a metastable melting. In case of formation of intermetallic compounds, too, the driving force for it is the deviation of

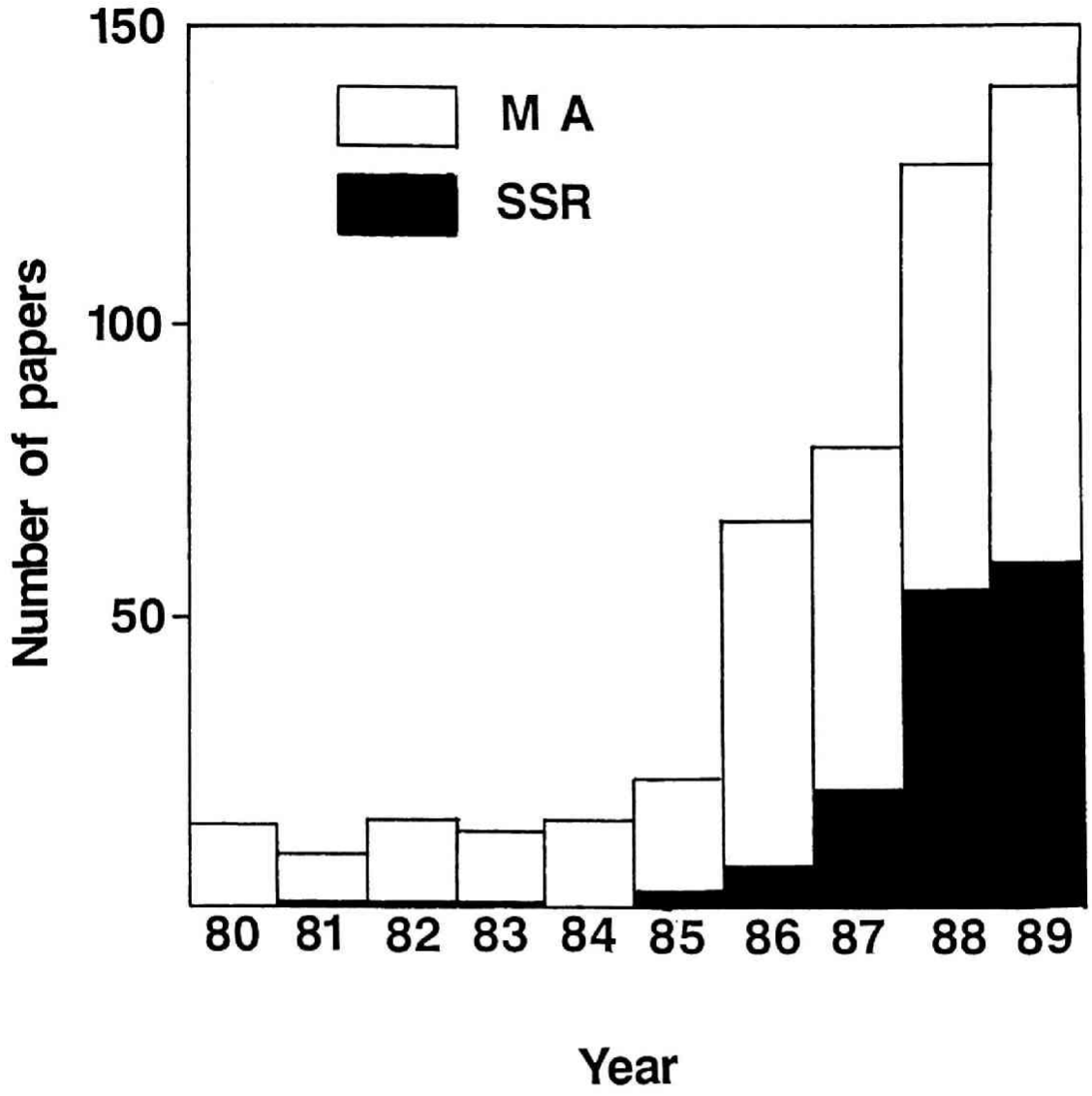

Fig.1.1 The numbers of papers on MA in the corresponding year from 1980 to 1989. Among them, number of papers on solid state state reaction by MA such as amorphization was shown in black.

Table 1.1 List of glass forming alloy systems by MA. ΔH is the heat of mixing and the value was calculated by Miedema model[12].

System	ΔH(KJ/mol)	Ref.	System	ΔH(KJ/mol)	Ref.
Ag-Cu	10	[13]	Fe-V	-29	[39]
Al-Cr	-43	[14]	Fe-W	0	[40]
Al-Fe	-11	[15]	Fe-Zr	-118	[28]
Al-Hf	-165	[16]	Ge-Nb	-97	[41]
Al-Nb	-74	[17]	Ge-Si	9	[42]
Al-Ta	-78	[18]	Hf-Ni	-144	[31]
Al-Ti	-118	[19]	Mg-Ti	59	[43]
Al-Zr	-189	[20]	Mg-Zn	-13	[44]
Au-La	-226	[21]	Mn-Zr	-74	[28]
Co-Gd		[22]	Mo-Ni	-27	[45]
Co-Mg	12	[23]	Nb-Ni	-135	[4]
Co-Nb	-111	[24]	Nb-Sn	-4	[41]
Co-Sn	1	[25]	Ni-Sn	-21	[46]
Co-Ti	-126	[26]	Ni-Ti	-154	[47]
Co-Y	-112	[27]	Ni-V	-75	[48]
Co-Zr	-197	[28]	Ni-Zr	-236	[28]
Cr-Nb	-32	[29]	Pd-Si	-145	[49]
Cr-Ta	-30	[30]	Pd-Ti	-26	[50]
Cu-Hf	-109	[30]	Pd-Zr	-117	[51]
Cu-Ta	9	[31]	Rh-Zr	-315	[35]
Cu-Ti	-40	[32]	Ru-Zr	-260	[35]
Cu-V	20	[33]	Si-Sn	30	[52]
Cu-W	101	[34]	Si-Ta	-165	[53]
Cu-Zr	-110	[28]	Si-V	-121	[53]
Fe-Hf	-71	[35]	Si-W	-58	[54]
Fe-Si	-75	[36]	Si-Zn	-3	[52]
Fe-Ta	-67	[37]	V -Zr	-17	[55]
Fe-Ti	-74	[38]			

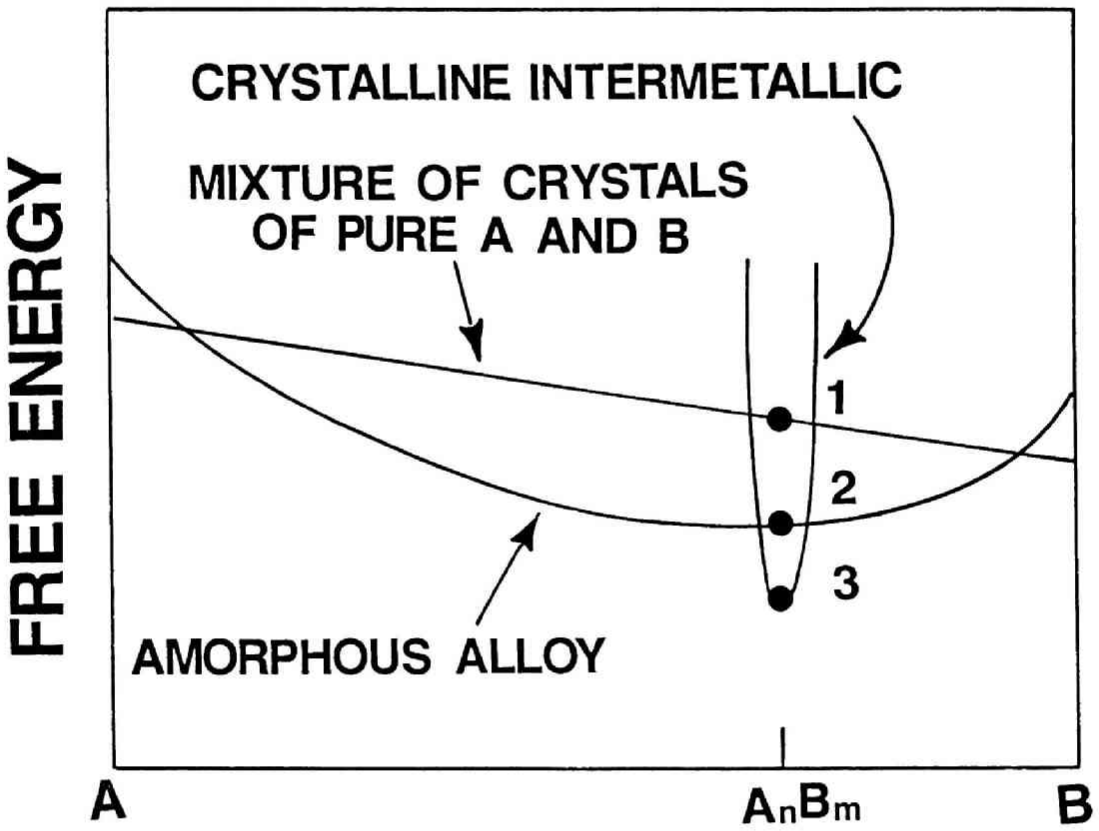

Fig.1.2 Schematically drawn relationship among free energies of amorphous, mixture of pure element and intermetallic compound.

free energy between mixtures of pure components (state 1) and intermetallic compounds (state 3). On the contrary, Schwarz reported a new different technique which is a grinding of crystalline alloys such as intermetallic compounds[58]. From a thermodynamic point of view, this phenomenon means the elevation of free energy (from state 3 to state 2 in Fig.1.3) and so MA was found to include the energizing process, too. Taking this fact into consideration, although the driving force for solid state amorphization was considered to be the negative heat of mixing, non-equilibrium phase may be formed even in the alloy system with positive heat of mixing where the mixture of pure components is thermodynamically stable and there is no chemical driving force. Positive heat of mixing means the existence of strong repulsive interaction with each other and in such alloy systems there is s large miscibility gap in their phase diagrams and alloying is impossible by conventional casting. So it is interesting to examine whether non-equilibrium phases were obtained in such alloy systems by MA. However, although many works on the solid state reaction induced by MA have been limited in the alloy systems with negative heat of mixing, works on solid state reaction in the alloy systems with positive heat of mixing have scarcely examined as shown in Table 1.2. Moreover, non-equilibrium or metastable crystalline formation has been scarcely studied compared with the systematic studies on amorphization. This situation is in contrast with that of the early stages of rapid quenching of liquid when Duwez first aimed at the creation of

Table 1.2 Alloy phases formed by MA in several alloy systems with positive heat of mixing by MA.

System	ΔH(KJ/mol)	Solid Solubility	Synthesized Phase (examined composition)	Ref.
Ag-Cu	8	14.1at%Cu in Ag 4.9at%Ag in Cu	Amor. (50at%Cu)	[13]
Ag-Fe	102	Negligible	bcc(SS) (8at%Ag) fcc(SS) (12at%Fe)	[59]
Al-Sb	11	Negligible	Compound AlSb (50at%Sb)	[60]
Bi-Mn	9	Negligible Mn in Bi 0.47at%Bi in Mn	Compound MnBi (50at%Mn)	[61]
Co-Mg	12	Negligible	Amor. (20-50at%Mg)	[23]
Co-Sn	1	2.5at%Sn in Co Negligible Co in Sn	Amor. (60at%Sn)	[25]
Cr-Cu	49	0.89at%Cr in Cu 0.20at%Cu in Cr	bcc(SS) (30,50at%Cu)	[62]
Cu-Ta	9	Negligible Ta in Cu	Amor. + fcc + bcc (44-61at%Ta) Amor. (70at%Ta)	[31]
Cu-V	21	0.1at%V in Cu 7.5at%Cu in V	Amor. + bcc(SS) (50at%V) bcc(SS) (70-90at%V)	[33]
Cu-W	101	Negligible	fcc(SS) + bcc(SS) (5-30at%W) Amor. + fcc(SS) + bcc(SS) (30-100at%W)	[34]
Fe-Sn	56	9.3at%Sn in Fe Negligible Fe in Sn	bcc(SS) (25at%Sn)	[63]
Ge-Si	9	entire composition	Amor. + diamond (0-100at%Si) diamond (0-100at%Si)	[42]
Mg-Ti	59	>0.075at%Ti in Mg 2.9at%Mg in Ti	hcp(SS) (0-6at%Mg) Amor. (10at%Mg)	[43] [64]
Si-Sn	30	Negligible	Amor.+diam.(SS)+tetrag.(SS) (0-20at%Sn) diam.(SS)+tetrag.(SS)+new tetrag. (20-30at%Sn)	[52]

non-equilibrium super-saturated solid solution in the Ag-Cu system[65]. In this work, the effectiveness of MA regarding the formation of non-equilibrium phase is examined in the alloy system with positive heat of mixing.

In chapter 2, the results of the studies on the formation of super-saturated solid solution in the Ag-Cu system by MA are given. By examining changes in the structure or X-ray diffraction pattern occurred during MA, the process of MA and the progress of solid state reaction are traced. Some properties, such as thermal stability of synthesized non-equilibrium phases, are also discussed[66].

In chapter 3, studies on mechanical alloying in the Fe-Cu system with different crystal structure and larger positive heat of mixing than Ag-Cu system are reported. In addition to some properties presented in chapter 2, results of the study on Mössbauer and magnetic property are given[67].

In chapter 4, formation of non-equilibrium phases by mechanical alloying in ternary Fe-Ag-Cu alloy is reported. Properties of the synthesized alloy are compared with the binary alloy[68].

In chapter 5, formation of non-equilibrium phases by repeated rolling method is examined. The repeated rolling method is compared with a conventional ball milling[69].

In chapter 6, a thermodynamical discussion on the formation of non-equilibrium phase and the elevation of free energy in the alloy system with positive heat of mixing is presented.

References

[1] W.Klement Jr, R.H.Willens and P.Duwez;Nature 187 (1960) 869.

[2] X.L.Yeh, K.Samwer and W.L.Johnson; Appl.Phys.Lett. 42 (1983) 242.

[3] S.Herd, K.N.Tu and K.Y.Ahn; Appl.Phys.Lett. 42 (1983) 597.

[4] R.B.Schwarz and W.L.Johnson; Phys.Rev.Lett. 51 (1983) 415.

[5] C.C.Koch, O.B.Cavin, C.G.Mckamey and J.O.Scarbrough; Appl.Phys.Lett. 43 (1983) 1017.

[6] J.S.Benjamin; Metall.Trans. 1 (1970) 2943.

[7] R.L.Cairns and J.S.Benjamin; J.Eng.Mater.Technol. 95 (1973) 10.

[8] J.J.Fischer, I.Astley and J.P.Morse, Proc. 3rd Int. Symp. on Superalloys at Seven Springs,Baton Rouge, Claitor (1970) 361.

[9] P.S.Jilman and W.D.Nix; Metall.Trans. 12A (1981) 813.

[10] R.C.Benn, L.R.Curwick and G.A.J.Hack; Powder Metall. 4 (1981) 191.

[11] P.S.Jilman and J.S.Benjamin; Ann.Rev.Mater.Sci. 13 (1983) 279.

[12] A.K.Niessen, F.R.de Boer, R.Boom, R.F.de Chatel, W.C.M. Mattens and A.R.Miedema; CALPHAD 7 No.1 (1983) 51.

[13] T.G.Richards and G.P.Johari; Phil.Mag.B 58 4 (1988) 445.

[14] K.F.Kobayashi, N.Tachibana and P.H.Shingu; J.Mater.Sci. 25 (1990) 3149.

[15] P.H.Shingu, B.Huang, J.Kuyama, K.N.Ishihara and S.Nasu;

Proc.DGM Conf.on New Material by MA Techniques,Claw-Hirsaw (1988) 319.

[16] R.B.Schwarz, J.W.Hannigan, H.Sheinberg and T.Tiainen; Proc. Modern Developments in Powder Metallurgy 21, Orland (1988) 415.

[17] E.Hellstern, L.Schultz, R.Borman and D.Lee;Appl.Phys. Lett. 53 15 (1988) 1399.

[18] M.S.E.Eskandarany, F.Itoh, K.Aoki and K.Suzuki; J.Non-Cryst.Solids 117/118 (1990) 729.

[19] L.Schultz; Mater. Sci.Eng. 97 (1988) 15.

[20] F.J.Fecht, G.Hau, Z.Tu and W.L.Johnson; J.Appl.Phys. 67 4 (1990) 1744

[21] P.I.Loeff and H.Bakker; Scrip.Metall. 22 (1988) 40.

[22] A.Ye.Yermakov, V.A.Barinov and Ye.Ye.Yurchikov; Phys.Met. Metall. 54 5 (1982) 90.

[23] A.Inoue and T.Masumoto; Proc.DGM Conf. on New Material by MA Techniques, Claw-Hirsaw (1988) 319

[24] H.Kimura, F.Takada and W.N.Myung; Mater.Sci.Eng. 97 (1988) 125.

[25] A.Hikata, M.J.Mckenna and C.Elbaum; Appl.Phys.Lett. 50 8 (1987) 478.

[26] E.Hellstern and L.Schultz; Mater.Sci.Eng. 93 (1987) 213.

[27] A.Ye.Yermakov, Ye.Ye.Yurchikov and V.A.Varinov; Phys.Met. Metall. 52 6 (1981) 50.

[28] E.Hellstern and L.Schultz; Appl.Phys.Lett. 48 2 (1986) 124.

[29] K.S.Kumar; "Solid State Powder Processing" A.H.Clauer and

J.J.deBarbadillo ed.,The Minerals and Metals & Materials Society (1990) 315.

[30] J.R.Thompson, C.Politis and Y.C.Kim; Mater.Sci.Eng. 97 (1988) 31.

[31] T.Fukunaga, K.Nakamura, K.Suzuki and U.Mizutani; J.Non-Cryst.Solids 117/118 (1990) 700.

[32] C.Politis and W.L.Johnson; J.Appl.Phys. 60 3 (1986) 1147.

[33] T.Fukunaga, M.Mori, K.Inou and U.Mizutani; Mater.Sci.Eng. A134 5 (1991) 863.

[34] E.Gaffet; Mater.Sci.Eng. A134 (1991) 1380.

[35] C.Politis; Z.Phys.Chem.N 157 (1988) 209.

[36] A.G.Escorial, P.Adeva, M.C.Christina, A.Martin, F.Carmona, F.Cebollada, V.E.Martin, M.Lenato and J.M.Gonzalez; Mater. Sci.Eng. A134 (1991) 1394.

[37] G.Veltl, B.Scholtz and H.D.Kunze; Proc. Modern Developments in Powder Metallurgy 20, Orland (1988) 707.

[38] J.Eckert,L.Schultz and K.Urban; J.Non-Cryst.Solids 127 (1991) 90.

[39] B.Fultz, G.Le Caer and P.Matteazzi; J.Mater.Res. 4 6 (1989) 1450.

[40] T.D.Shen, K.Y.Wang, M.X.Quan, J.T.Wang and W.D.Wei; Mater.Sci.Forum 88-90 (1992) 391.

[41] C.Politis; Physica B&C 135 (1985) 286.

[42] E.Gaffet, F.Faudot and M.Harmelin;Mater.Sci.Forum 88-90 (1992) 375.

[43] R.Sundaresan, A.G.Jackson, S.Krischnamurthy and F.H.Froe; Mater.Sci.Eng. 97 (1988) 115.

[44] A.Calka and A.P.Radlinsky; Mat.Sci.Eng. A118 (1989)131.

[45] G.Cocco, S.Enzo, N.Barrett and K.J.Roberts; J.Less Common Met. 154 (1989) 177.

[46] T.J.Tiainen and R.B.Schwarz; ibid. 140 (1988) 99.

[47] R.B.Schwarz, R.R.Petrich and C.K.Saw; J.Non-cryst. Solids 76 (1985) 281.

[48] Y.Honma, T.Fukunaga, K.Suzuki, and U.Mizutani; Mater. Sci.Forum 88-90 (1992) 339.

[49] T.Nasu, K.Nagaoka, S.Takahashi, T.Fukunaga and K.Suzuki; Mater.Trans.Jpn.Inst.Met. 30 2 (1989) 146.

[50] J.R.Thompson and C.Politis; Europhys.Lett. 3 2(1987) 199.

[51] P.I.Loeff, F.H.M.Spit and H.Bakker; J. Less Common Met. 145 (1988) 271.

[52] E.Gaffet and H.Harmelin; Colloq.de Physique C4 (1990) 139.

[53] R.K.Eiswanadham, S.K.Mannan and S.Kumar; Scrip.Metall. 22 (1988) 1011.

[54] J.H.Ahn, H.S.Chung, R.Watanabe and Y.H.Park; Mater.Sci. Forum 88-90 (1992) 347.

[55] A.W.Weeber and H.Bakker; J.Phys.F 18 (1988) 1359.

[56] A.Weeber and H.Bakker; J.Phys.Chem.N 157 (1988) 209.

[57] E.Hellstern and L.Schultz; Appl.Phys.Lett. 49(1986)1163.

[58] R.B.Schwarz and C.C.Koch; Appl.Phys.Lett. 49 (1986) 146.

[59] J.Kuyama, H.Inui, S.Imaoka, S.Nasu, K.N.Ishihara and P.H.Shingu; Jpn.J.Appl.Phys.2 6 (1991) L854.

[60] K.Uenishi, K.F.Kobayashi,K.N.Ishihara and P.H.Shingu; Mater.Sci.Forum 88-90 (1992) 453.

[61] R.M.Davis, B.Mcdermott and C.C.Koch; Met.Trans.A 19A (1988) 2867.

[62] Y.Ogino and R.Sakai;J.Non-Cryst.Solids 117/118(1990) 737.

[63] S.Nasu, S.Imaoka, S.Morimoto, H.Tanimoto, B.Huang, T.Tanaka, J.Kuyama, K.N.Ishihara and P.H.Shingu; Mater.Sci.Forum 88-90 (1992) 569.

[64] R.Sundaresan and F.H.Froe;Proc. DGM Conf. on New Materials by Mechanical Alloying Techniques,Claw-Hirsau (1988) 243.

[65] P.Duwez,R.H.Willens and W.Klement Jr; J.Appl.Phys. 31 (1960) 1136.

[66] K.Uenishi, K.F.Kobayashi, K.N.Ishihara and P.H.Shingu; Mater.Sci & Eng. A134 (1991) 1342.

[67] K.Uenishi, K.F.Kobayashi, S.Nasu, H.Hatano, K.N.Ishihara and P.H.Shingu; Z.Metallkd 83 2 (1992) 132.

[68] K.Uenishi, K.F.Kobayashi, K.N.Ishihara and P.H.Shingu; Mater.Sci.Forum 88-90 (1992) 459.

[69] P.H.Shingu, K.N.Ishihara, K.Uenishi, J.Kuyama, B.Huang and S.Nasu; Solid State Processing, A.H.Clauer and J.J.de Barbadillo ed. (1990) 21.

Chapter 2

Formation of super-saturated solid solution in the Ag-Cu system

2.1 Introduction

The heat of mixing of Ag and Cu is about 10kJ/mol in positive. The positive heat of mixing means that interaction between Ag and Cu atoms is repulsive. Figure 2.1 shows the phase diagram[1] for this system. The solubility of Ag in Cu is 0.05at% and that of Cu in Ag is 0.3at% at room temperature[2]. When Ag and Cu are conventionally melt and cast from liquid, they will not solve each other and separate. Duwez[3] first aimed at the creation of non-equilibrium solid solution by rapid quenching from liquid in this system. By undercooling below To curve[4] induced by rapid quenching, the nucleation of pure elements which needs long distance diffusion was kinetically suppressed and so the super-saturated solid solution was successfully prepared. Afterwards, this alloy system has been frequently used to test or optimize newly designed rapid quenching equipment; ie. plasma jet spraying[5]. Amorphous has been obtained by vapor quenching to 77K and subsequent annealing at 253K[6]. As in the study on MA in the same system, Richards et al.[7] had already reported the formation of amorphous. However, the amorphization was confirmed only from the broadness of the diffraction peak in X-ray diffraction pattern and the effect of O and N was not negligible.

In this chapter, MA containing a energizing process was investigated to know how effective it is to form non-

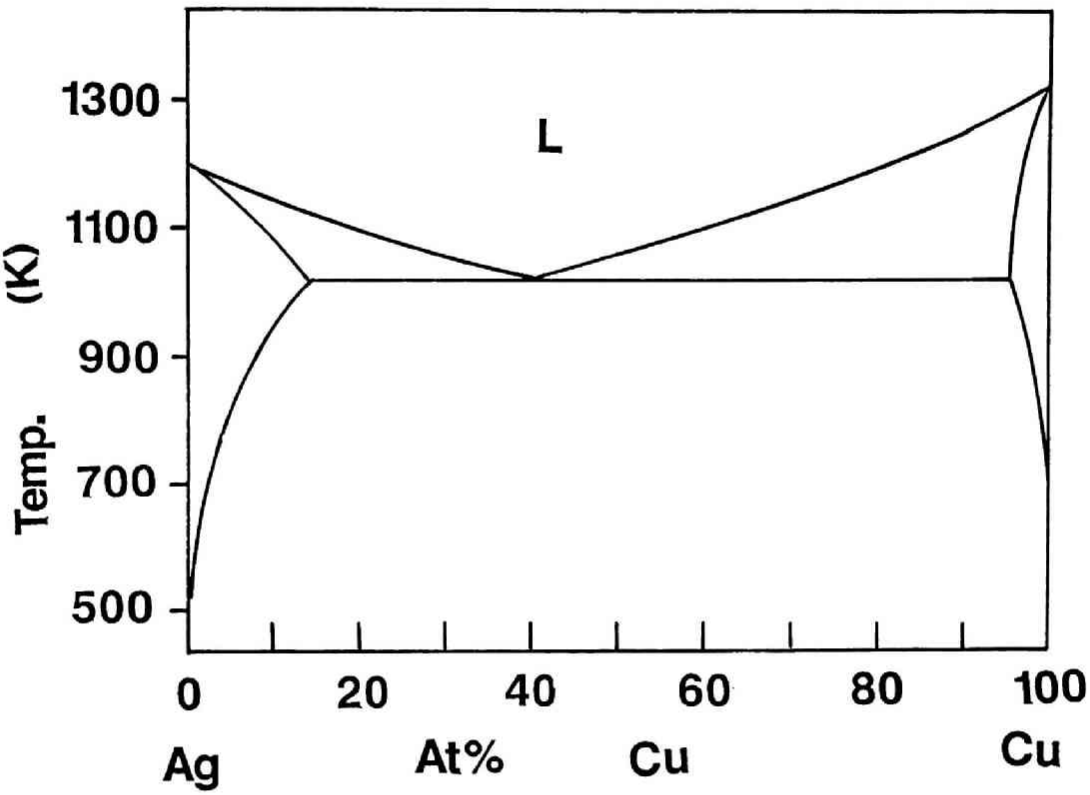

Fig.2.1 Phase diagram for Ag-Cu system[1].

equilibrium phases in the Ag-Cu system. The super-saturated solid solution formed by MA was compared with that by rapid quenching.

2.2 Experimental

2.2.1 Mechanical alloying

In this study, Mechanical alloying was performed by conventional ball milling. To avoid the rise of temperature induced by too hard mechanical milling and to realize the solid state reaction at low temperatures, ball milling with lowest temperature rise was adopted although the fracturing ability was not very strong. 99.9% Ag and Cu powders with average particle size of about 30μm were used as starting materials. These powders were blended to desired compositions and sealed in a cylindrical stainless vial with the stainless balls in an argon atmosphere. The stainless vial, balls and apparatus are shown in Fig.2.2. The stainless vial was 100mm in inner diameter and 140mm in height and 1700cm^3 in volume. The stainless balls were about 9mm in diameter and one thousand balls were loaded in the vial. The total powder weight was 50g and so the ball to powder ratio was 80:1. The vial with balls and sample powders was rotated at a rate of 90rpm on the rotating frame. To investigate the changes of the powder during MA, small amount of powders was removed in an Ar atmosphere by nominal length of MA time.

2.2.2 Chemical analysis

Mechanically alloyed powders were afraid to contain many

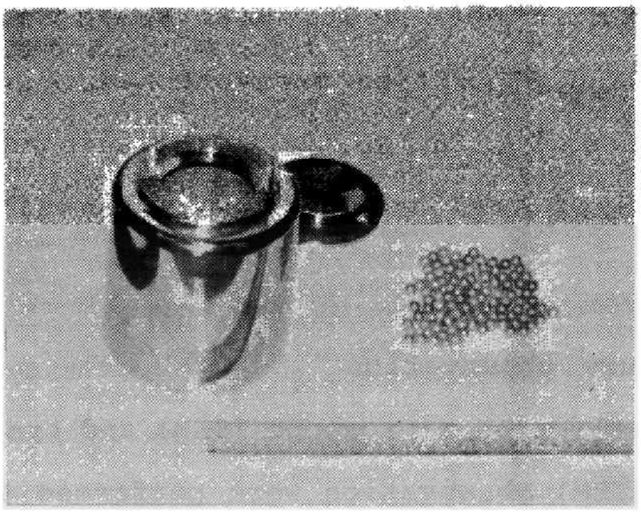

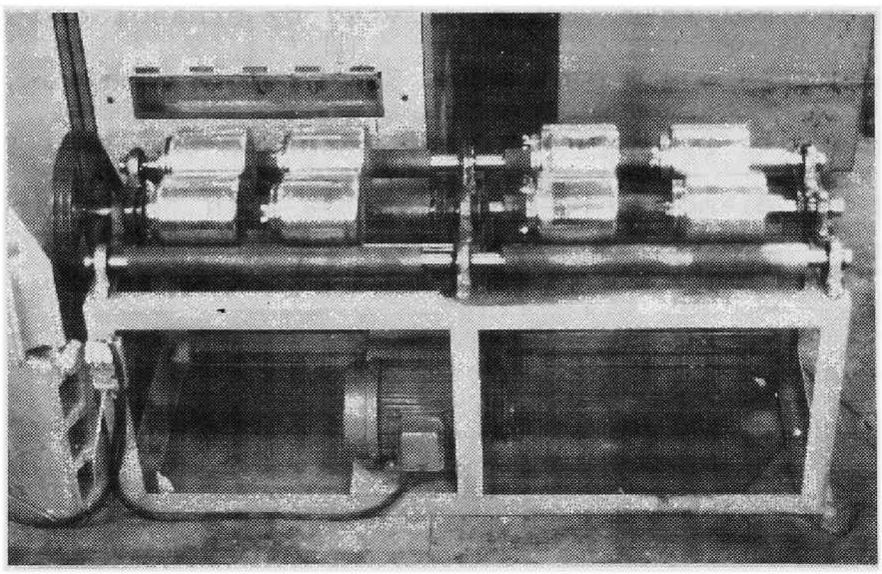

Fig.2.2 The ball milling apparatus.

contaminations such as Fe from stainless apparatus. Moreover, MA powders were rich in the surface activity, so the effect of surrounding gas, such as O_2 and N_2 were not negligible. In fact, Richards reported that O_2 affected strongly on the amorphization in this system[7]. In the present study, the composition and impurities were checked by chemical analysis. Metal elements, Ag, Cu, Fe, Cr and Ni were analyzed by ICP, and O_2 and N_2 gases were analyzed by gas analyzer (HORIBA EMGA 2200).

2.2.3 Structure observation

Scanning electron microscope (SEM) and transmission electron microscope (TEM) observation were performed to investigate the structural changes caused by MA and subsequent heat treatment. For SEM observation, the powders were embedded in the epoxy resin and polished. $FeCl_3$ diluted by ethanol and HCl was used as a etching solution of Cu. For TEM observation, the sample embedded in epoxy resin (TAAB 812 set) was thin sliced using glass and diamond blade. The ultra-thin sectioning instrument (LKB 2188 ultratome NOVA) was used to slice.

2.2.4 X-ray diffraction (XRD) analysis

Phases formed by MA and heat treatment was identified by XRD analysis. The used X-ray was Cu Ka radiation.

The lattice parameter of fcc phase was measured form (211) peak by using the following equation.

$$a = \lambda / 2 (h^2 + k^2 + l^2)^{1/2} \sin\theta$$

where λ is wave length of X-ray 0.154nm, θ is diffraction

angle, and h,k,l is the crystal plane index of diffraction peak.

The correction of the diffraction angle was performed by using standard diffraction peaks of Si.

Effective crystallite size was evaluated by using Scherrer formula[8]. The Scherrer formula is

$D = 0.9\lambda / B \cos\theta$

where D is crystallite size and B is the half value width of the diffraction peak.

2.2.5 Thermal analysis

The thermal stability was examined by measuring differential scanning calorimetry (DSC). DSC was performed at the heating rate of 0.33K/sec under Ar flow atmosphere by using Perkin-Elmer DSC 7. The sample powder was canned in pure Al pan and the difference in heat input to keep the temperature difference between the sample and the standard reference (Al pan without sample) to be zero was measured.

2.2.6 Electrical Resistivity

The change in the electrical resistivity upon heating was measured at the same heating rate as DSC, 0.33K/sec, in an Ar atmosphere. The resistivity was measured by four-point-prove technique. Mechanically alloyed powders were consolidated to a thin plate by cold rolling. Al leading wires were resistance welded on the each corner of the sample. Constant current of 100mA was sent and the voltage was measured.

2.3 Results and discussion

2.3.1 Chemical composition of mechanically alloyed powders

Table 2.1 shows the results on chemical analysis of Ag-Cu alloy powders mechanically alloyed for 400h. From these results, the atomic ratio of Ag to Cu was hardly changed compared with that before MA. In case of MA, weldabilty of the powders to the balls and vial is different by the element, so the compositional change is likely induced. It was interpreted, however, not to be the matter in this case from these results.

MA is known to be the subjectable process of impurity due to the intense friction between balls and vials. In this work, some means were performed to avoid the impurities. The ball milling technique with relatively weak friction was adopted. MA was preparatory performed for 50h on the corresponding composition and the alloy powders were thin coated to the balls and vials. By using this coated balls and vial, stainless to stainless friction was diminished and the contamination was reduced. However, Fe, Cr and Ni from stainless balls and vial were still recognized as the impurities. The total contamination was about 4at% although the value was smaller than that in the case by the other apparatus such as attritor with more intense friction.

The contamination of O_2 and N_2 was 0.273wt% and 0.004wt% respectively. In Richards' report[7], chemical analyses were not performed and the simple comparison with the present work was difficult, but when MA powders were heated over 550K Cu_2O was detected in Richards' sample while any oxides were not

Table2.1 Chemically analyzed composition of Ag-Cu powder mechanically alloyed for 400h.

	Chemically analyzed composition (at%)				
	Ag	Cu	Fe	Ni	Cr
Ag-10at%Cu	88.71	9.94	0.88	0.23	0.24
Ag-20at%Cu	76.65	19.37	2.85	0.41	0.71
Ag-30at%Cu	68.39	29.85	1.26	0.22	0.27
Ag-40at%Cu	53.15	41.67	3.97	0.50	0.71
Ag-50at%Cu	49.33	46.60	3.00	0.43	0.64
Ag-60at%Cu	37.30	55.68	5.05	0.74	1.22
Ag-70at%Cu	29.06	67.69	2.41	0.35	0.48
Ag-80at%Cu	18.90	75.93	3.83	0.49	0.85
Ag-90at%Cu	9.35	87.47	2.39	0.28	0.51

detected in this work. So the effect of O_2 was considered to be less than in the case of Richards' work.

2.3.2 Structural evolution by MA

Figure 2.3 shows the morphologies and of Ag-70at%Cu powders mechanically alloyed for various time. On the early stage of MA, such as 25h MA, the constituent powders were deformed and the welded to each other and as the result, the particle size became about 10 times larger than starting powders. By prolonged MA as shown in the SEM images of the MA powders for 50 hours, the coarse composite particles became equiaxed and fine. But even by further MA such as 100 and 400h MA, the morphology and particle size hardly changed. MA is a fracturing and welding process. So, the particle size is determined by the balance between the two process. On the early stage of MA, the welding took place dominantly because constituent metal powders had some ductility and were easy to be deformed, so the particle were coarsened. But by further MA, the powders were excessively deformed and hardened[9]. The deformability decreased and powders became fracturable. So the fracturing frequency became larger and the particle became fine and equiaxial.

Figure 2.4 shows the microstructure of the MA powders. On the early stage of MA, such as 2 hour, the particles took on layered composite structure of starting constituents. The original starting constituents were identifiable within the composites. In this figure, the dark contrasted area was consisted of Ag and bright in Cu. By further MA such as 10h and

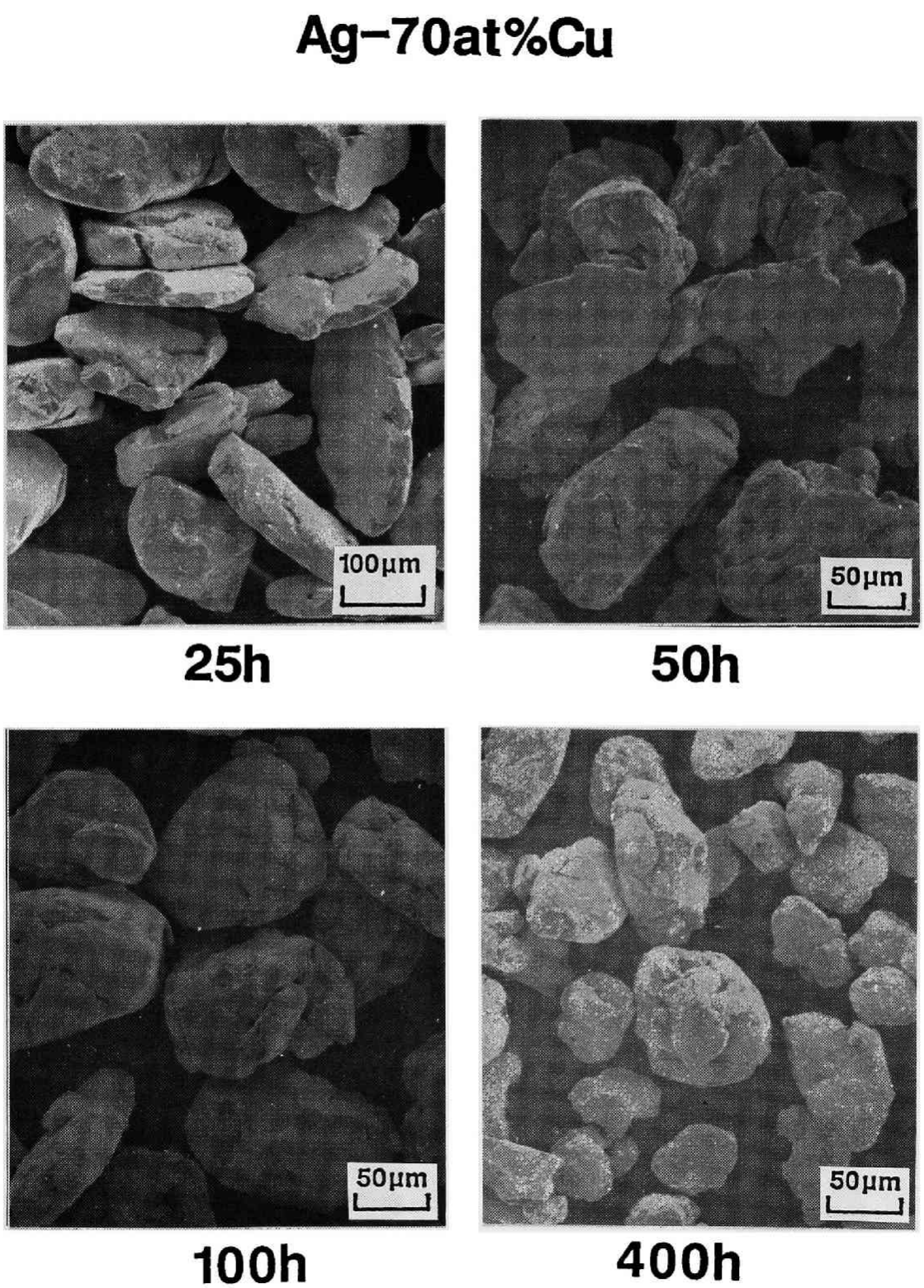

Fig.2.3 Changes of morphology of Ag-70at%Cu MA powder as a function of MA time.

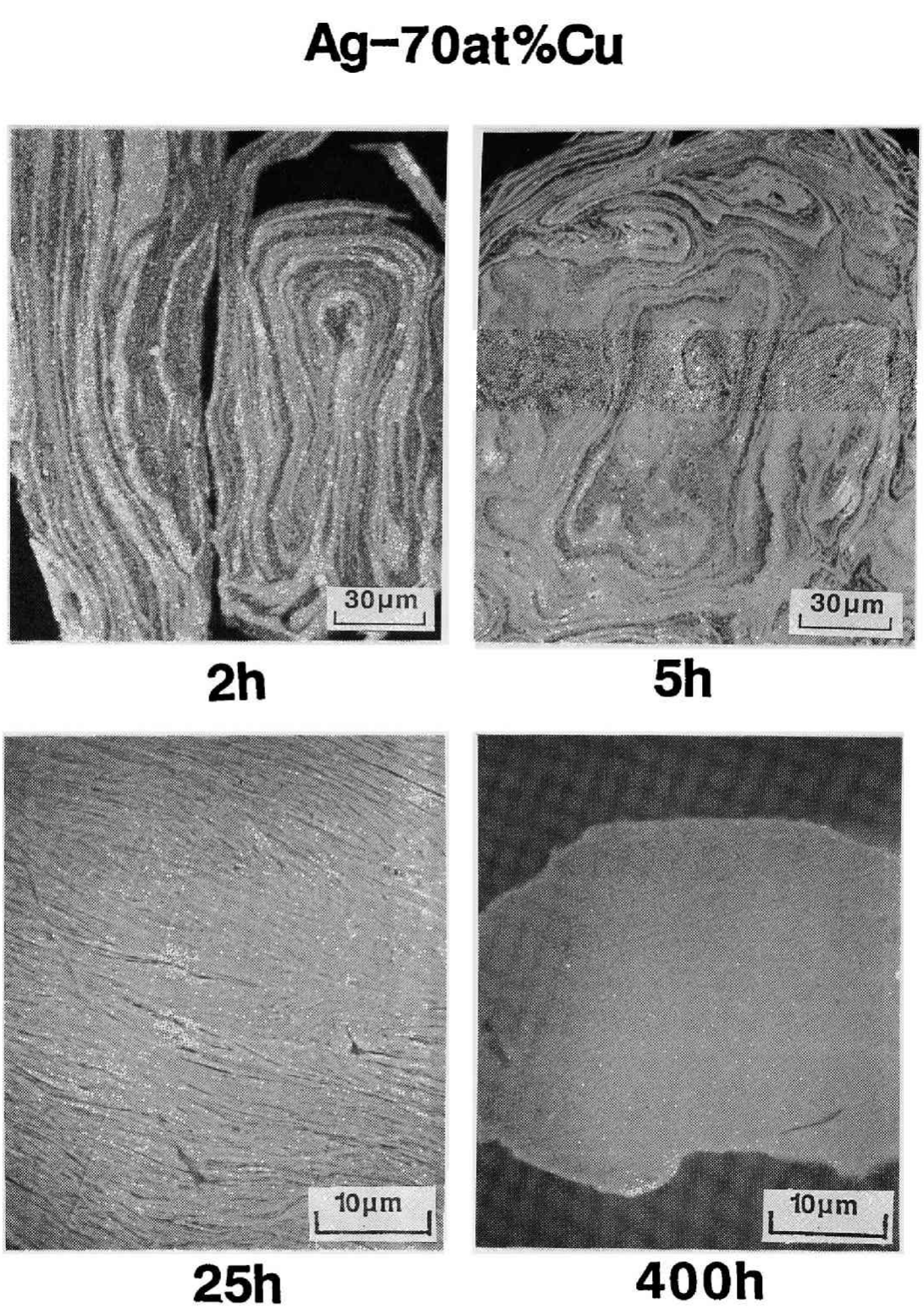

Fig.2.4 Changes of the microstructure of Ag-70at%Cu MA powder as a function of MA time.

25h, these composites were further refined and convoluted as the kneading (rolling and folding) was repetitively performed. And on the final stage of MA, such as 400h MA, no structure were observed within the resolution ability of SEM.

2.3.3 Formation of super-saturated solid solution

When the mixture of pure Ag and Cu powders were mechanically alloyed, both of the XRD peaks of fcc Ag and Cu became broader and smaller with increasing the MA time as shown in Fig.2.5. However, the peak position of Ag and Cu hardly changed with MA time. For Ag-70at%Cu powder, after MA 25h, a new diffraction peak appeared between pure Ag and Cu (111) peaks. The new peak became larger with increasing the MA time, and after MA for 100h, peaks of pure Ag and Cu finally disappeared and only the new fcc peaks were left. By further MA, the diffraction pattern hardly changed. These results indicate that a non-equilibrium fcc super-saturated solid solution was formed by MA. The powder mechanically alloyed for 400h was found, by TEM observation to have a homogeneous and fine structure with average grain size of about 10nm as shown in Fig.2.6.

The changes of XRD pattern of MA powders as a function of composition are shown in Fig.2.7. The diffraction peak became broader as the composition became equiatomic. Fig.2.8 shows the changes of grain size estimated from XRD patterns as a function of composition. The minimum value exhibited about 10nm.

The peak position was confirmed from Fig.2.7 to shift to the higher angle with increasing the Cu content. In Fig.2.9, the lattice parameter of synthesized fcc phase is shown against

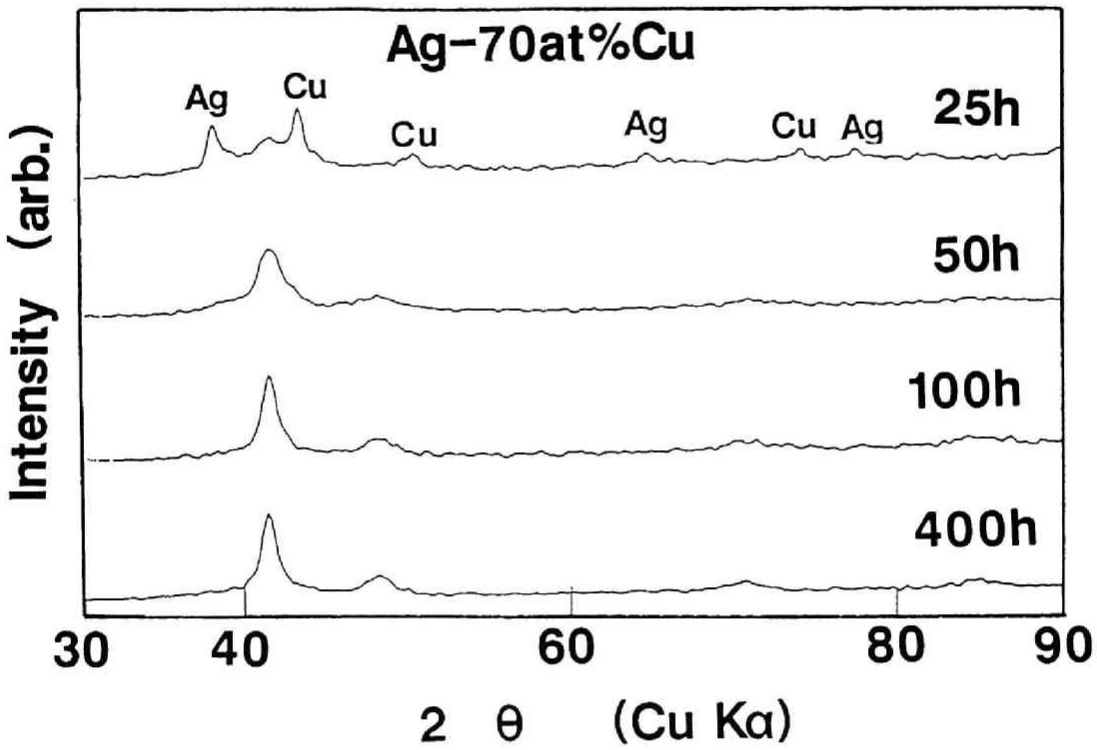

Fig.2.5 Changes of XRD patterns of Ag-70at%Cu MA powder as a function of MA time.

Ag-70at%Cu MA 400h

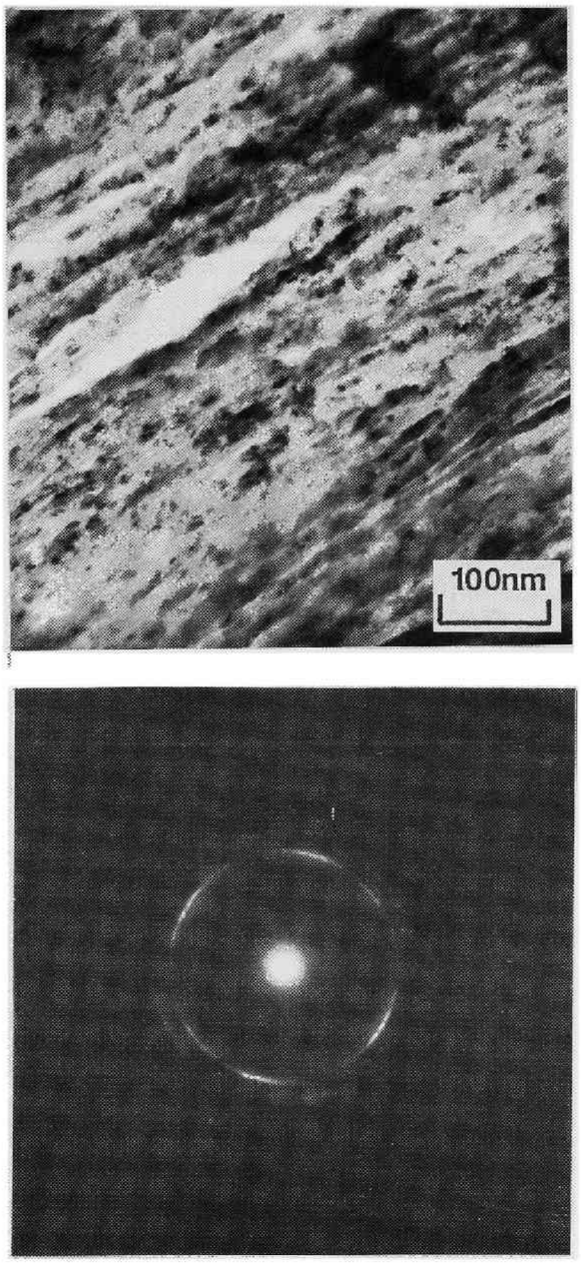

Fig.2.6 TEM images of Ag-70at%Cu powder mechanically alloyed for 400h.

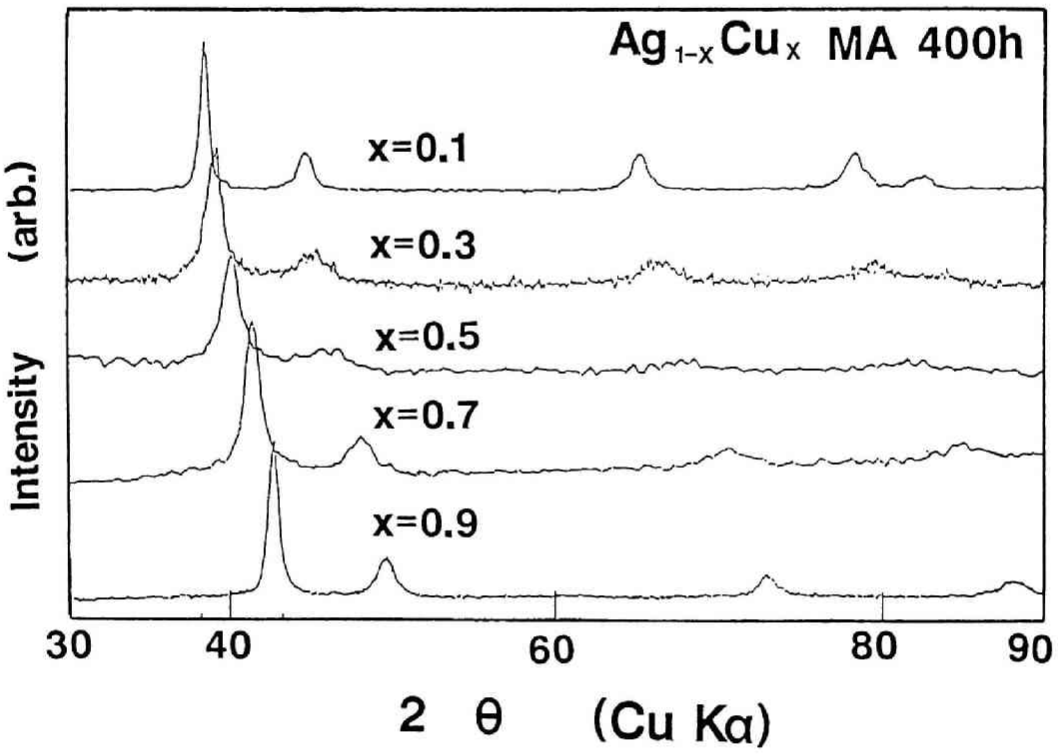

Fig.2.7 XRD patterns of Ag-Cu MA 400h powder having various compositions.

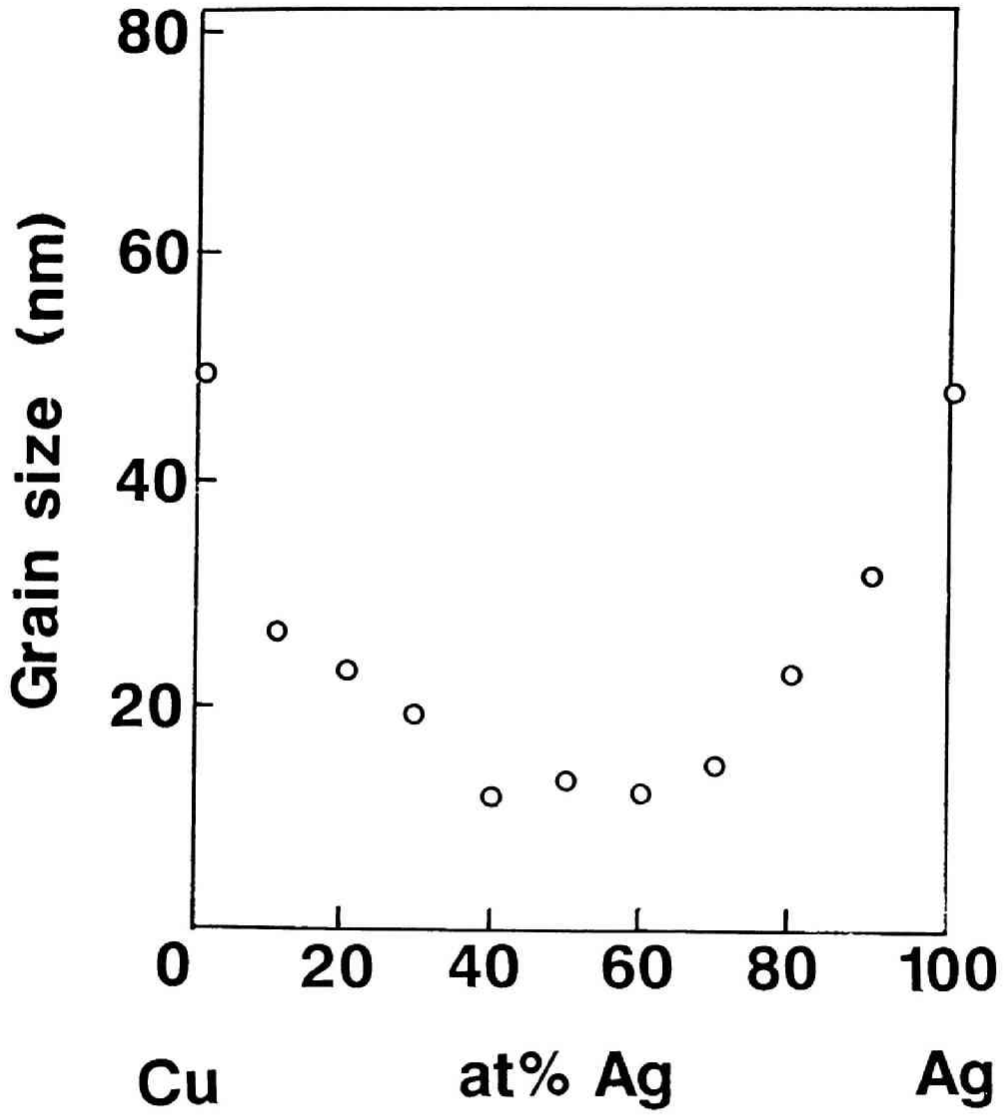

Fig.2.8 Grain size of Ag-Cu MA 400h powder evaluated by Scherrer formula.

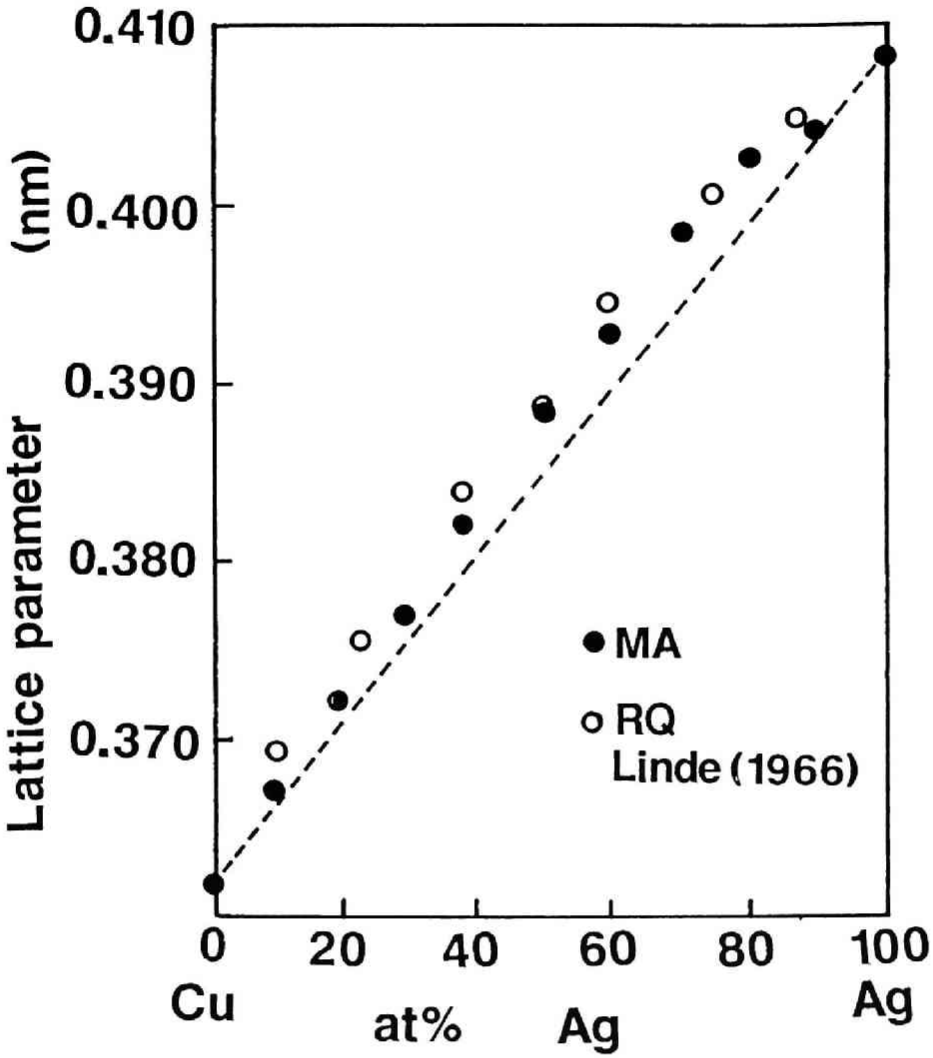

Fig.2.9 Lattice parameter of Ag-Cu alloy produced by 400h MA and by rapid quenching[10].

the corresponding composition. The measured lattice parameters were slightly higher than those estimated from Vegard's law. The slight positive deviation from Vegard's law was consistent with the small positive value of the heat of mixing of Ag and Cu. The matching with the reported data by rapid quenching method[10] was quite good.

2.3.4 Thermal stability of super-saturated solid solution

In Fig.2.10, the changes of DSC curves of Ag-70at%Cu are shown as a function of MA time. The broad exothermal peaks became larger with increasing the MA time up to 100h, but hardly changed by prolonged MA. In Fig. 2.11, DSC curves of mechanically alloyed Ag-Cu powders having various compositions are shown. In the DSC curves of MA powders, for example Ag-70at%Cu powder, two broad exothermal peaks from about 430K to 590K and from 430K to 830K were confirmed. The X-ray diffraction patterns of Ag-70at%Cu powders continuously heated up to various temperatures are shown in Fig.2.12. The position and width of diffraction peaks showed no changes by heating up to 430K before the first exothermal peak. However, by heating up to 590K, which was a higher temperature than the first exothermal peak, the broad peaks corresponding to pure Ag and Cu appeared. These peaks from Ag and Cu were broader than those of as mechanically alloyed solid solution phase. Such broadening in the diffraction peaks were caused by the precipitated extremely fine structure of Ag and Cu precipitates. By heating up to 870K, a higher temperature than the second exothermal peak, the peaks of Ag and Cu became

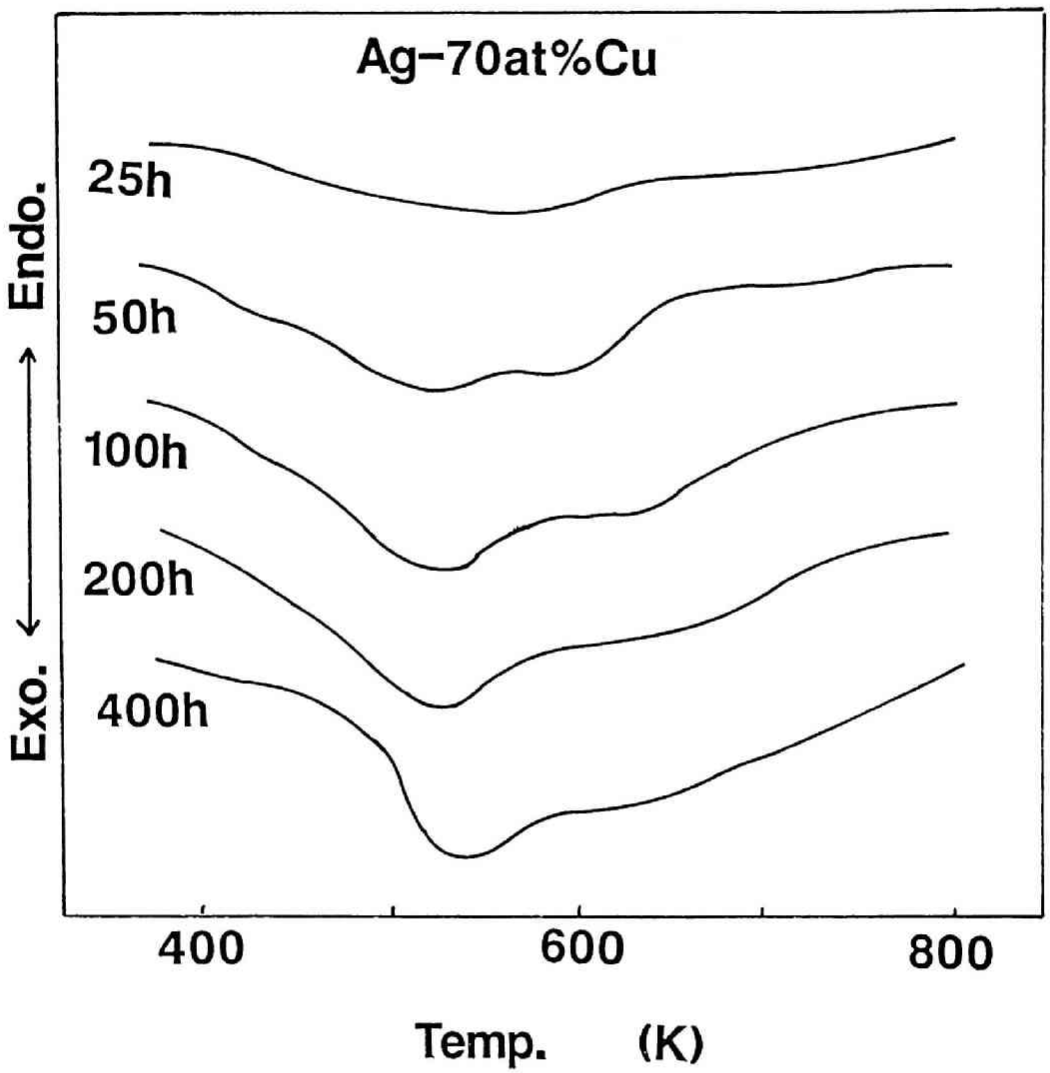

Fig.2.10 Changes of DSC curves of Ag-70at%Cu MA powder continuously heated at a rate of 20K/min. as a function of MA time.

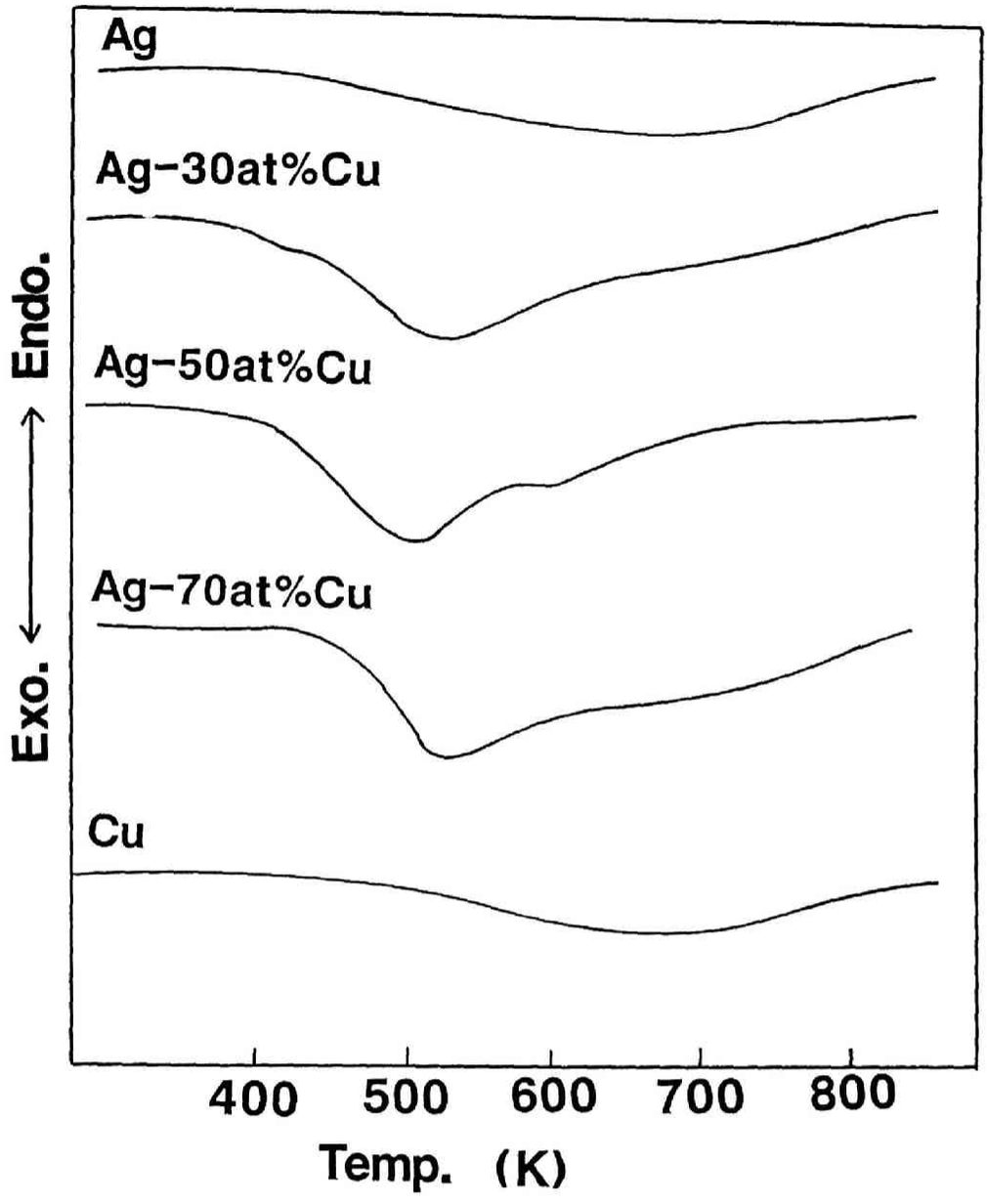

Fig.2.11 DSC curves of Ag-Cu MA 400h powder having various compositions at a heating rate of 20K/min.

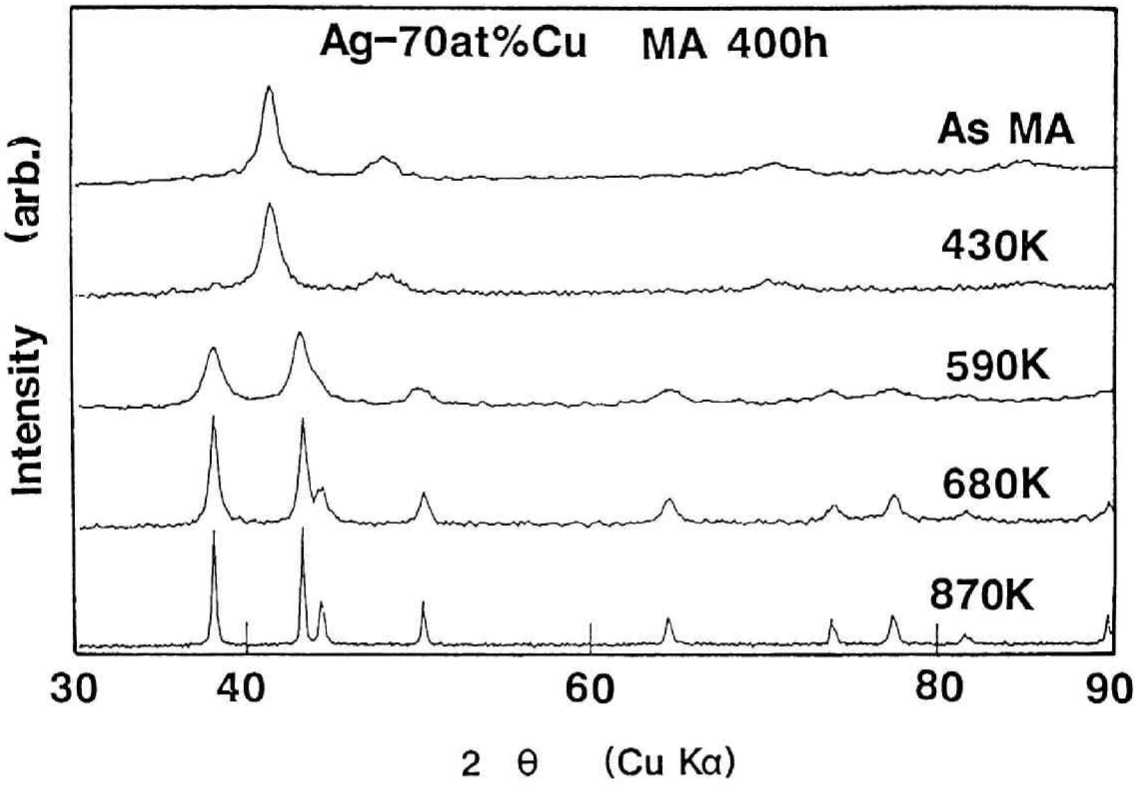

Fig.2.12 XRD pattern of Ag-70at%Cu powders continuouly heated up to various temperature at a rate of 20K/min.

sharper showing the occurrence of the grain growth. These results indicated that the solid solution was stable and any grain growth did not occur below the first exothermal peak. The solid solution decomposed to fine Ag and Cu at the temperature corresponding to the first exothermal peak. The second exothermal peak correspond to the grain growth of the precipitated fine Ag and Cu. These results were also confirmed by TEM observation in Fig.2.13 of the same samples. The estimated grain size from XRD pattern was 16nm, 16nm, 15nm and 75nm respectively, which matched well with the observed grain size by TEM.As to the thermal stability of super-saturated solid solution,the decomposition temperature matched well with those produced by the other techniques[6][11]. About the stability of the nanocrystalline structure,the similar results were reported in Cu-Ti alloy by Abe et al.[12]. According to the report, the segregation of Cu atoms in grain boundaries suppressed the the grain growth and no grain growth took place until the intermetallic $CuTi_2$ nucleated. In this work, such segregation was not confirmed. The decomposition behaviors of the solid solution were examined by many researchers[6][11][13], but there were no report on the 10nm order precipitates formation. In the samples produced by the other techniques, the grain size of the precipitates was about several hundred nm which value was ten times larger than that by MA. The samples stored stress in excessively high density, which generated the many nucleation site in the decomposition and suppressed the grain growth.

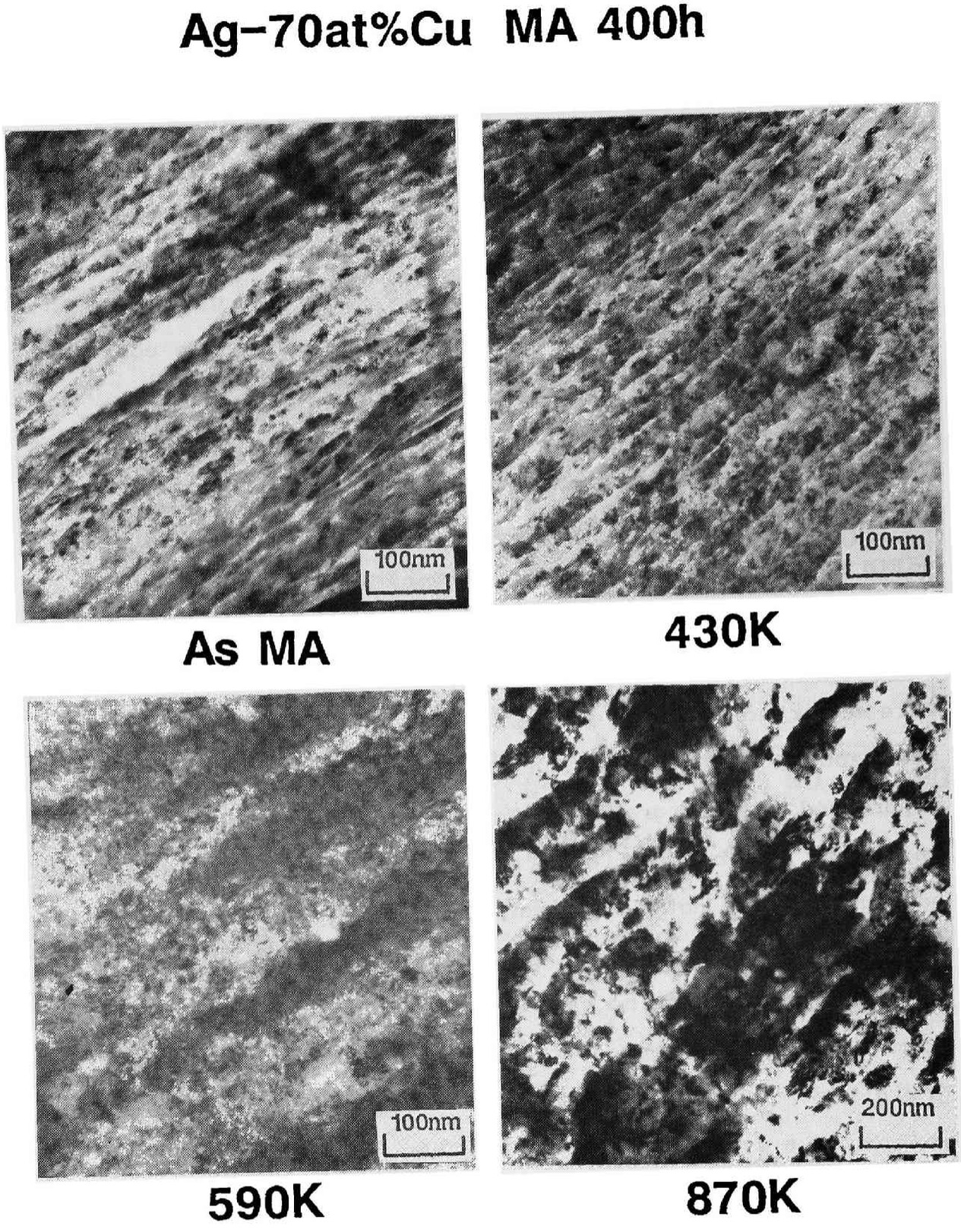

Fig.2.13 TEM images of Ag-70at%Cu powders continuously heated up to various temperature at a rate of 20K/min.

The total heat output of the exothermal peaks was compared with the thermodynamically calculated[14] value of heat of mixing as shown in Fig.2.14. The measured exothermal heat was about 5 kJ/mol larger than the heat of mixing to form super-saturated fcc phase. The reason for this large heat output may be due to the heat of grain growth or recovery.

The changes of the electrical resistivity with the temperature was shown in Fig.2.15. The resistivity of as mechanically alloyed Ag-60at%Cu and Ag-80at%Cu powders was about 60 and 25$\mu\Omega$cm respectively. It linearly increased with increasingthe temperature. But when the decomposition of solid solution to Ag and Cu took place at 450 or 550K, the resistivity gradually decreased. The decomposition was confirmed to finish completely about 600K from DSC analyses, but the resistivity still went on decreasing. The resistivity of solid solution produced by the other techniques exhibited sharper decrease in decomposition. In the case of MA, the precipitated Ag and Cu were fine on the early stage of decomposition, which made the resistivity large and the grain growth made the resistivity decreased. When the sample heated to about 770K was cooled to room temperature, the resistivity was about one fifth of the initial state for the Ag-60at%Cu sample.

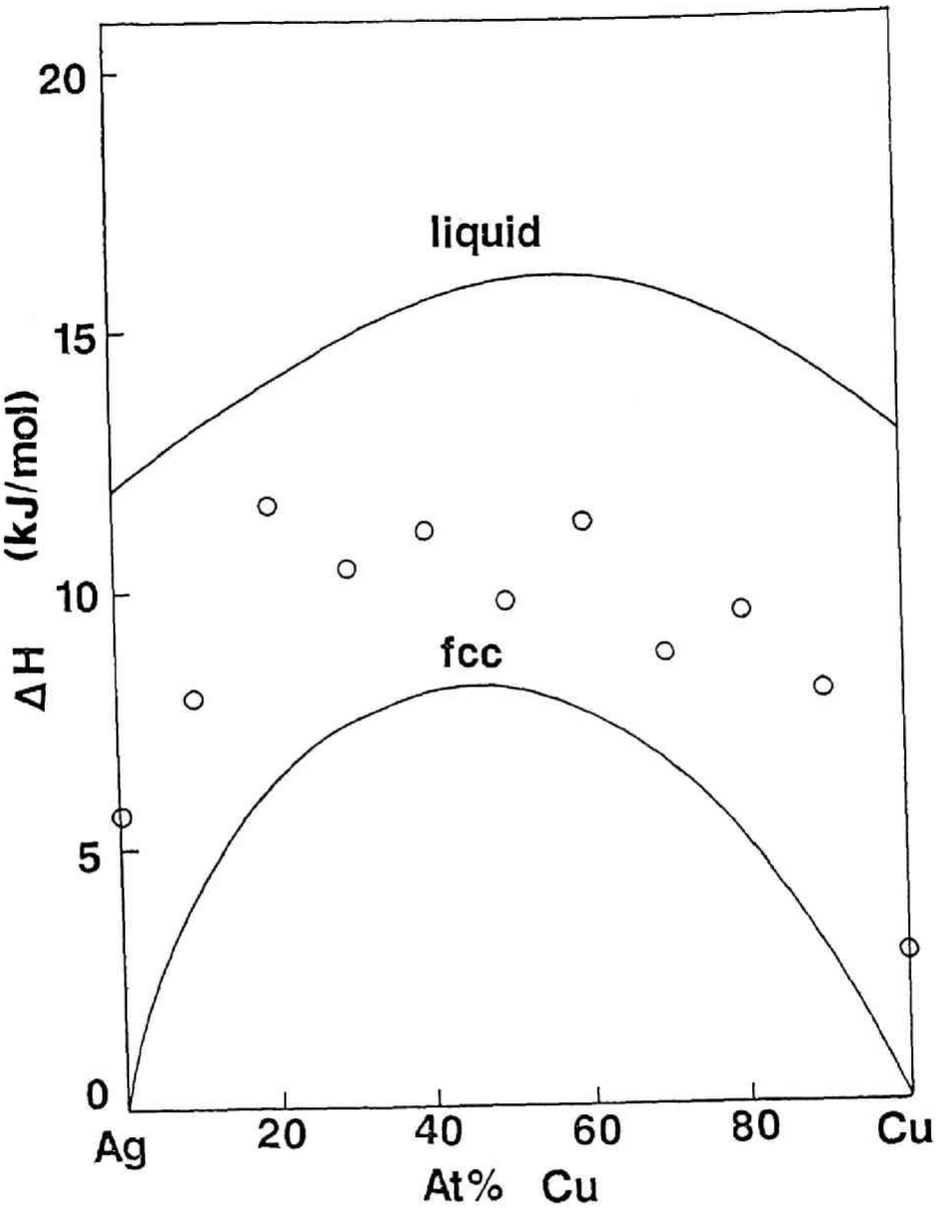

Fig.2.14 Total heat output of exothermal peaks in DSC curves of Ag-Cu MA 400h powders. Thermodynamically calculated enthalpy of liquid and fcc phases is also shown in solid line.

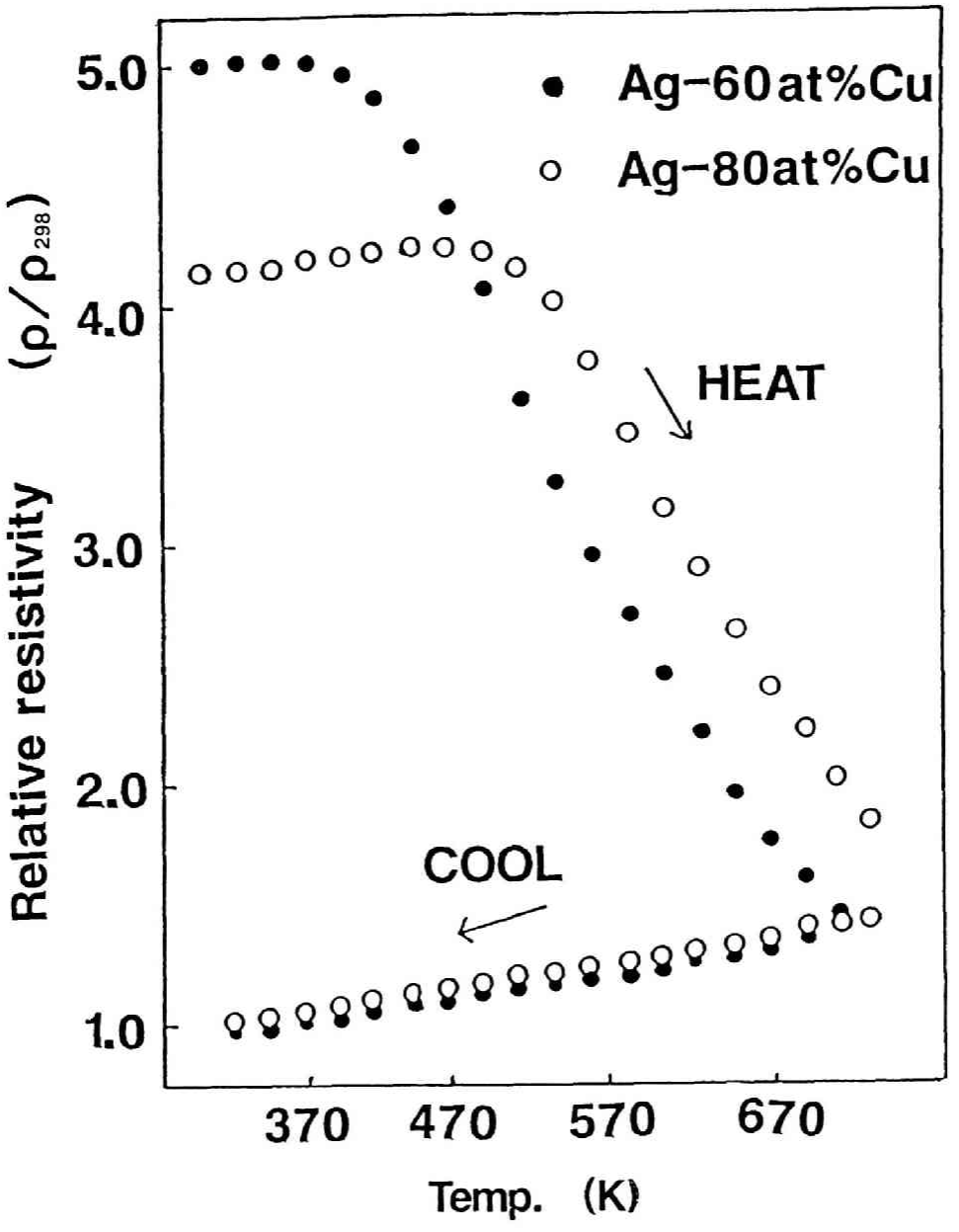

Fig.2.15 Changes of the electrical resistivity of MA 400h Ag-60at%Cu and Ag-40at%Cu powder compact with temperature at a heating rate of 20K/min.

2.4 Conclusion

Mechanial alloying by ball milling was performed in the Ag-Cu system. Non-equilibrium super saturated fcc solid solution was formed in entire composition range. The mechanical alloying which is a greatly different processing technique in comparison with the rapid quenching (RQ) was proved, in this work, to be just as effective as RQ in producing the complete solid solution in the Ag-Cu system. The nanocrystal structure with grain size of 10nm of super-saturated solid solution was thermally stable until the decomposition took place. The decomposition of super-saturated solid solution took place by heating the mechanically alloyed sample over 430K. The decomposition was accompanied by a gradual decrease in electrical resistivity. At the initial stage of decomposition, the grain size of decomposed phases remained in ten nano-meter size. Only by heating over about 600K, the grain growth took place.

References

[1] W.C.Giessen; Bul.Alloy Phase Diagram 1 1 (1986) 41.

[2] I.V.Salli and L.P.Limina; Tsvet.Met. 4 (1965) 117.

[3] P.Duwez, R.H.Willens and W.Klement Jr; J.Appl.Phys. 31 (1960) 1136.

[4] K.N.Ishihara and P.H.Shingu; Mater.Sci.&Eng. 63 (1984) 251.

[5] M.Moss, D.L.Smith and R.A.Lefever; Appl.Phys.Lett. 5 (1964) 5.

[6] S.Mader, A.S.Novick and H.Widner; Acta.Met. 15 (1967) 203.

[7] T.Richards and G.P.Johari; Phil.Mag.B 58 4 (1988) 445.

[8] B.D.Cullity "Elements of X-ray diffraction" Addision-Wesley Pub. Company Inc., USA (1978) 102.

[9] M.Zdujic, K.F.Kobayashi and P.H.Shingu; Z.Metallkde. 81 H.5 (1990) 380.

[10] R.K.Linde; J.Appl.Phys.37 (1966) 934.

[11] B.Y.Tsaur, S.S.Lau and J.W.Mayer; Appl.Phys.Lett. 36 (1980) 823.

[12] Y.R.Abe and W.L.Johnson; Mater.Sci.Forum 88-90 (1992) 513.

[13] R.Stoering and H.Conrad; Acta.Metal. 17 (1969) 933.

[14] J.L.Murray, Metall.Trans.15A (1984) 262

Chapter 3

Mechanical alloying in the Fe-Cu system

3.1 Introduction

In the previous chapter 2, results on super-saturated solid solubility in Ag-Cu system were reported. In this chapter, MA was performed in Fe-Cu system with different crystal structure and larger positive heat of mixing, about 50kJ/mol, than that of Ag-Cu system. Phase diagram of Fe-Cu system[1] is shown in Fig.3.1. The crystal structure of Fe is bcc and of Cu is fcc. Fe and Cu are almost immscible around room temperature. Preparation of alloy phases, super-saturated solid solution in this system has been tried by liquid quenching and vapor quenching. The results on the synthesized phases were reviewed in Fig.3.2. By solid quenching, about 1 at% solubilty was obtained[2][3] and Klement reported preparation of 20at% super-saturated solid solubility in both sides by liquid quenching[4]. Moreover, Kneller[5] and Sumiyama[6] reported the larger solubility by thermal evaporation and by sputtering respectively. The attempt of MA for this system was first reported by Benjamin[7] before the discovery of amorphization by MA. In his paper, only fine homogeneous structure formation was briefly mentioned.

3.2 Experimental

The starting powders were 99.9% Cu and 99% Fe powders with the average particle size of about 30 μm and 50 μm respectively. These powders were blended to desired

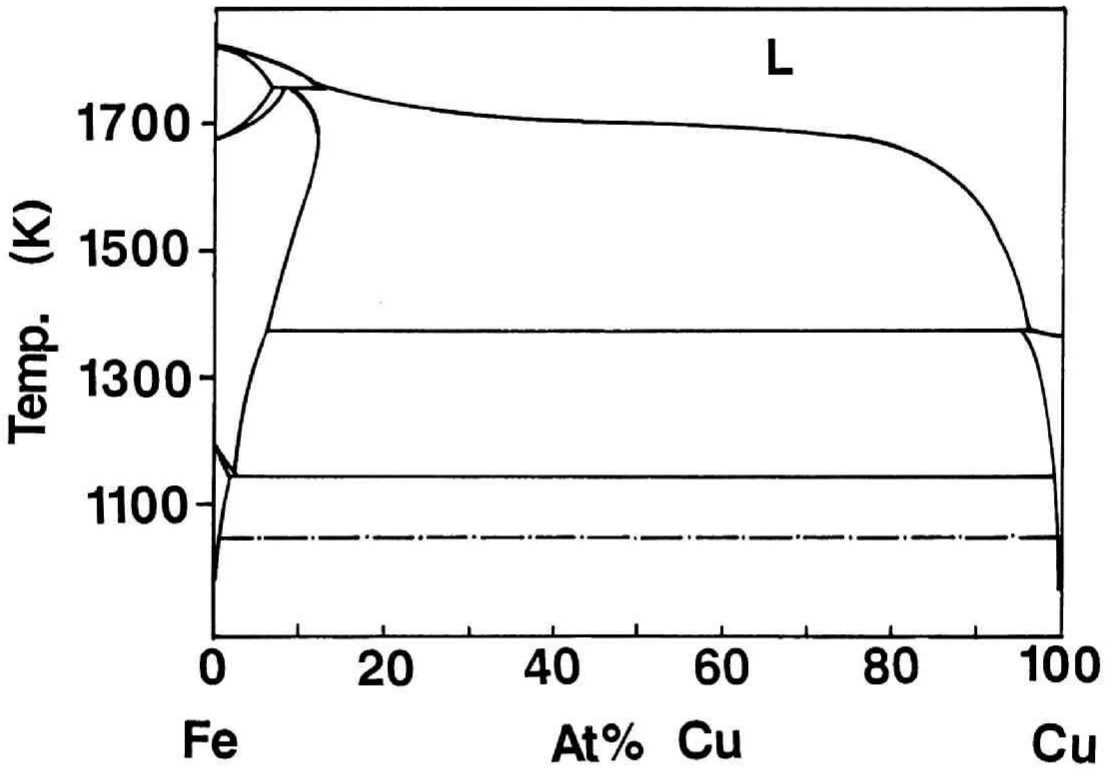

Fig.3.1 Phase diagram for Fe-Cu system[1].

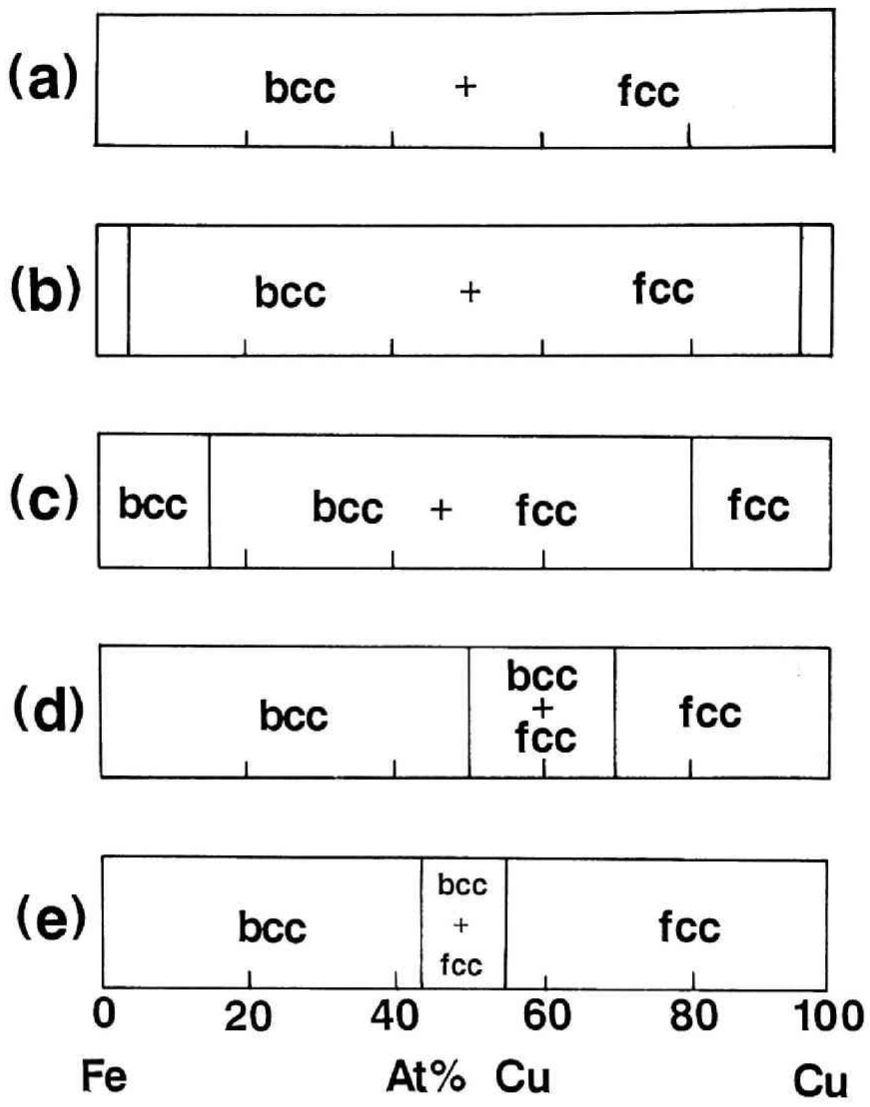

Fig.3.2 Phase obtained in Fe-Cu alloy by various treatments, (a)equilibrium[1],(b)solid quenched [2][3], (c)liquid quenched[4], (d)thermally evaporated[5] and (e)sputter deposited alloys[6].

compositions and sealed in a cylindrical stainless vial with the stainless balls in an argon atmosphere. The weight ratio of the ball to the powder was 80:1. To avoid the adhesion of the powders to the vial and balls, methyl alcohol as a process control agent (PCA) was put in the vial in the amount of about 0.2mass% of the capacity of the vial. The MA powders were characterized by XRD analysis, SEM observation and TEM observation. The thermal stability was examined by DSC.

^{57}Fe Mössbauer transmission measurements were performed at room temperature to examine the changes of the environments around the Fe atom during MA.

The magnetic moments were examined by measuring the magnetization at 77K with a balance magnetometer.

3.3 Results and Discussion

Table 3.1 shows the chemical composition of Fe-Cu alloy powders mechanically alloyed for 400h. Cr and Ni were detected as the contaminants from the stainless vial and balls. However, volume fraction of Fe was nearly the same as the starting one.

The XRD patterns of Fe-30at%Cu and Fe-70at%Cu MA powders for various MA time are shown in Fig.3.3 and Fig.3.4. For the Fe rich alloy, it was found that peaks of fcc Cu became broad with increasing the MA time and finally disappeared and only broad bcc peaks were left in Fig.3.3. For the Cu rich alloy, bcc Fe peaks gradually disappeared and only fcc peaks were finally left as shown in Fig.3.4. In Fig.3.5, the XRD patterns of the mechanically alloyed powder for 400h having various compositions are shown. Alloys up to 30at%Cu were bcc and

Table 3.1 Chemically analyzed composition of Fe-Cu powders mechanically alloyed for 400h.

	Chemically analyzed composition (at%)			
	Fe	Cu	Ni	Cr
Fe-10at%Cu	89.38	10.32	0.11	0.19
Fe-20at%Cu	78.91	20.99	0.05	0.05
Fe-30at%Cu	70.34	29.39	0.10	0.17
Fe-40at%Cu	60.62	38.66	0.24	0.48
Fe-50at%Cu	51.83	46.68	0.50	0.99
Fe-60at%Cu	39.85	60.23	0.01	0.01
Fe-70at%Cu	30.45	69.21	0.13	0.21
Fe-80at%Cu	19.31	79.98	0.23	0.48
Fe-90at%Cu	9.10	90.77	0.05	0.08

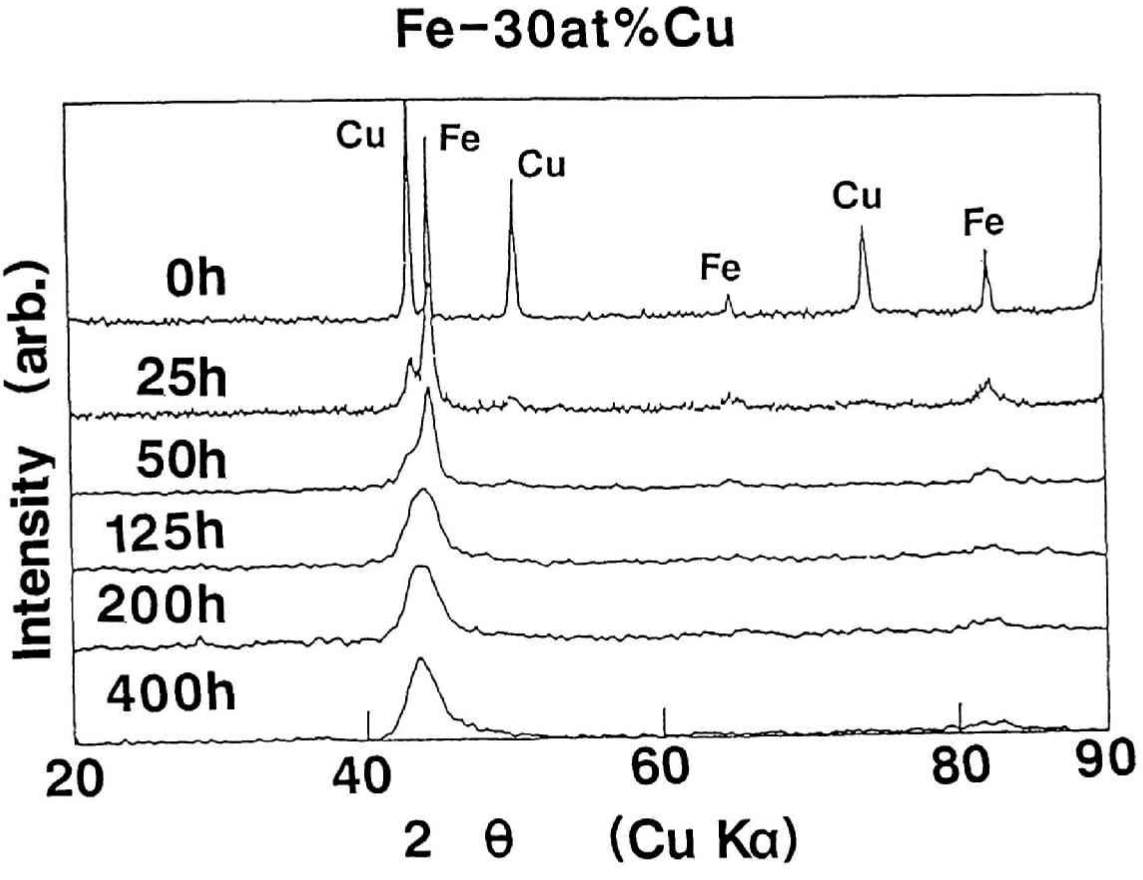

Fig.3.3 Changes of XRD patterns of Fe-30at%Cu MA powders as a function of MA time.

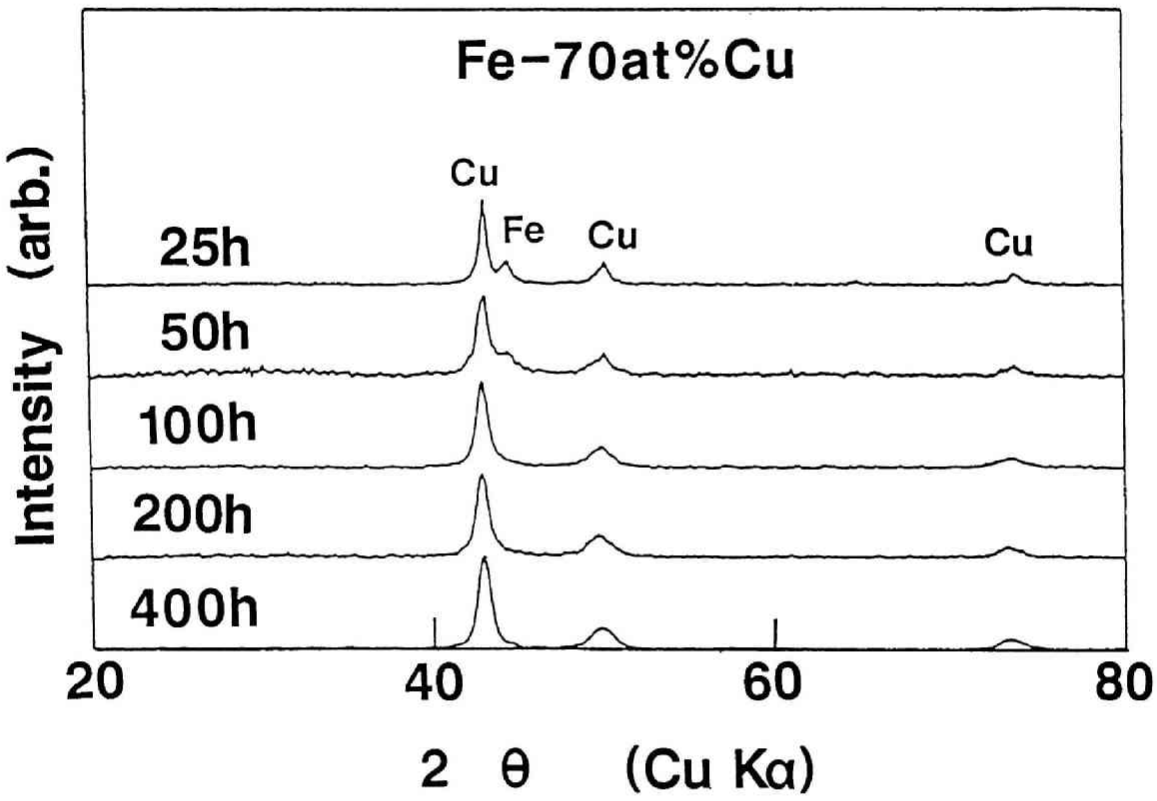

Fig.3.4 Changes of XRD patterns of Fe-70at%Cu MA powders as a function of MA time.

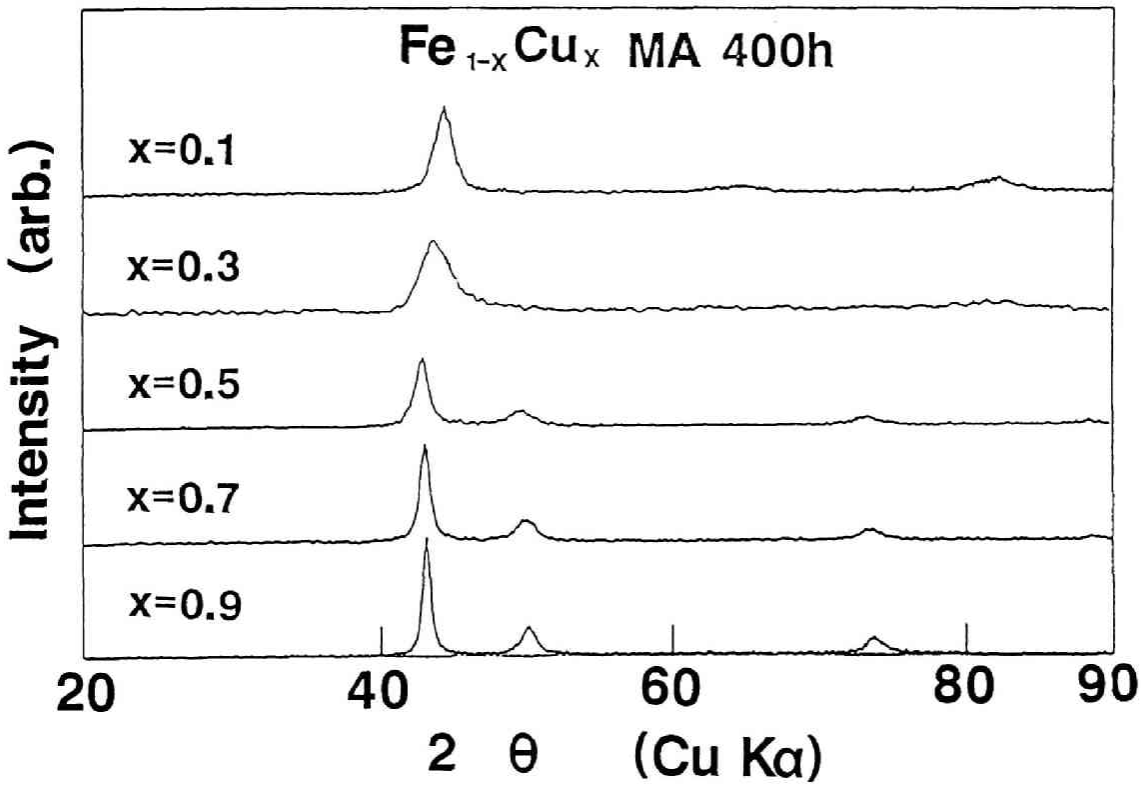

Fig.3.5 XRD pattern of Fe-Cu MA 400h powders having various compositions.

alloys from 40 to 100at%Cu were fcc. As introduced in 2.1, by the other techniques, there was wide composition range where two phases coexisted and the complete solubility could not be obtained. In this work, however, in the any composition two phase coexistence was not found by the XRD analysis. In Fig.3.6, the lattice parameters of the solid solution calculated from (110) of bcc and (220) of fcc phase are shown against the corresponding composition. The lattice parameter of bcc increased with increasing the Cu content. This is similar to the case of rapid quenching and vapor quenching. The lattice parameter of fcc also increased with increasing the Fe content. In the composition from 40 to 70at%Cu, the lattice parameter of fcc produced by MA nearly corresponds to the value extrapolated from the lattice parameter of single fcc phase obtained by rapid quenching. The recent study on MA in this system by Ivanov[8] reported the similar data. From these results, it may be concluded that the non-equilibrium phase forming range was extended by MA.

In Fig.3.7 and 3.8, TEM images of the Fe-30at%Cu and Fe-70at%Cu powders mechanically alloyed for 400h are shown. The structure was fine and homogeneous with the average grain size of about a few nm for Fe-30at%Cu and ten nm for Fe-70at%Cu. This difference of the grain size agreed well with the calculated grain size from the width of the XRD peaks shown in Fig.3.9.

Figure 3.10 shows the DSC curves of the Fe-Cu powders mechanically alloyed for 400h. DSC curves of bcc solid solution from 10 to 30at%Cu showed two exothermal peaks around 580K and

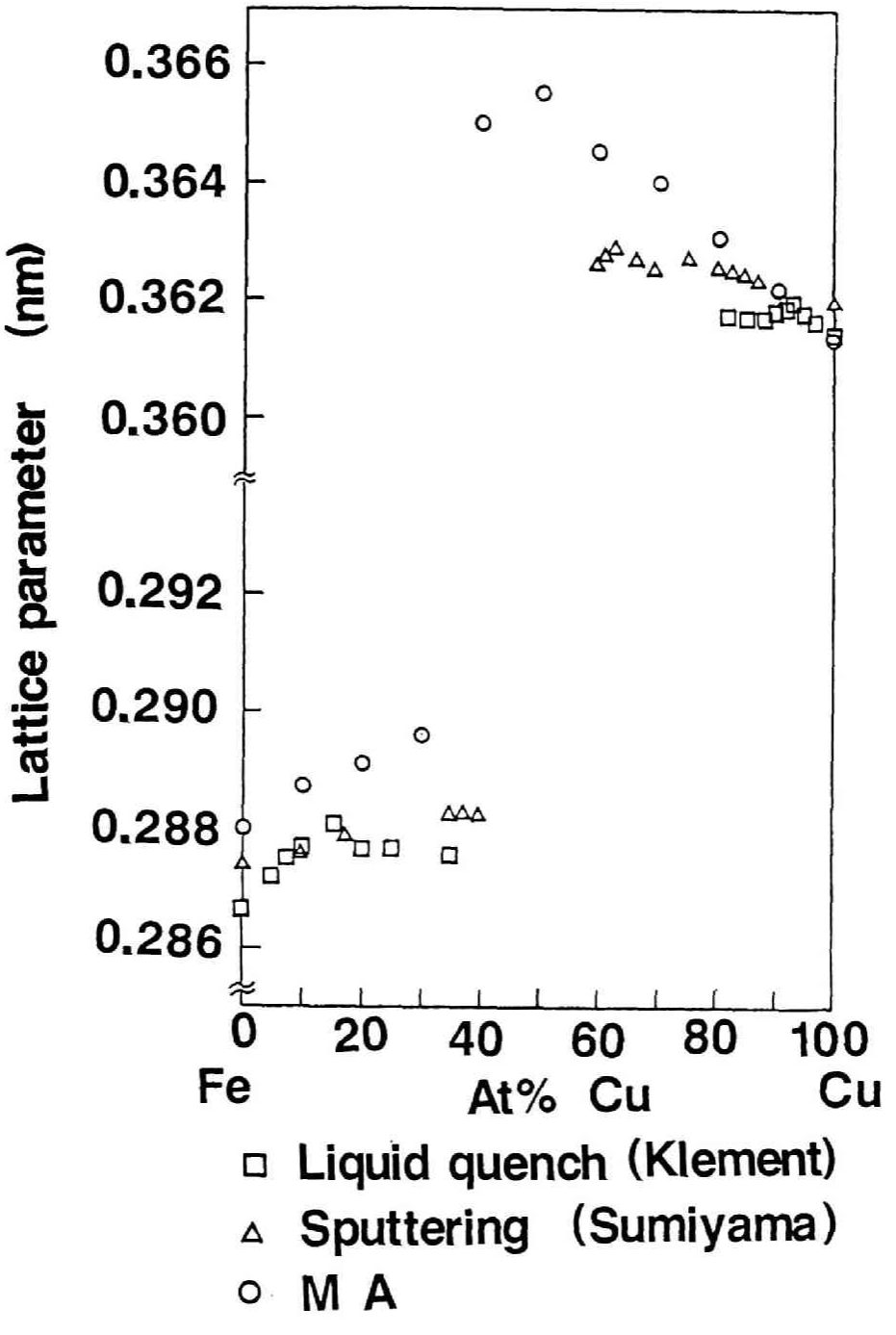

Fig.3.6 The lattice parameter of Fe-Cu alloy produced by MA 400h, liquid quenching[4] and sputtering[6].

Fe-30at%Cu MA 400h

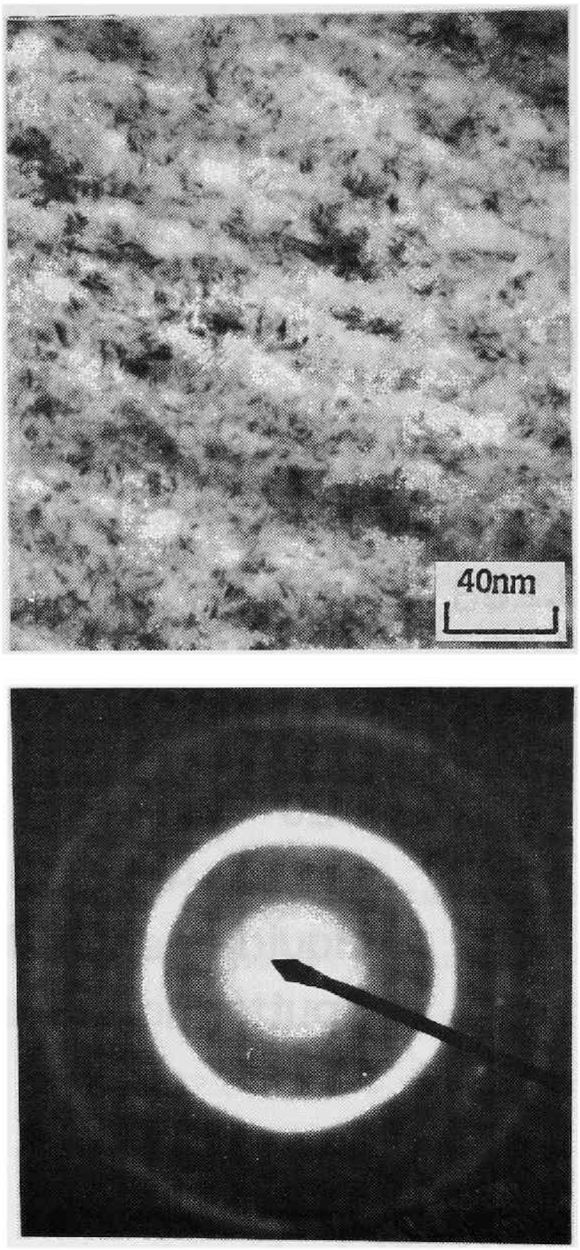

Fig.3.7 TEM images of Fe-30at%Cu powder mechanically alloyed for 400h.

Fe-70at%Cu MA 400h

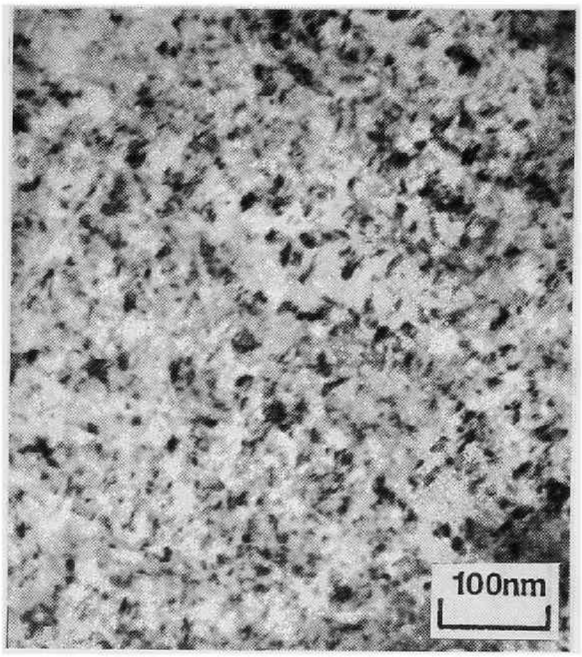

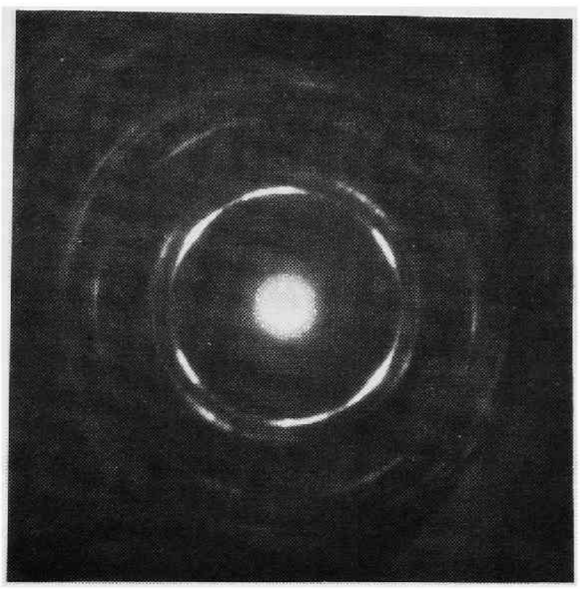

Fig.3.8 TEM images of Fe-70at%Cu powder mechanically alloyed for 400h.

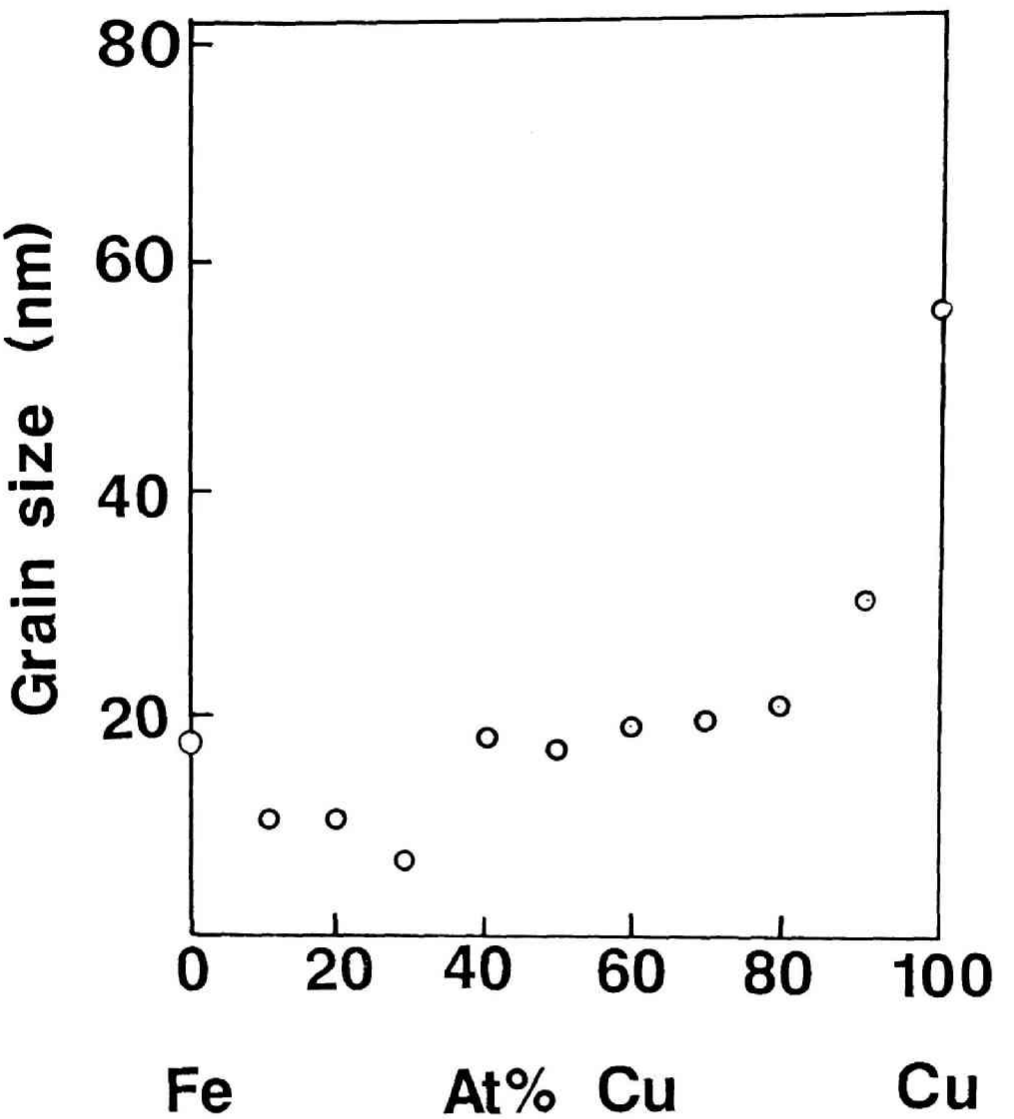

Fig.3.9 Grain size of Fe-Cu MA 400h powders evaluated from Scherrer formula.

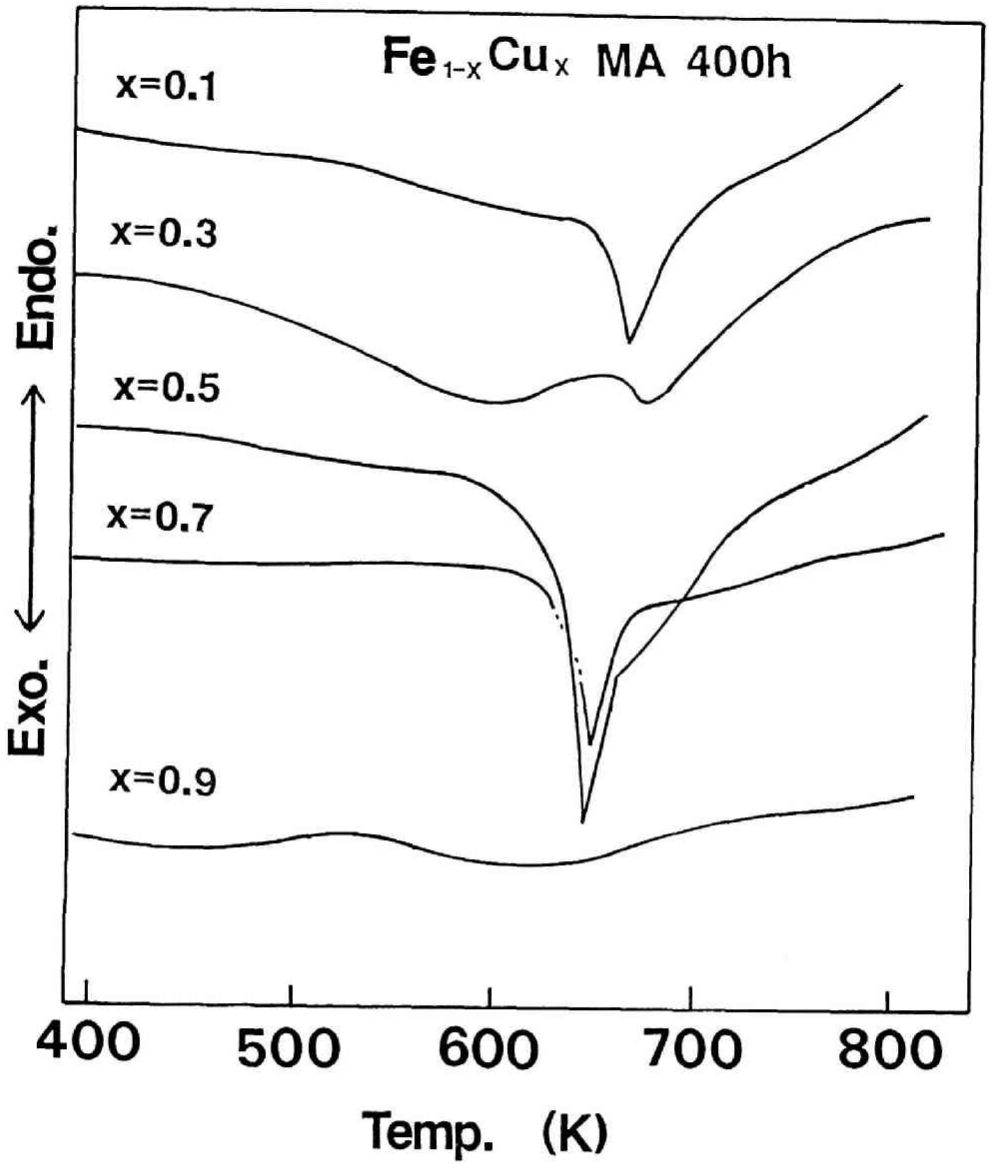

Fig.3.10 DSC curves of Fe-Cu MA 400h powders having various compositions at a heating rate of 20K/min.

around 650K, whose tendency was similar to the case of Ag-Cu system. In the case of the sample which was rich in Cu, the first exothermic peak was very small and the second one lies around 630K. After these peaks, solid solution decomposed to pure Fe and Cu. Figure 3.11 shows the Mössbauer spectra at room temperature of the Fe-30at%Cu powder mechanically alloyed for various time. In the spectra of Fe-30at%Cu, intensity of the sextet of pure ferromagnetic Fe spectrum became broader with increasing the MA time, which indicates that the Fe and Cu were mixed in the atomic level and the environment around the Fe atom changed. In Fe-90at%Cu as shown in Fig.3.12, the sextet of ferromagnetic Fe became smaller with increasing the MA time and new paramagnetic doublet appeared. When Fe was solid solved and was isolated in Cu, the magnetic splitting of Fe to six energy level did not occur due to the magnetic transformation of Fe from ferromagentic to paramagnetic. And the transmission peak exhibits the quadropole splitting due to the existence of the gradient of magnetic field caused by non-cubic symmetric surrounding around Fe. The spectra shows the doublet by the disappearance of magnetic splitting and the quadropole splitting. In the sample mechanically alloyed for 400h, the sextet transmission peaks completely disappeared and only the doublet was left, which showed the alloying in the atomic level was completed by MA. This doublet spectrum was matched well with that of fcc super-saturated solid solution produced by sputtering[9]. Figure 3.13 shows the changes of Mössbauer spectra of Fe-Cu alloy mechanically alloyed for 400h as a

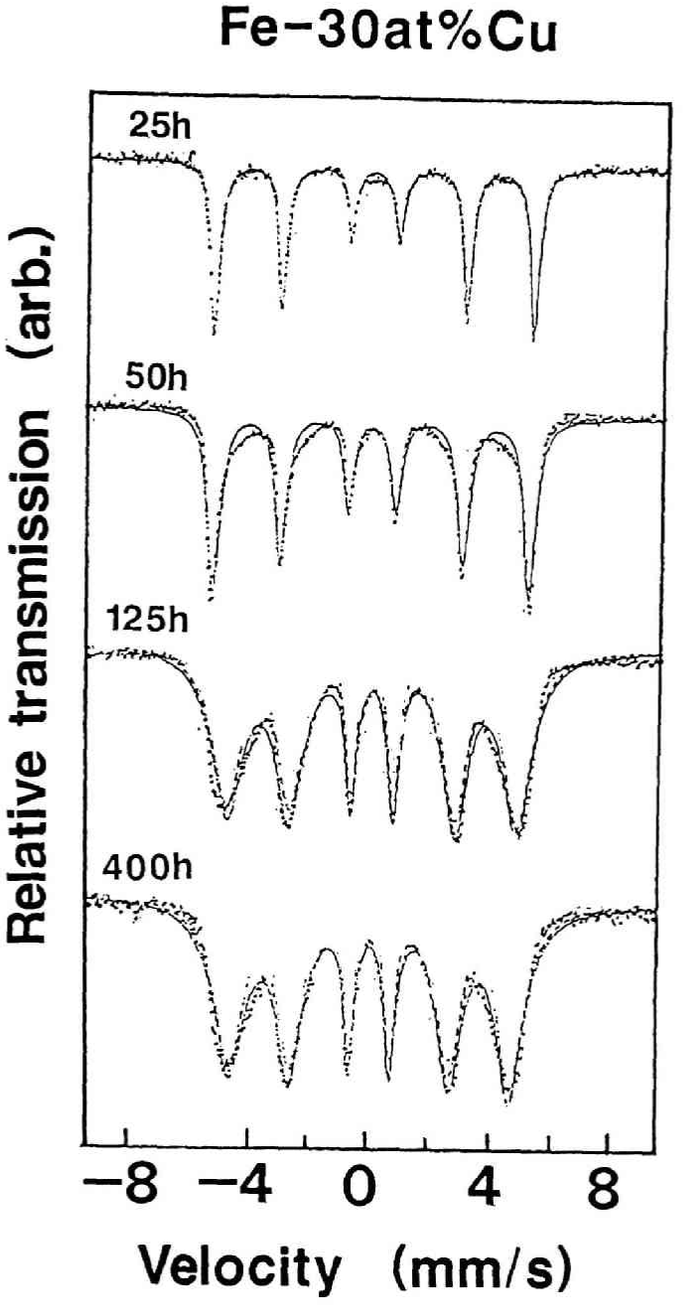

Fig.3.11 Changes of Mossbauer spectra of Fe-30at%Cu powder as a function of MA time.

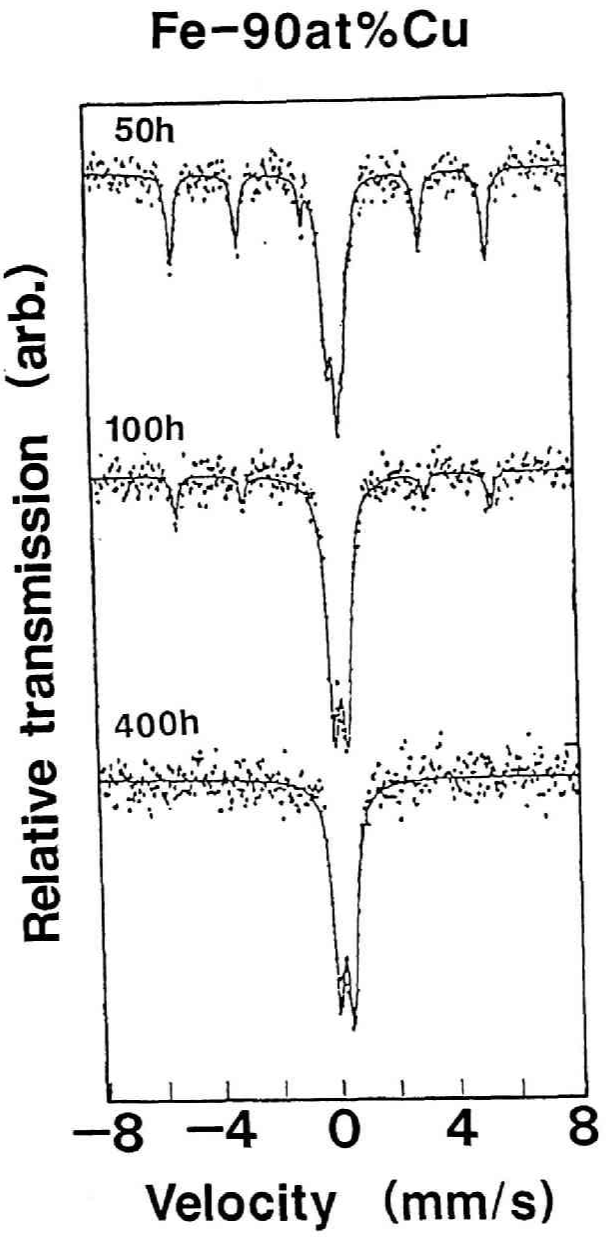

Fig.3.12 Changes of Mossbauer spectra of Fe-90at%Cu powder as a function of MA time.

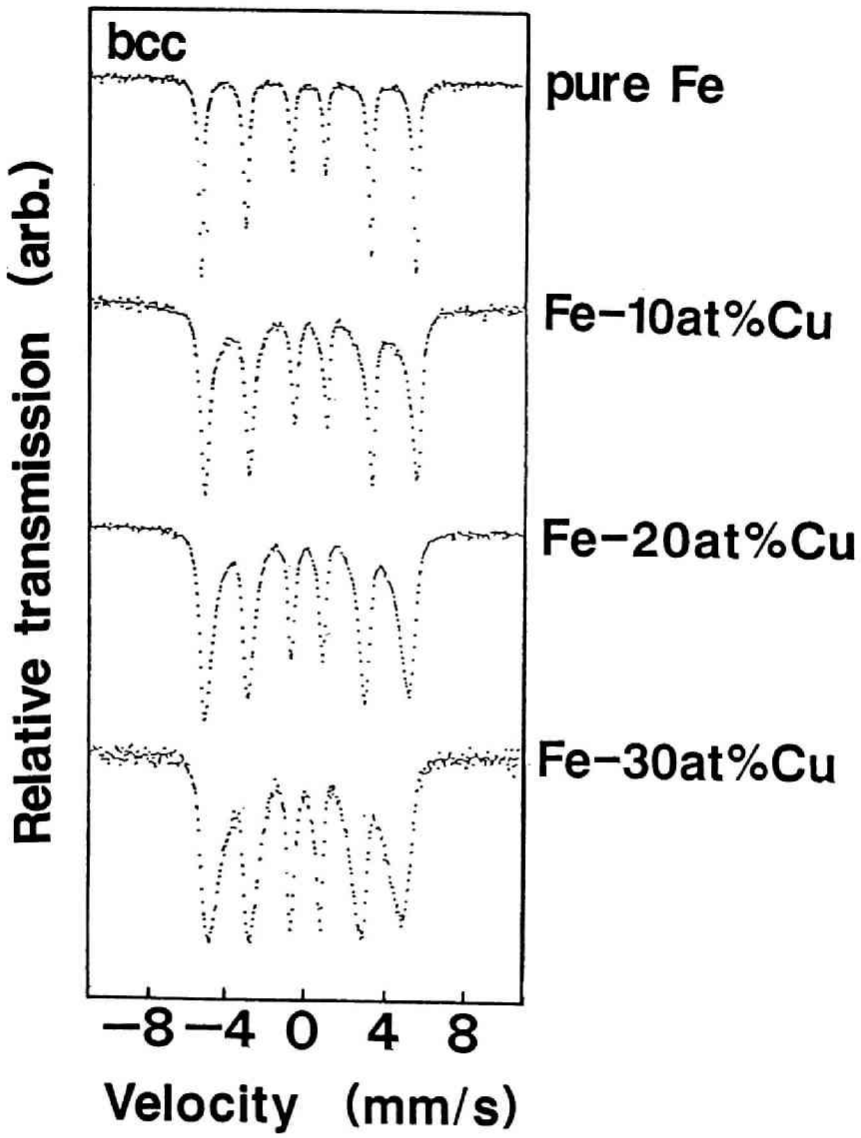

Fig.3.13 Mossbauer spectra of MA 400h Fe-Cu powders having various compositions.
The spectra were divided by the crystal structure of synthesized phases, bcc and fcc.

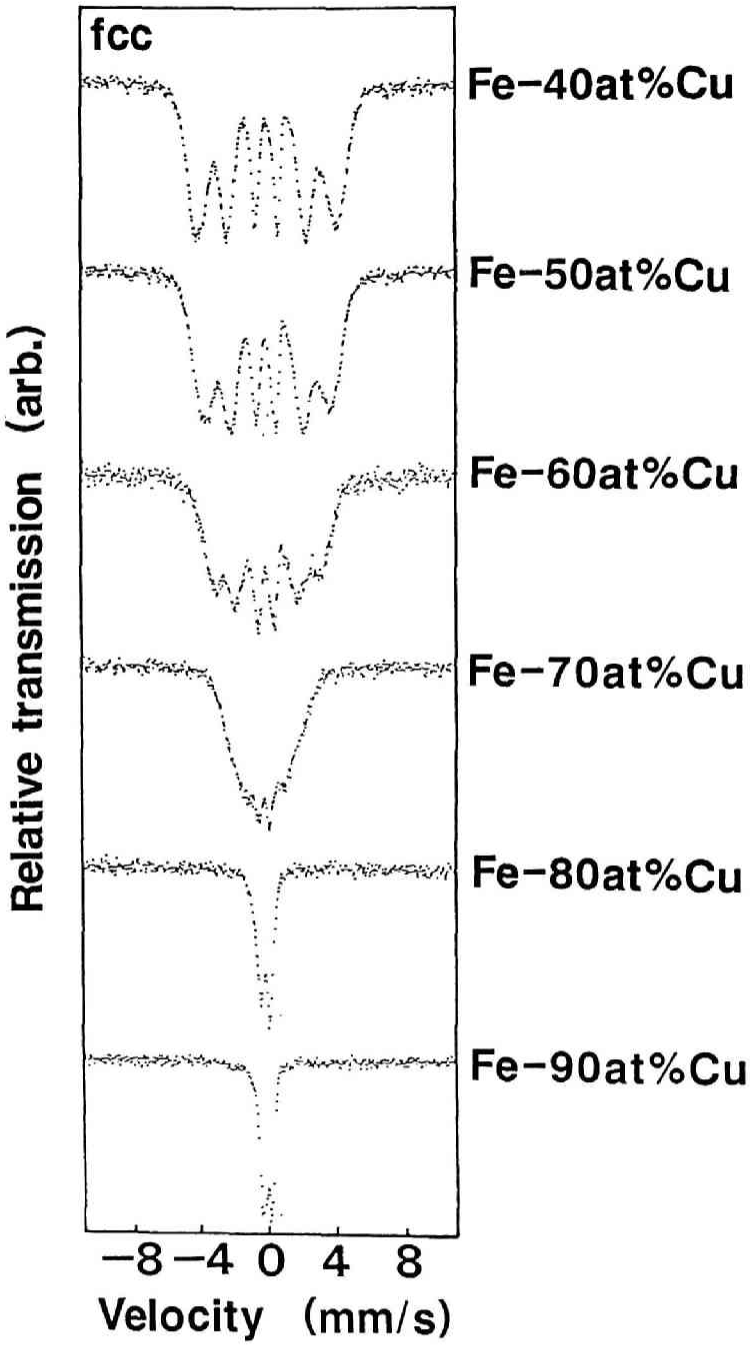

Fig.3.13contd. Mossbauer spectra of Fe-Cu MA 400h powders having various compositions.

function of the composition. Up to 70at%Cu, the spectra were consisted of sextet and above 70at%Cu, the spectra were consisted of doublet. In the ferromagnetic sample with sextet spectra, as the volume fraction of Cu increased the peaks became broad. The distance from the first to sixth peak, which corresponds to the internal magnetization hardly changed in bcc alloys up to 30at% Cu while it was sensitively decreased with the decrease of Fe in fcc alloys from 40 to 90at%Cu. In the two phases, bcc and fcc, coexisting alloy such as Fe-50at%Cu alloy prepared by sputtering, the spectrum exhibited the mixture of ferromagnetic and paramagnetic as shown in Fig.3.14. In all of the samples prepared by MA, however, the spectra were consisted of one component showing that there were no two phase co-exist region.

The magnetic moments per Fe atom, μ_{Fe}, of mechanically alloyed powders of various composition at 77K and sputter deposited films at 4.2K[9] are shown against the composition in Fig.3.15 by assuming that Cu atoms have no magnetic moment. In bcc phases from 0 to 30at%Cu, the magnetic moment showed little changes with the concentration, while that of fcc phase from 40 to 100at%Cu is sensitive to the composition. It is confirmed experimentally and from band theoretical calculation that magnetic moment, μ_{Fe}, becomes larger as increasing the atomic volume and the tendency is more prominent in fcc structure than in bcc structure[10][11]. These data matched well with the Mössbauer analyses. Above results fairly agreed with the results from the sputtered film.

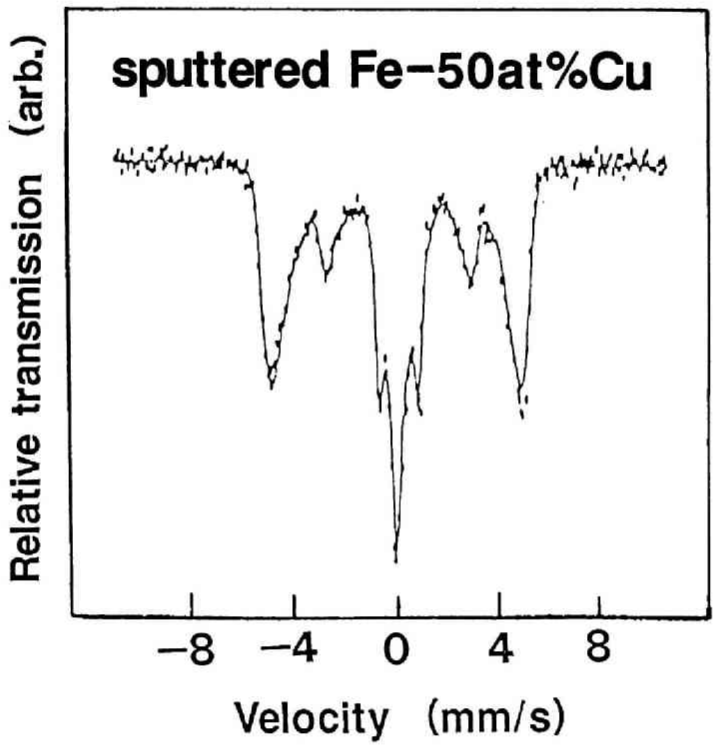

Fig.3.14 Mossbauer spectrum of sputter deposited Fe-50at%Cu alloy[9].

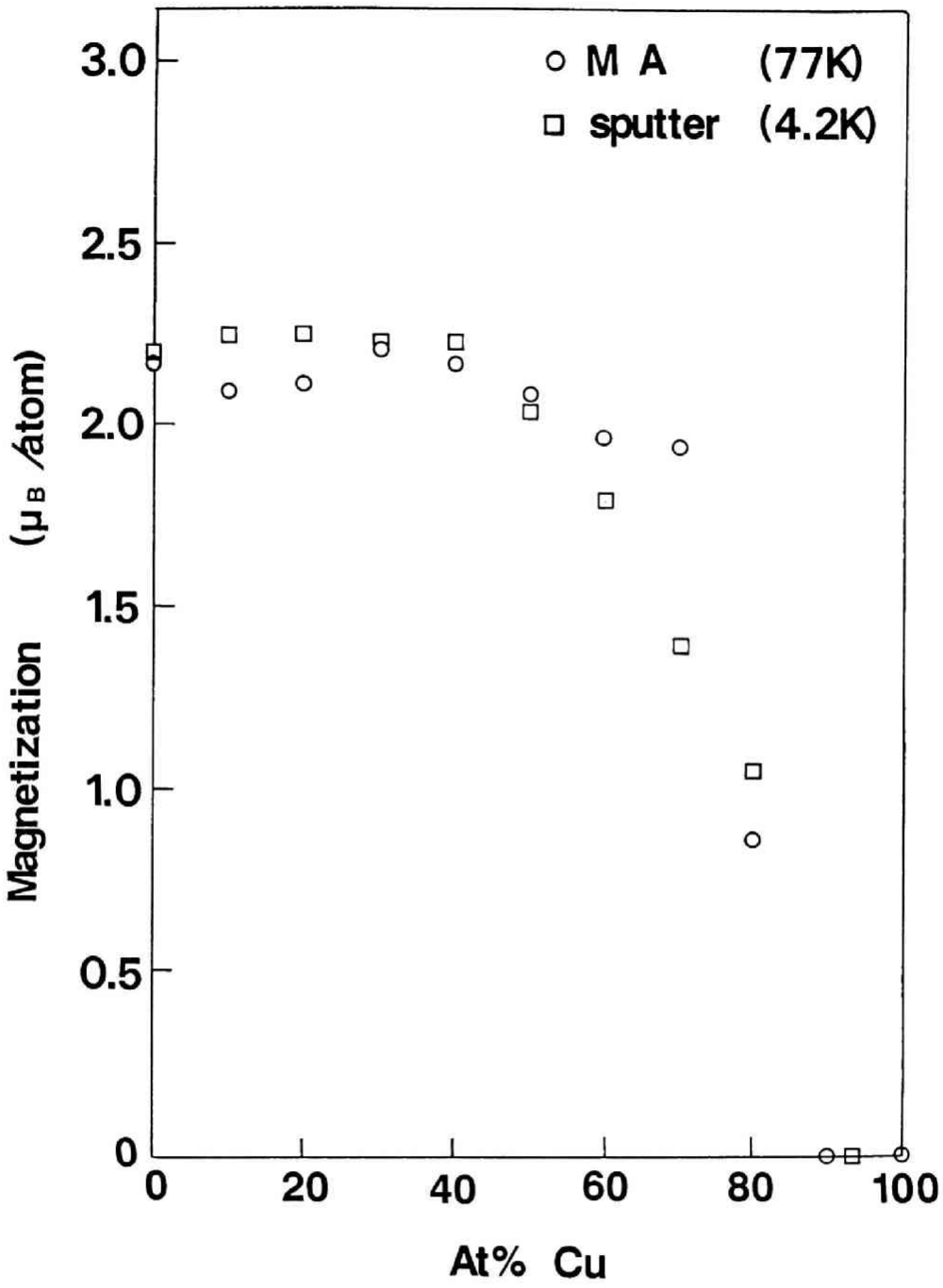

Fig.3.15 Magnetization of Fe-Cu alloy produced by MA 400h and sputtering[9].

3.4 Conclusion

It was confirmed by X-ray diffraction analysis, TEM observation and Mössbauer study that non-equilibrium super-saturated solid solution was formed in entire composition in the Fe-Cu system by MA(Fig.3.16), which has been impossible by the other techniques. Above 700K at a heating rate of 20K/min, the synthesized solid solution decomposed to equilibrium bcc Fe and fcc Cu. The magnetization of mechanically alloyed powder exhibited similar value to that prepared by the sputtering.

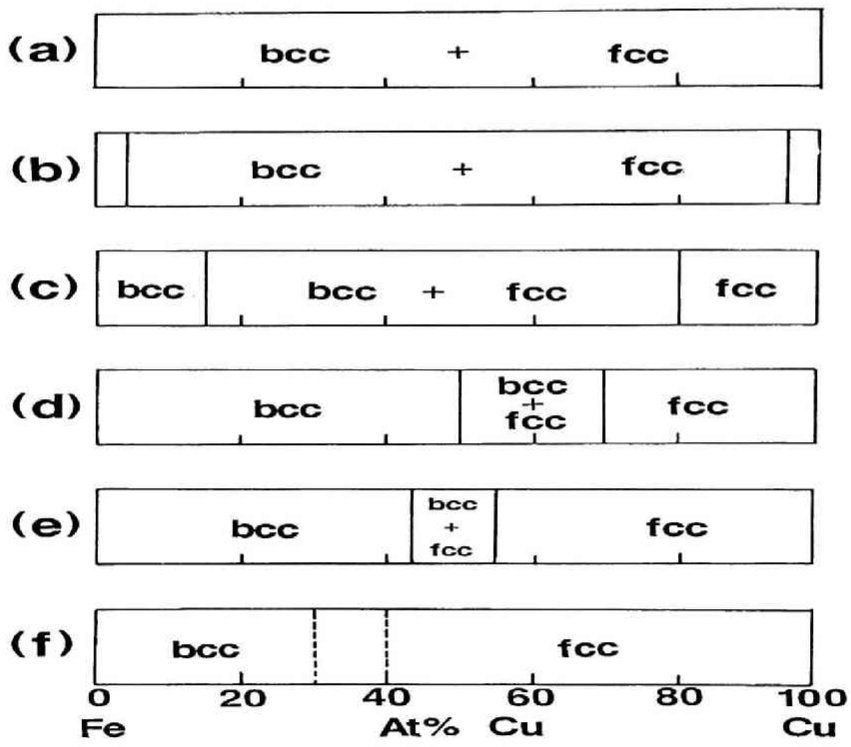

Fig.3.16 Phase obtained in Fe-Cu alloy by various treatments, (a)equilibrium[1], (b)solid quenched [2][3], (c)liquid quenched[4], (d)thermally evaporated[5], (e)sputter deposited alloys[6] and (f)MA.

References

[1] T.M.Massalski; Binary Alloy Phase Diagram, American Society for Metals, New York (1986) 915.

[2] A.T.Aldred; J.Phys.C 1 (1968) 1103.

[3] B.Window; Phil.Mag. 26 (1972) 681.

[4] W.Klement Jr; Trans.Metall.Soc.AIME 233 (1965) 1180.

[5] E.F.Kneller; J.Appl.Phys. 35 (1964) 2210.

[6] K.Sumiyama,T.Yoshitake and Y.Nakamura; Acta Metall. 33 (1985) 1791.

[7] P.S.Jilman and J.S.Benjamin, Ann.Rev.Mater.Sci. 13 (1983), 279

[8] K.Gerasimov, A.Gusev and E.Ivanov; Proc. Int.Sympo. on Mechanical Alloying, Kyoto (1991)

[9] K.Sumiyama, T.Yoshitake and Y.Nakamura; Trans.Jpn. Inst.Met. 26 4 (1985) 217.

[10] O.K.Anderson, J.Madsen, U.K.Poulsen and J.Kollar; Physica 86-88B (1977) 249.

[11] M.Shiga; Solid State Commun. 10 (1972) 1233

Chapter 4

Non-equilibrium Phases Formation in the Fe-Ag-Cu system by Mechanical Alloying

4.1 Introduction

In chapter 3 and 4, the formation of super-saturated solid solution in Ag-Cu and Fe-Cu systems with positive heat of mixing was reported. In the ternary Fe-Ag-Cu system, too, the solid solubilities are very little in the equilibrium state as well as in constituent binary systems. The study on non-equilibrium phase was performed by Sumiyama et al.[1]. According to the report, amorphous as well as super-saturated solid solution were prepared by sputtering on the equiatomic composition range while amorphous was not prepared in the binary system. In this chapter, in addition to these binary systems, the possibility of amorphous formation by MA was examined in this ternary system. MA in the binary Fe-Ag was first examined by Shingu et al.[2][3]. Although Fe and Ag are immiscible even in the liquid state, about 10at% solubility was obtained by MA according to the report. The enhancement of the solubility of Fe and Ag was examined, too, by adding Cu which is completely miscible with Fe and Ag by MA. When Fe and Ag became miscible, it is predicted that the lattice parameter of bcc Fe becomes larger and some change in the property such as the increase of magnetization. In this chapter, the ternary alloy produced by MA is compared with the binary Fe-Cu alloy and the effect of Ag addition is discussed as well.

4.2 Experimental

MA was performed by the same procedure as mentioned in chapter 2 and 3. The mechanically alloyed powders were characterized by XRD analysis and TEM observation. The thermal stabilities were examined by DSC. Mossbauer transmission spectra measurements at room temperature were performed to examine the environments around the Fe atom. Magnetic moments of the MA powders were examined by measuring the magnetization at 77K with a balance magnetometer.

4.3 Results and discussion

The XRD patterns of MA powders were divided into four types, bcc, fcc, fcc+bcc and halo. The representative XRD patterns are shown in Fig.4.1 and changes of the XRD pattern as a function of the composition are shown in Fig.4.2. Within the broken circle, halo patterns as well as crystalline peaks were observed. The tendency of non-equilibrium phase formation was similar to the case by RF sputtering[1] shown in Fig.4.3.

In the Fe rich composition range, such as Fe-10at%Ag-10at%Cu alloy, bcc X-ray diffraction lines were revealed and in the Cu rich composition range such as Fe-10at%Ag-70at%Cu alloy, fcc lines were revealed. In the binary Fe-Cu system, super-saturated bcc solid solutions up to 30at%Cu and fcc solid solutions above 40at%Cu were obtained. In the case of an Fe-10at%Ag-Cu alloy, too, super-saturated bcc solid solutions up to 30at%Cu and fcc solid solutions above 40at%Cu were obtained. In Fig.4.4, the lattice parameters of Fe-Cu and Fe-10at%Ag-Cu alloys were shown against the composition, at% of Fe. The

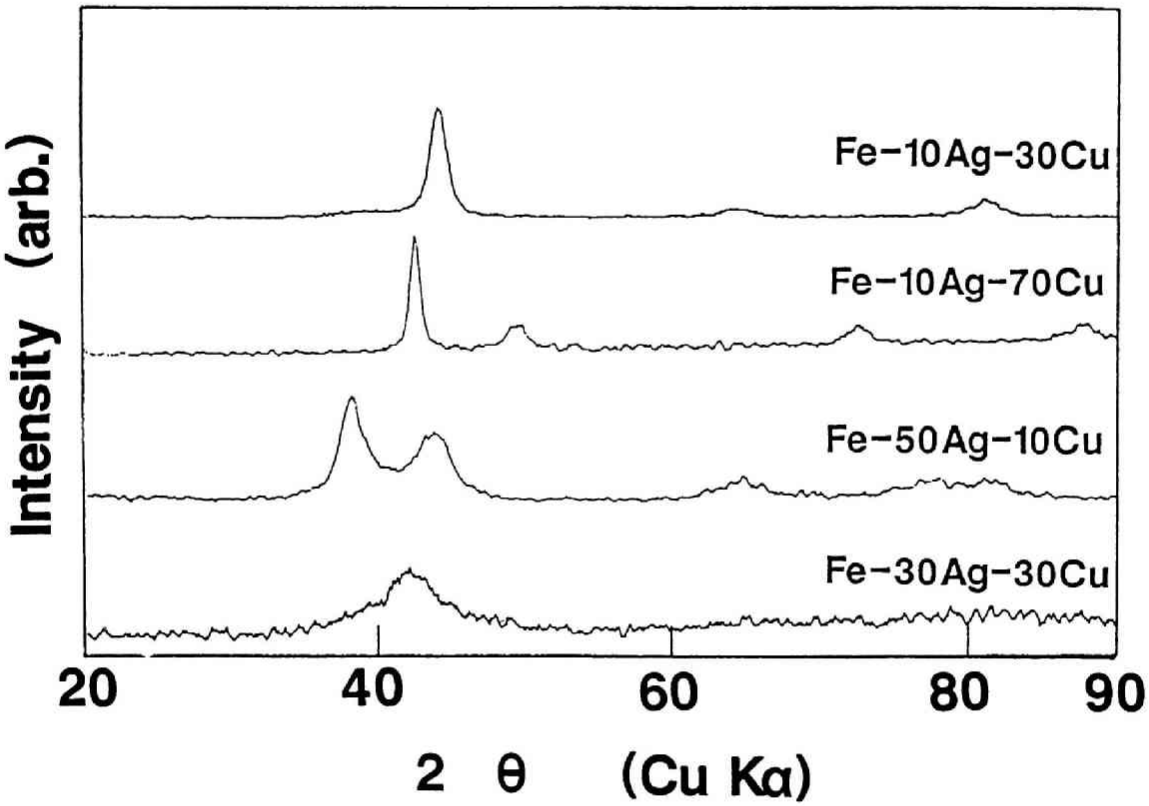

Fig.4.1 XRD patterns of Fe-Ag-Cu MA 400h powders having various compositions.

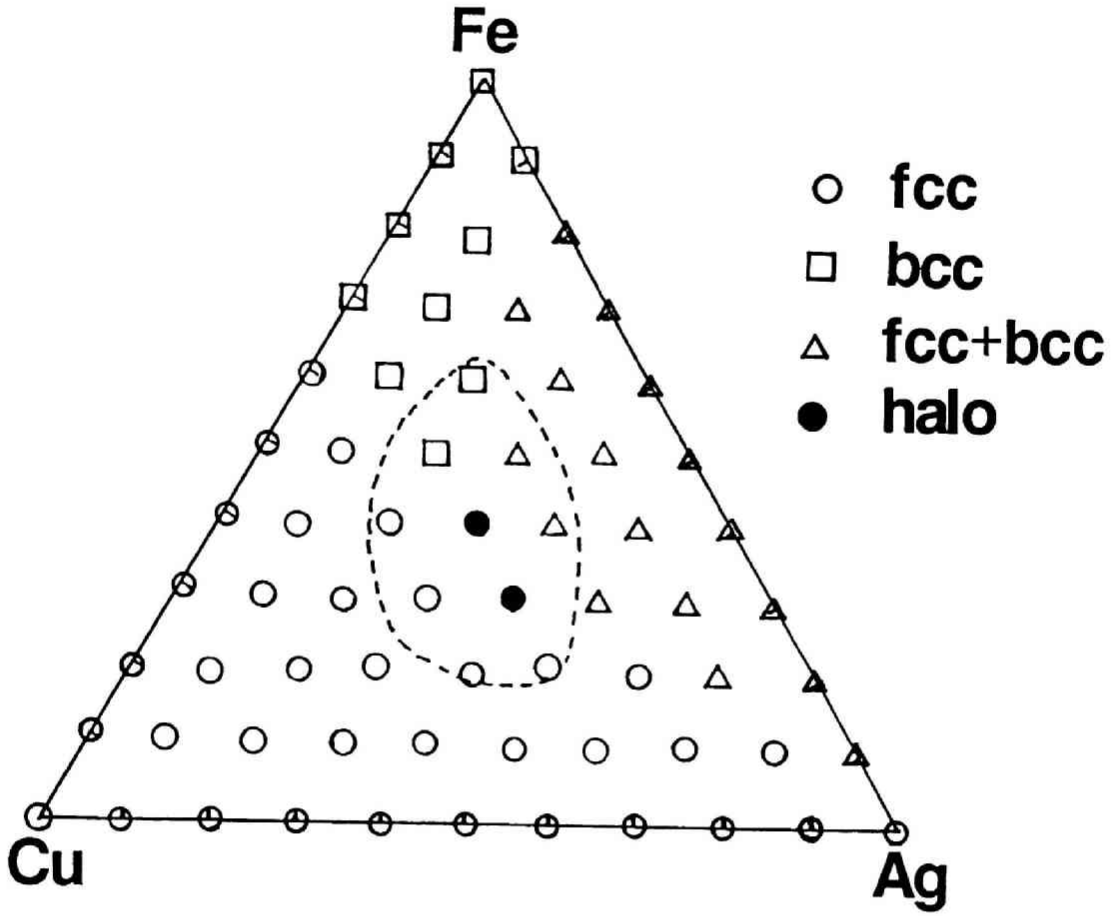

Fig.4.2 Results of XRD analysis of Fe-Ag-Cu alloy produced by MA 400h.

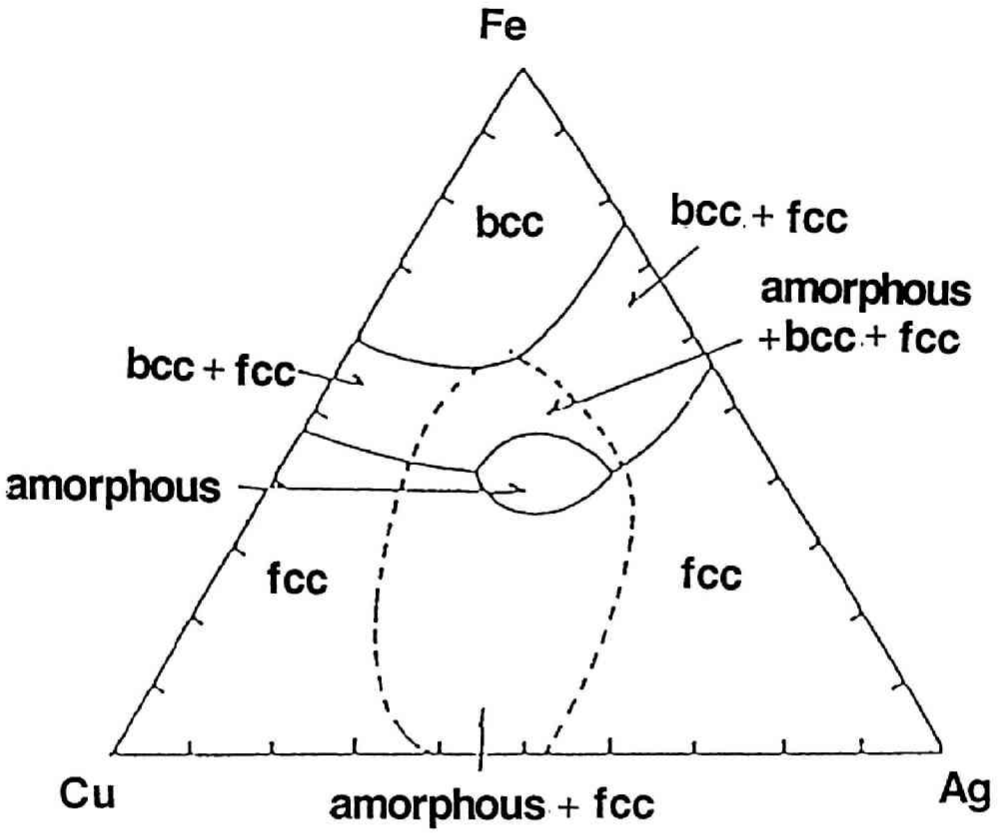

Fig.4.3 Synthesized phases by RF sputtering[1].

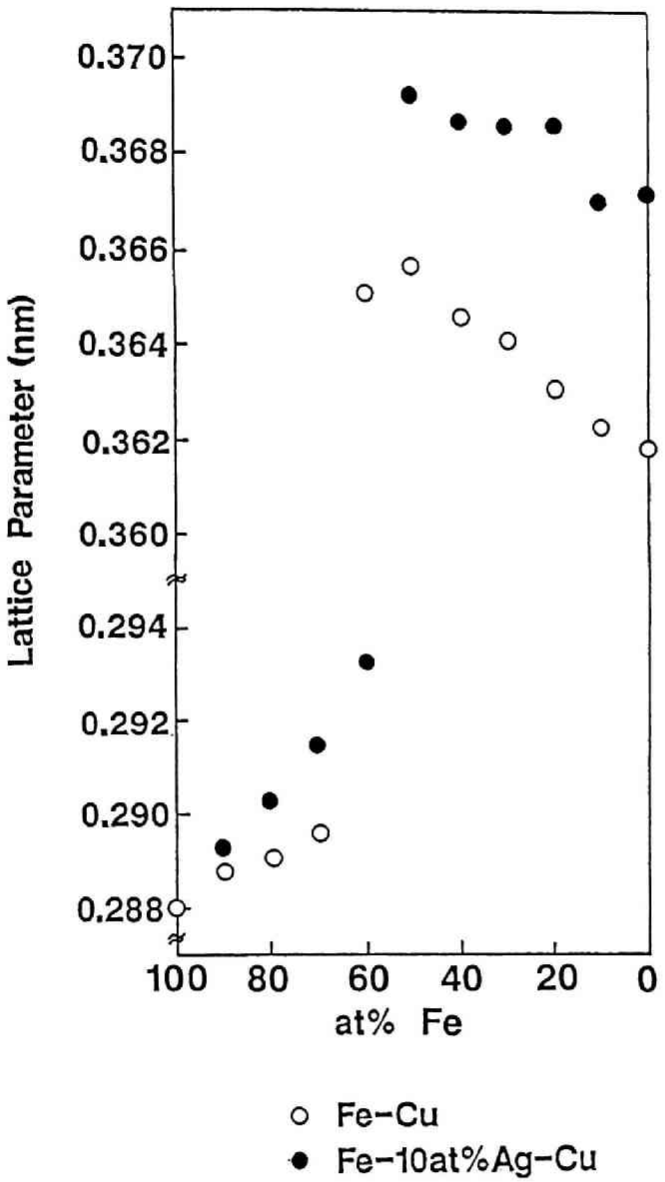

Fig.4.4 Lattice parameter of Fe-Cu and Fe-Ag-Cu alloy produced by MA 400h.

lattice parameter of bcc increased with increasing the Cu content and that of fcc increased with increasing the Fe content. The lattice parameters of Fe-Ag-Cu alloy were larger than those of Fe-Cu alloy. When Fe, Ag and Cu were completely miscible, the lattice parameter became larger by replacing smaller Fe and Cu atoms with larger Ag atoms. While the extended solubilities of Fe and Ag by MA were only about 10at% in the binary Ag-Fe system, Fe and Ag were confirmed to be miscible in the Cu rich composition range. However, in the Cu poor composition range such as Fe-50at%Ag-10at%Cu, the XRD pattern revealed the two phases, bcc and fcc, lines. As the peak position of bcc (110) and fcc (200) was nearly the same, although the detected peak position corresponded to fcc line, the relative intensity of the peak from (200) was larger.

Mössbauer spectra of mechanically alloyed Fe-Ag-Cu alloys are shown in Fig.4.5. The sextet of ferromagnetic Fe became broader in an Fe-10at%Ag-30at%Cu alloy than that of pure Fe, and in an Fe-10at%Ag-70at%Cu alloy the sextet of ferromagnetic Fe completely disappeared and new doublet of paramagnetic Fe appeared, which shows the complete solid solution formation. However, in an Fe-30at%Ag-10at%Cu and Fe-70at%Ag-10at%Cu alloy which were rich in Ag compared with the Cu content, the changes of the Mössbauer spectra were slight in comparison with the case of the Cu rich alloy. Especially in an Fe-70at%Ag-10at%Cu alloy, the sextet of ferromagnetic Fe were left although sputter deposited single-fcc Fe-71at%Ag alloy was reported to show paramagnetic doublet[4]. These results indicate that Fe and Ag were not completely miscible in the Cu poor composition

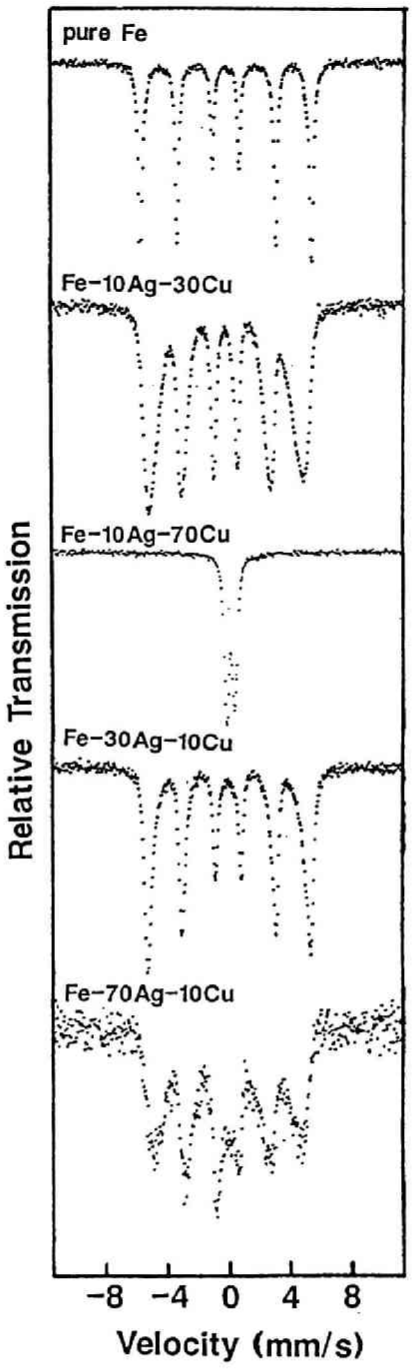

Fig.4.5 Mossbauer spectra of Fe-Ag-Cu MA 400h alloy having various compositions.

range.

In the equi-atomic composition range such as Fe-30at%Ag-30at%Cu, the XRD pattern in Fig.4.1 revealed halo pattern, whose tendency was similar to the case of the formation of amorphous phase by RF sputtering[1], so this halo diffraction pattern may suggest the formation of amorphous phase. In Fig.4.6,the calculated grain size of Fe-Ag-30at%Cu MA powder are shown. The grain size of bcc was smaller than that of fcc alloy which tendency was the same as Fe-Cu alloy and around the equi-atomic composition range, the grain size discontinuously decreased. However, as shown in Fig.4.7, DSC curves did not show the sharp exothermal peak in crystallization while the sharp exothermal peak due to the crystallization was observed in the sputter deposited amorphous Fe-30at%Ag-30at%Cu alloy.

In Fig.4.8, many crystallites and no amorphous region were observed by TEM observation although the grains of crystallite were a few nm fine in size while the electron diffraction pattern revealed halo pattern as well as the XRD pattern. The peak broadening is considered mainly due to the fine grain size. However, as seen in the XRD pattern, small shoulder peak was observed around 40 in 2θ and the halo was asymmetric. Moreover, as shown in Fig.4.9, the Mössbauer spectra of the MA powder considerably differed from sputtered deposited amorphous alloy. So the synthesized phase were considered not to be single phase but two phases, bcc and fcc with similar composition as Fe-30at%Ag-30at%Cu and the peak broadening was due to the two phases coexistence as well as due to the fine

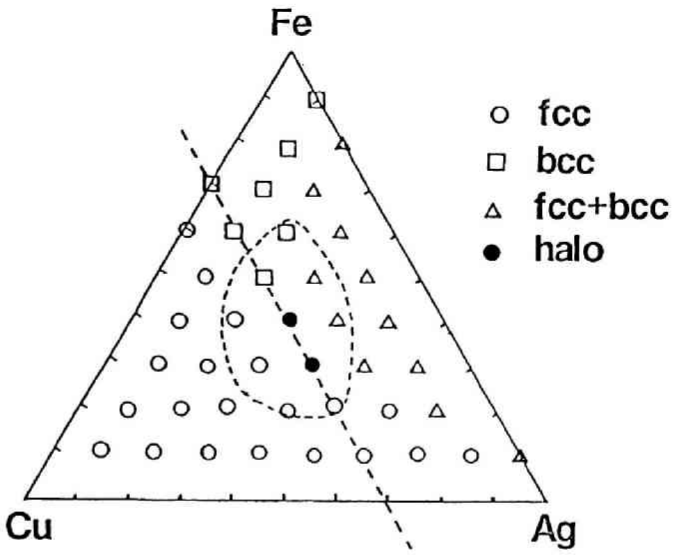

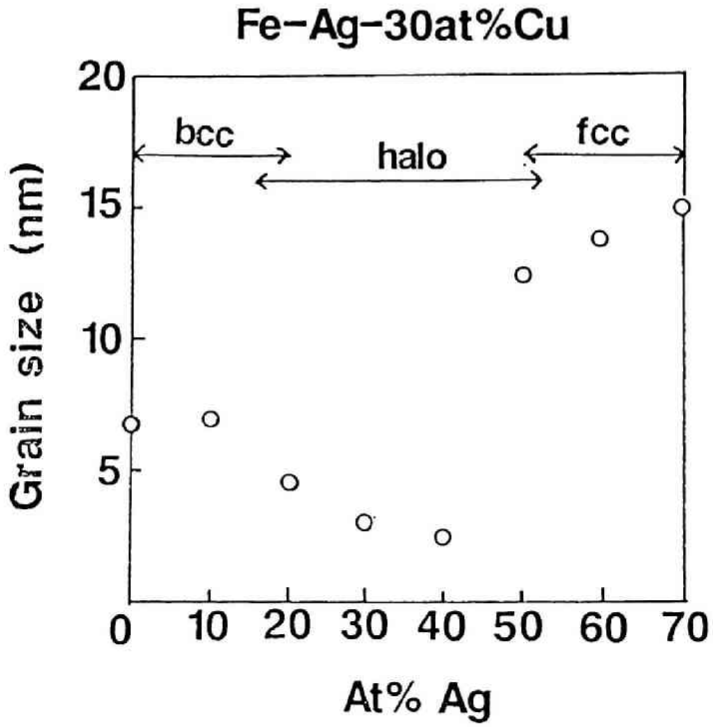

Fig.4.6 Grain size of MA 400h Fe-Ag-30at%Cu alloy evaluated from Scherrer formula.

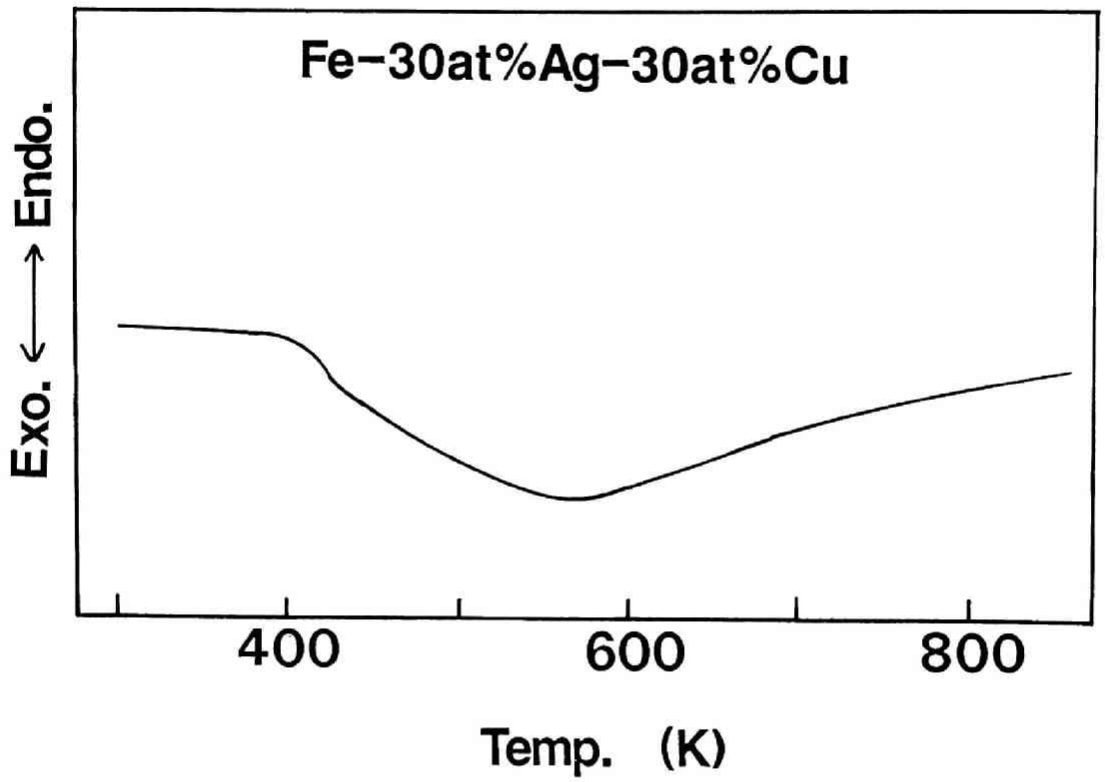

Fig.4.7 DSC curves of Fe-30at%Ag-30at%Cu powder mechanically alloyed for 400h at a heating rate of 20K/min.

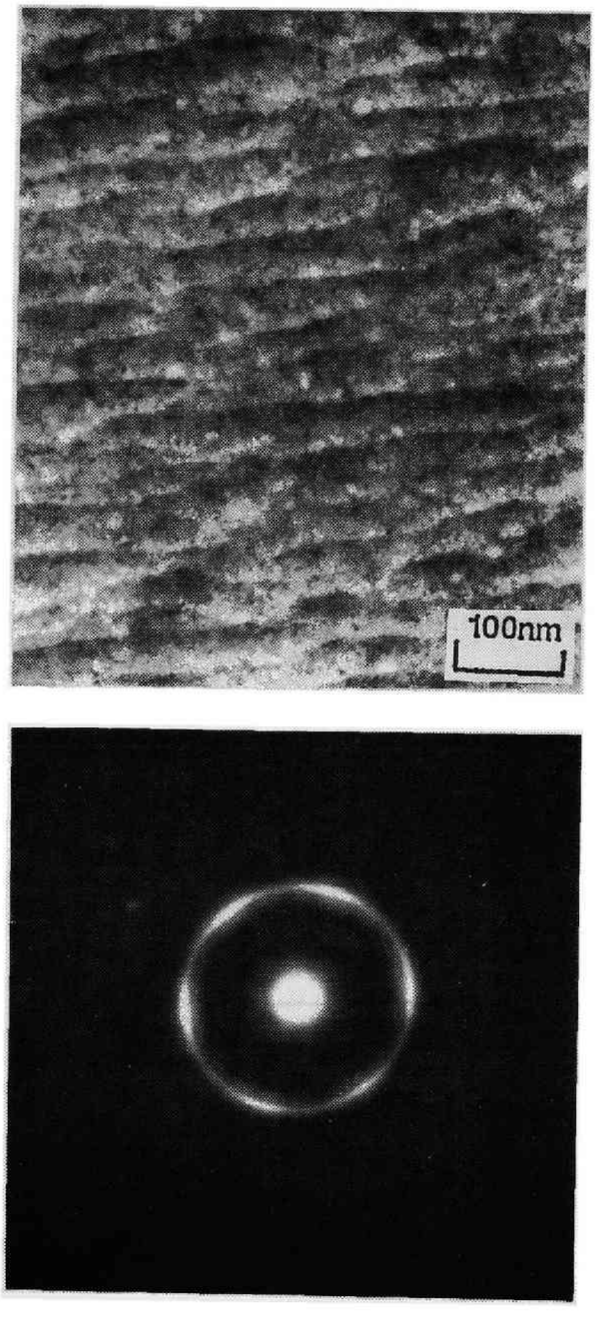

Fig.4.8 TEM images of Fe-30at%Ag-30at%Cu powder mechanically alloyed for 400h.

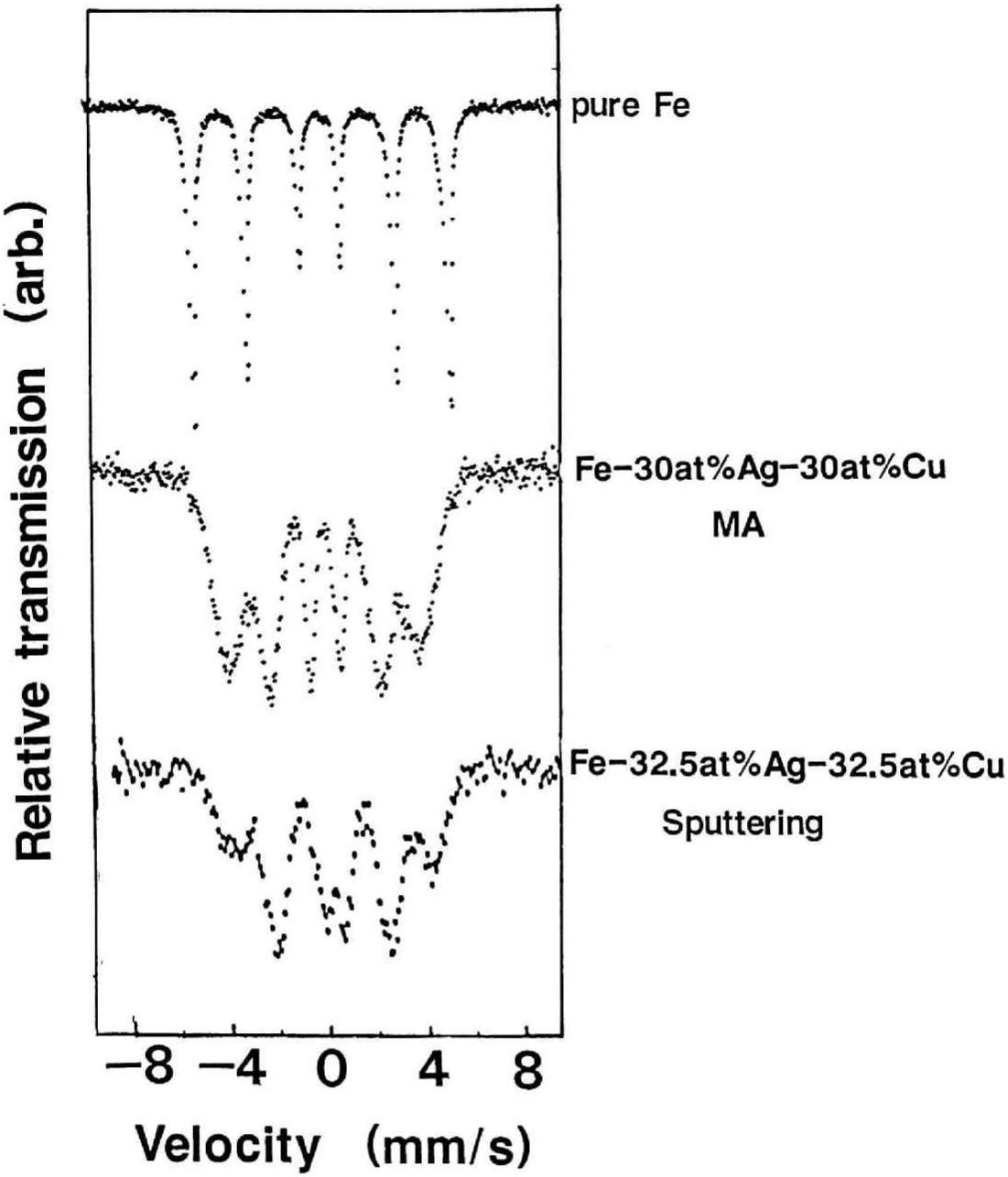

Fig.4.9 Mossbauer spectra of pur Fe, MA 400h Fe-30at%Ag-30at%Cu and sputter deposited Fe-32.5at%Ag-32.5at%Cu alloy.

grain size. In Fig.4.10, the magnetic moment, μ_{Fe}, at 77K assuming Ag and Cu have no magnetic moments was shown for Fe-10at%Ag-Cu and Fe-Cu alloys. The magnetic moment of Fe-Ag-Cu alloys was larger than that of Fe-Cu alloys especially in the case of 20at%Fe, Fe-10at%Ag-70at%Cu and Fe-80at%Cu. Generally, it is known that the lattice expansion of Fe induces the increase of the magnetic moment especially in fcc alloy[5] and this result corresponded to the results on the expansion of lattice parameter shown in Fig.4.4. The magnetic moments exhibited the maximum value, $2.4\mu_B$, which was larger than that of pure Fe in an Fe-10at%Ag-30at%Cu alloy. In the sputter deposited alloy, the magnetic moments exhibited the maximum value was about $2.7\mu_B$ on the composition of Fe-60at%Ag, in which composition the single phase super-saturated solid solution was not obtained by MA.

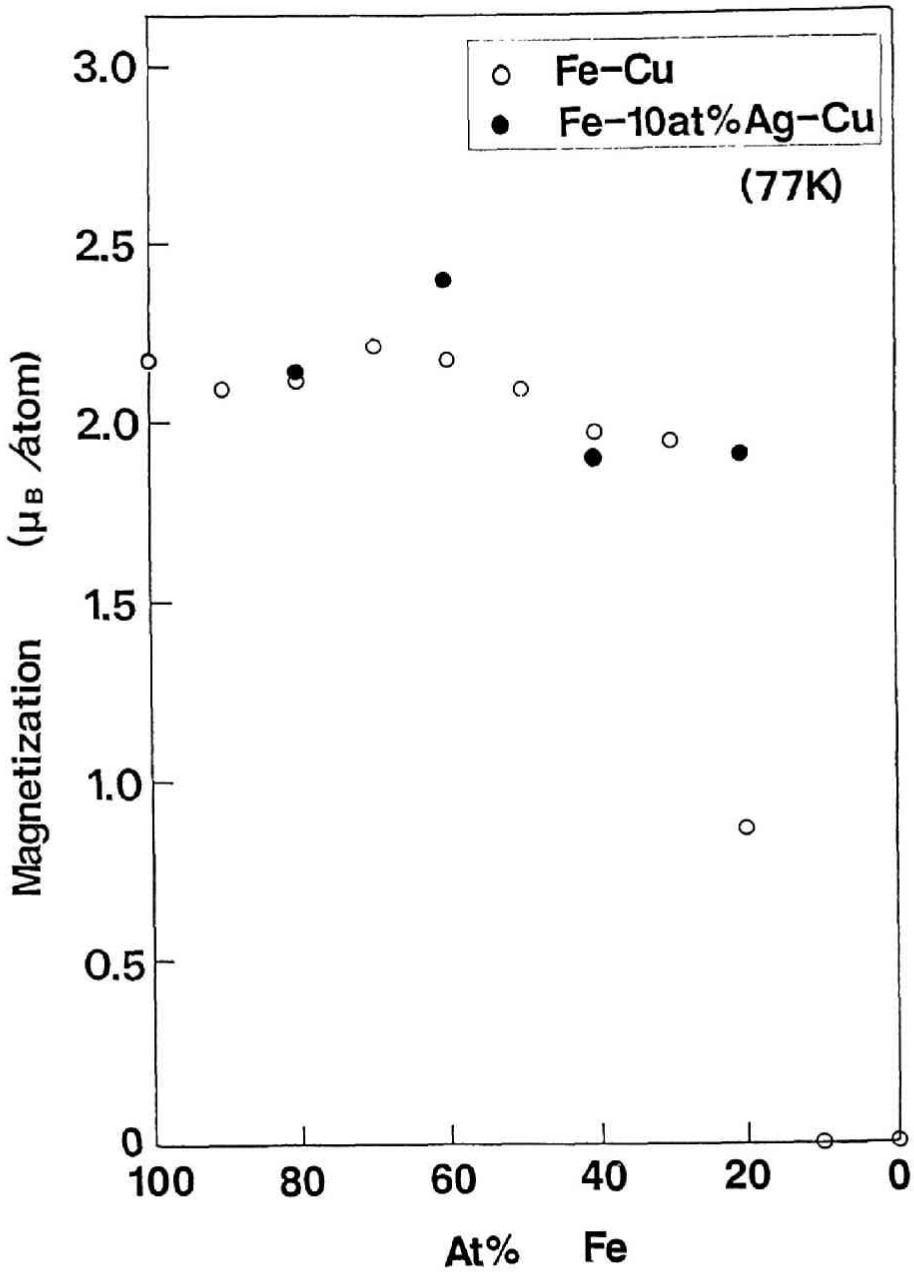

Fig.4.10 Magnetization at 77K of Fe-Cu and Fe-10at%Ag-Cu alloy produced by MA for 400h.

4.4 conclusion

In the ternary Fe-Ag-Cu alloy system, the super-saturated solid solution was obtained in wide composition range. The synthesized phases by mechanical alloying of elemental powders are shown in Fig. 4.9. Except in the Cu poor composition range, complete bcc or fcc super-saturated solubility was confirmed. In the intermediate composition range, the XRD pattern revealed halo pattern, but by TEM observation the alloy was found to be not an amorphous and to be consisted of fine crystallite with the average grain size of a few nm.

By adding Ag in Fe-Cu alloy, the magnetic moment increased due to the lattice expansion and in an Fe-10at%Ag-30at%Cu alloy, it became larger than that of pure Fe due to the expansion.

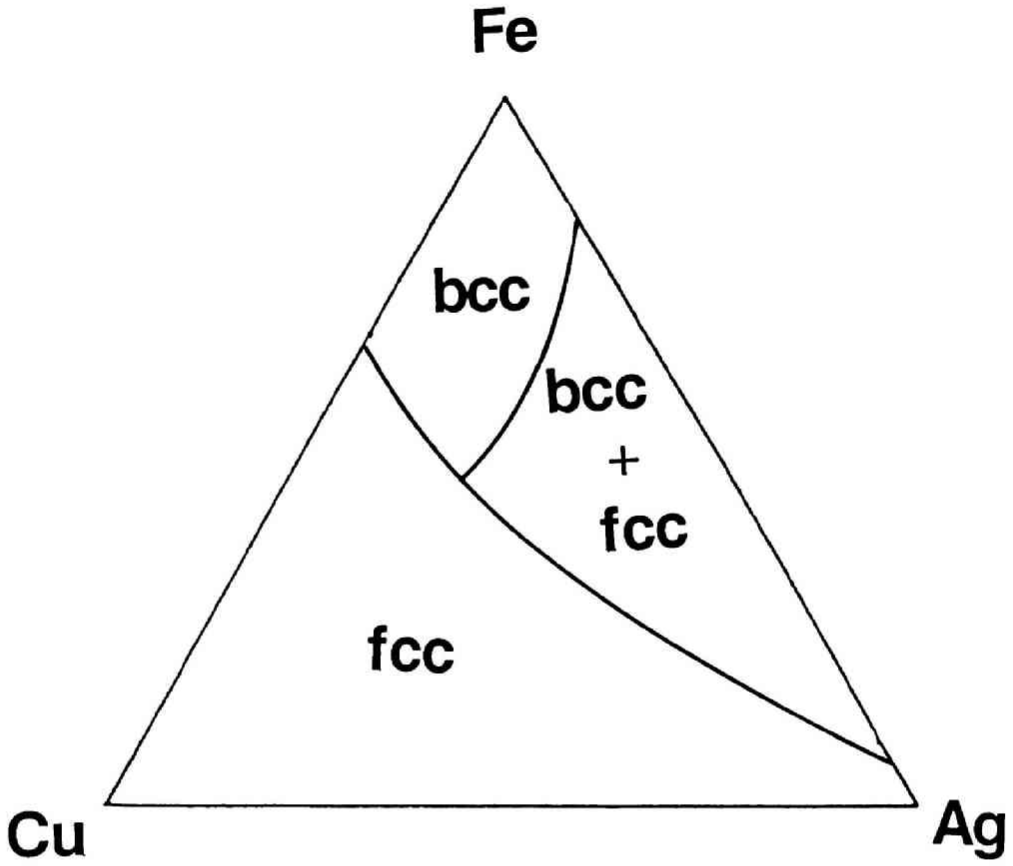

Fig.4.11 Synthesized phases by MA 400h.

References

[1] K.Sumiyama, Y.Kawawake and Y.Nakamura, phys.stat.sol.(a) 96 (1986), K107.

[2] P.H.Shingu, B.Huang, J.Kuyama, K.N.Ishihara and S.Nasu; Proc.DGM Conf. on New Material by MA Techniques, Claw-Hirsaw (1988) 319.

[3] J.Kuyama, H.Inui, S.Imaoka, S.Nasu, K.N.Ishihara and P.H.Shingu; Jpn.J.Appl.Phys.2 6 (1991)

[4] K.Sumiyama and Y.Nakamura; Proc. 5th Int. Conf. on Rapidly Quenched Metals (1985) 859.

[5] O.K.Andersen, J.Madsen, U.K.Poulsen and J.Kollar, Physica B 86-88 (1977) 249.

Chapter 5

Formation of non-equilibrium phases by repeated rolling

5.1 Introduction

In the previous chapters, formation of non-equilibrium phases was reported in the alloy systems with positive heat of mixing by conventional ball milling. It was recognized that the powders subjected to ball milling became fine and homogeneous by repeated fracturing and welding. However, the ball milling process is not clear because of its complex fracturing mechanism. In the present chapter, mechanical alloying by repeated rolling was performed. MA by repeated rolling was previously studied by Atzmon[1] and Huang[2]. According to their reports, amorphous was successfully prepared by repeated rolling. However, the examined alloy system was restricted to the alloy system with negative heat of mixing. In this chapter, repeated rolling was performed to prepare non-equilibrium phase in the Ag-Cu and Fe-Cu systems with positive heat of mixing and the synthesized alloy was compared with that synthesized by ball milling.

5.2 Experimental

The schematic process of the repeated rolling method was shown in Fig.5.1. The starting elemental powders were the same as in case of ball milling. The powders, previously blended to desired compositions, were packed in a stainless tube with 20mmOD and 18mmID. The stainless tube with the sample powder was cold pressed to a thickness of 8mm by a hydraulic press for

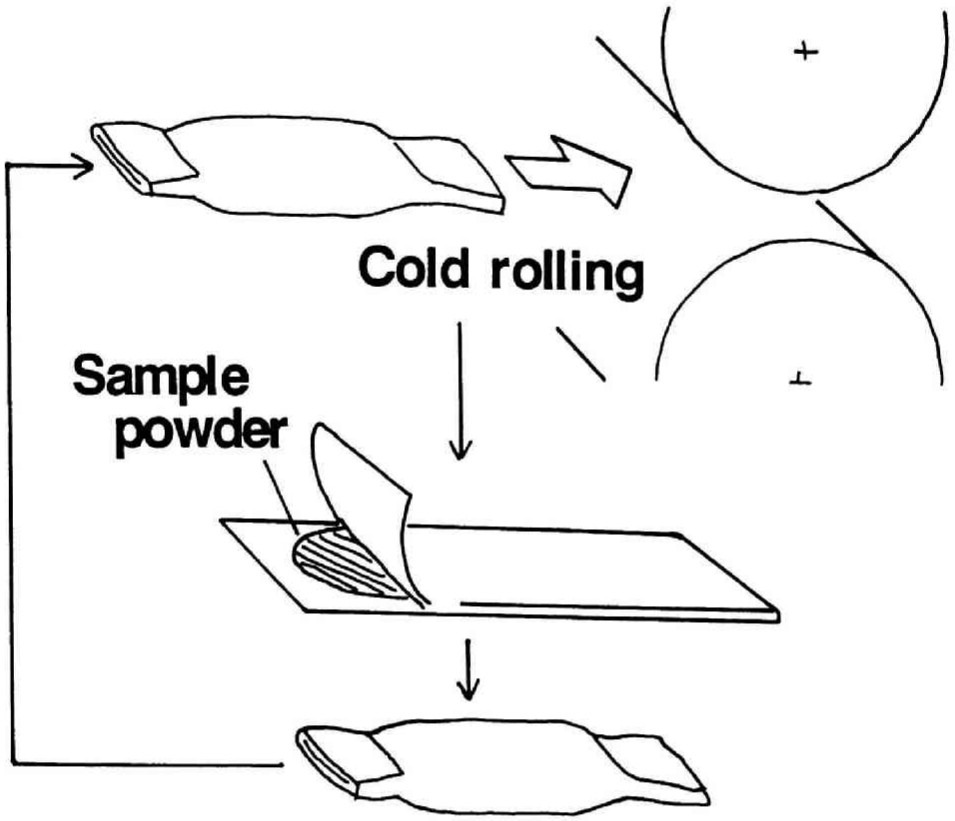

Fig.5.1 Schematically drawn process of repeated rolling method. Sample powders packed in stainless pipe were cold rolled. Rolled sample was taken by removing the stainless sheath. The sample was packed again in stainless tube and rolled. These procedure was continuously repeated.

making it easy to insert the pipe between the rolls. Then the pipe was repeatedly cold rolled to a thickness of about 0.5mm. The thickness of the sample after removal of the stainless sheath was about 0.2mm. The rolled sample was packed again into the stainless tube with the same size, and pressed and rolled by the same procedure. This process was repeated up to 30 times. Small amount of the sample after each cycle of rolling was saved for the XRD, DSC, SEM and TEM analyses.

5.2 Results and Discussion

5.2.1 Structural evolution

Figure 5.2 shows the changes of the structure of repeatedly rolled Ag-70at%Cu alloy as a function of the repetition times of rolling. The powders revealed the same lamellae structure as in the case of ball milling. Subjected to the repeated kneading, the structure became fine and homogeneous like by the ball milling process. If the repeated rolling process in this work caused folding and rolling of the sample powders, the lamellae spacing of the sample, d, after n-th cycle of repeated rolling would roughly obey the following equation of kneading,

$$d = d_0 \, (1/a)^n$$

where d_0 is the initial particle size and 1/a is the reduction ratio per one cycle of rolling. In this work, the spacing of the sample roughly obeyed the kneading equation on the early stages of rolling. However, the overall spacing showed a steady decrease because of the decrease of ductility of the metal powders from deformation induced hardening. From XRD analysis, the grain size of the samples, too, was confirmed to decrease

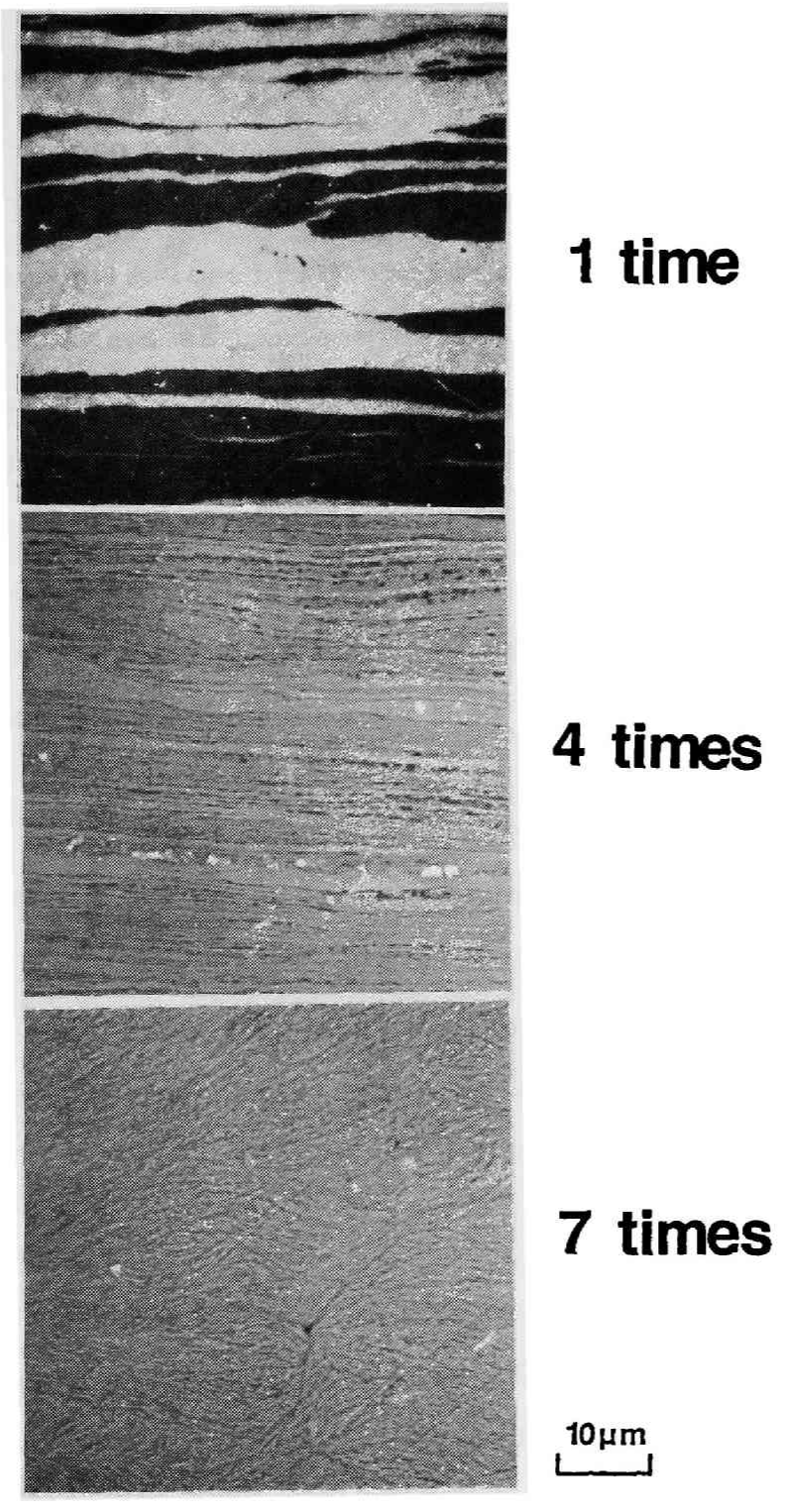

Fig.5.2 Changes of SEM images of Ag-70at%Cu alloy as a function of rolling time.

down to ten nm order evaluated from Scherrer equation.

5.2.2 Non-equilibrium phase formation

Ag-Cu system

Figure 5.3 shows the changes of the XRD patterns of the Ag-70at%Cu sample by repeated rolling and ball milling. It is evident the super-saturated solid solution was formed by repeated rolling in the same process as by MA. In Fig.5.4 the lattice parameter of super-saturated solid solution produced by repeated rolling was plotted against the composition with the data by ball milling reported in Chapter 2. The lattice parameter of the solid solution produced by repeated rolling was smaller than that by MA. This is because Ag and Cu was not completely solved and residual Cu peaks were not completely disappeared even after 30 times of rolling. TEM images of the Ag-70at%Cu alloy synthesized by ball milling and repeated rolling is shown in Fig.5.5. In both cases, the fine and homogeneous structures with average grain size of 10nm were observed while some texture was observed in repeatedly rolled sample. The grain size of 10nm fairly agreed well with the evaluated value from XRD analysis.

Fe-Cu system

Figure 5.6 shows the XRD pattern of Fe-70at%Cu as mixed, rolled 30 times and ball milled for 400h. By repeated rolling while residual Fe was observed, formation of fcc solid solution was confirmed. Figure 5.7 shows the changes of ^{57}Fe Mössbauer spectra of Fe-70at%Cu sample as a function of rolling time and

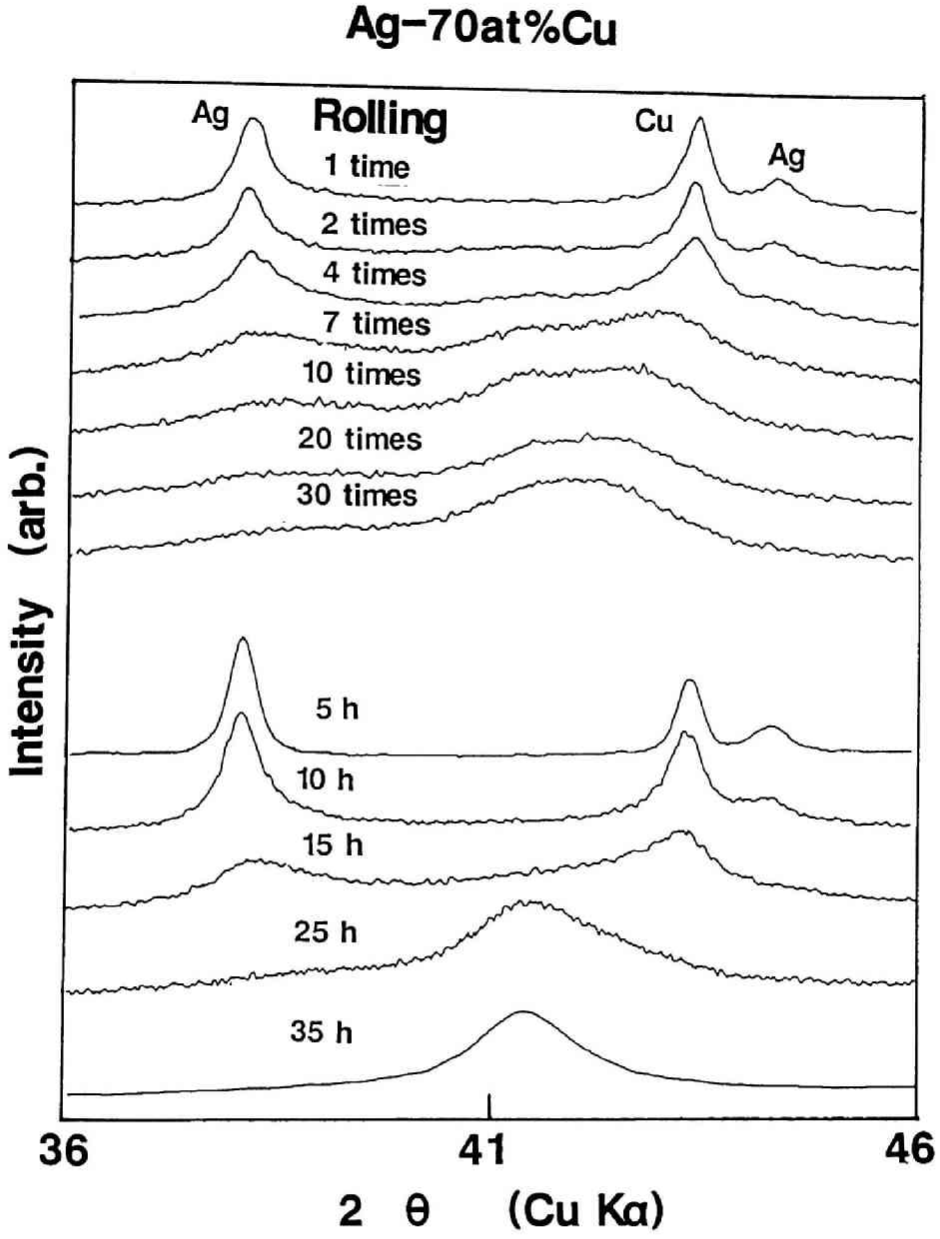

Fig.5.3 Changes of XRD patterns of Ag-70at%Cu powders as a function of rolling times and ball milling time.

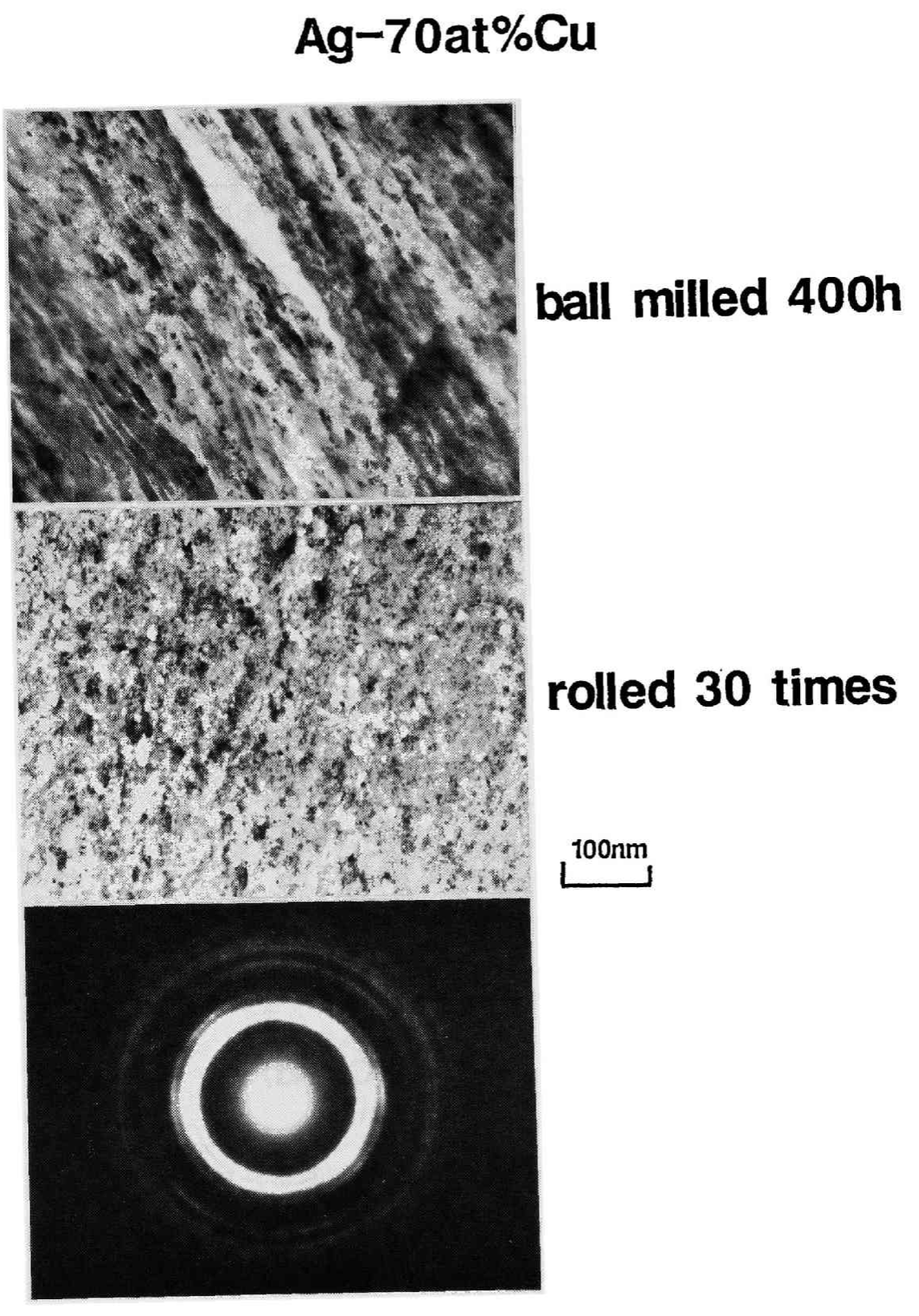

Fig.5.4 TEM images of Ag-70at%Cu powder produced by ball milling and repeated rolling.

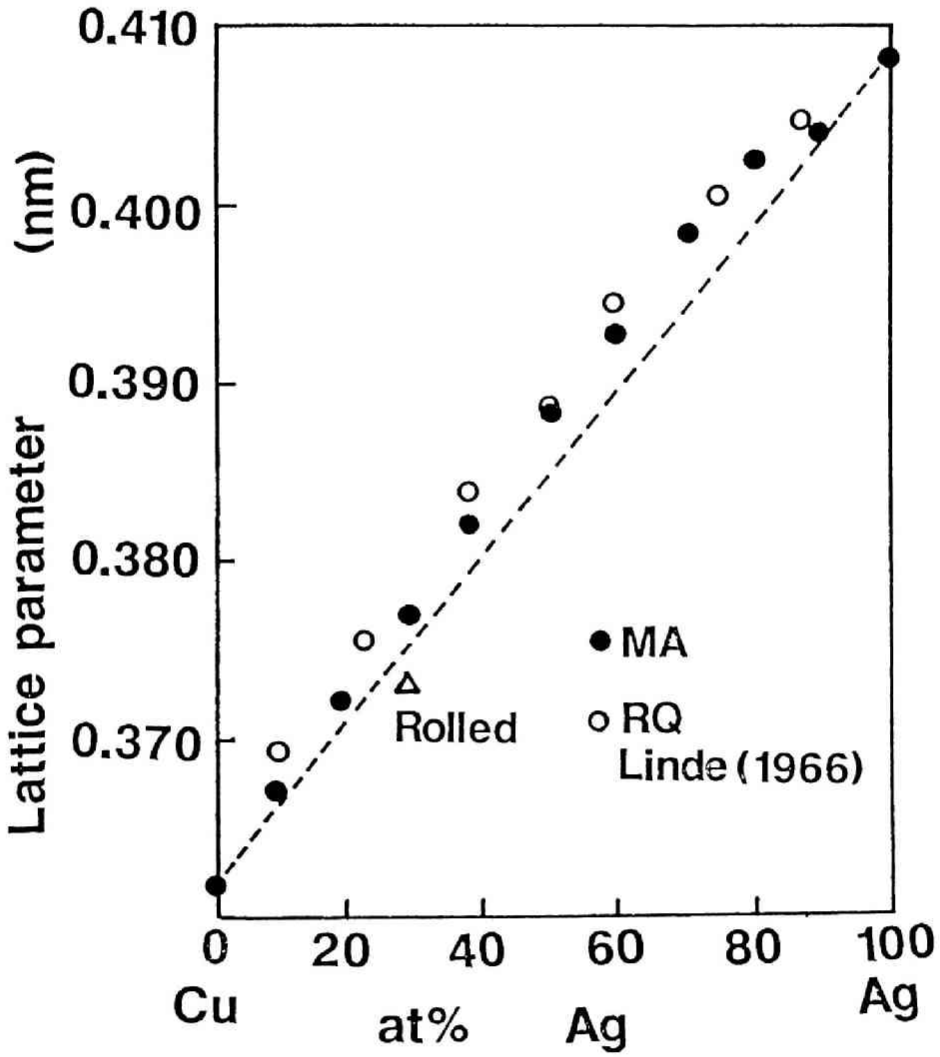

Fig.5.5 Lattice parameter of Ag-70at%Cu powders produced by repeated rolling 30 times and ball milling.

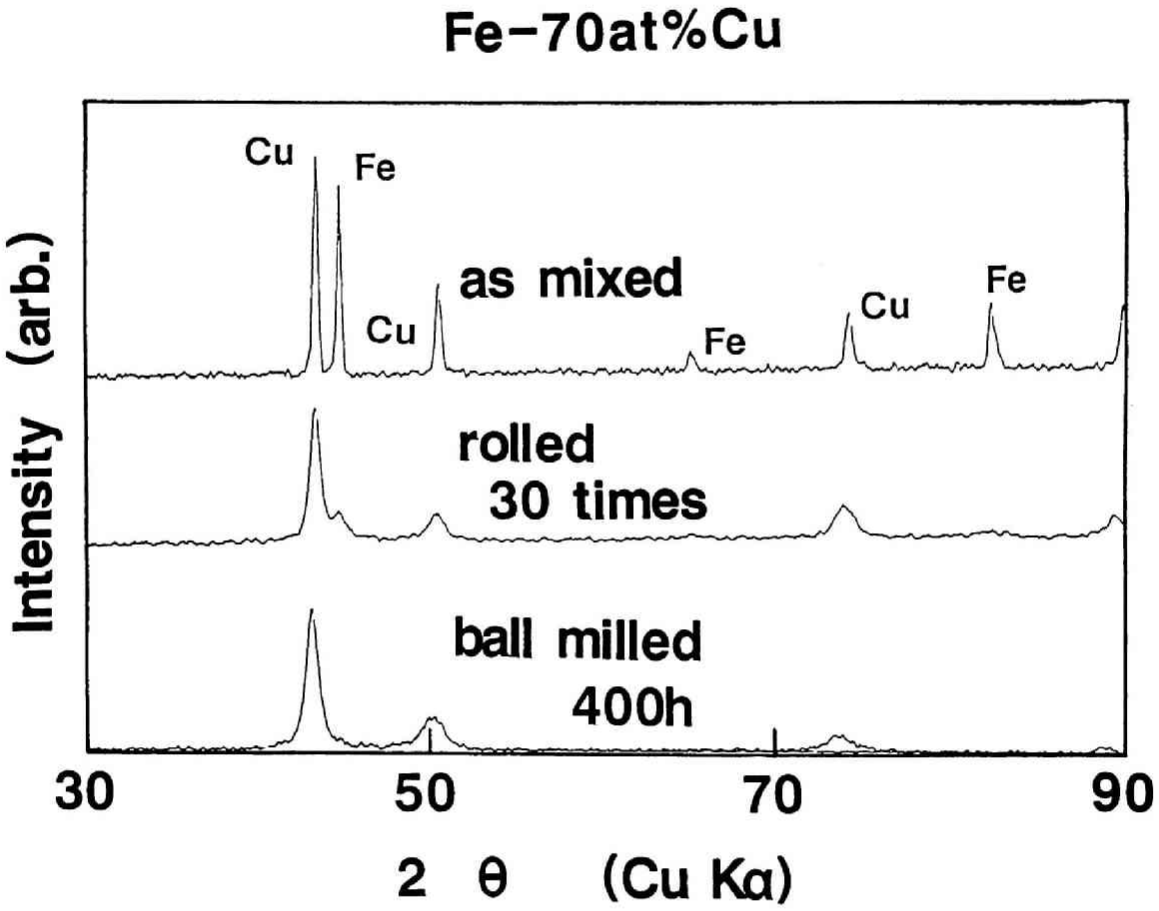

Fig.5.6 XRD patterns of as mixed, ball milled, and repeatedly rolled Fe-70at%Cu powder.

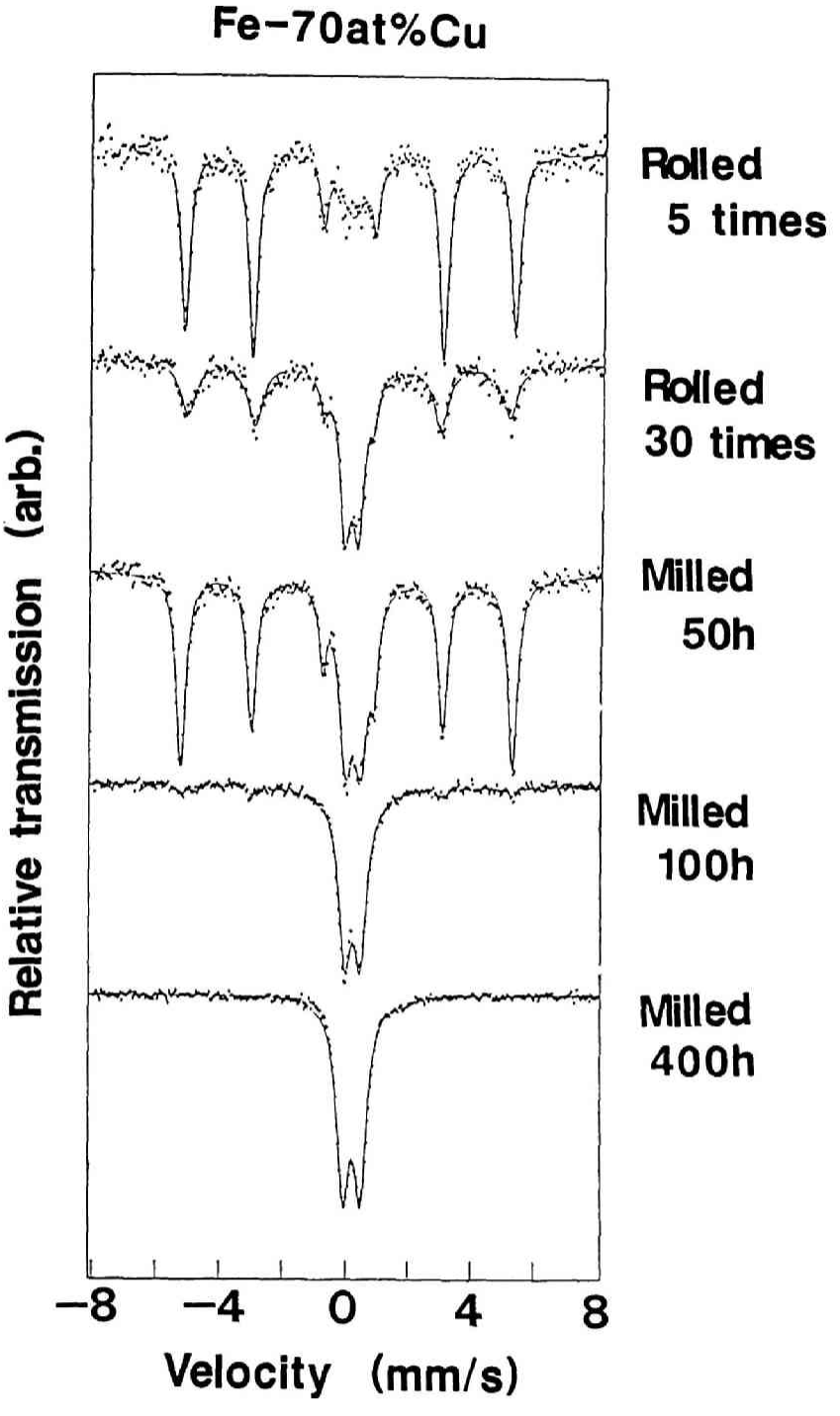

Fig.5.7 Changes of Mossbauer spectra of MA Fe-70at%Cu powder as a function of milling time and rolling time.

ball milling time. The sample repeatedly rolled 30 times exhibited the doublet spectra although residual sextet of ferromagnetic Fe was not completely disappeared. The process of solid solution formation was nearly the same. The repeated rolling 30times was judged to correspond to the ball milling for about 80h. Figure 5.8 shows the TEM images of Fe-70at%Cu sample prepared by ball milling and repeated rolling. The fine and homogeneous structure with average grain size of 10nm was observed in both methods as well as in the Ag-Cu system.

5.2.3 Conclusion

MA by the repeated rolling was performed in Ag-70at%Cu and Fe-70at%Cu alloy. In both alloy systems structural refinement in nm order due to the repeated kneading was achieved by repeated rolling as well as ball milling. The super-saturated solubilities were also achieved in both alloys although complete solubilities were not obtained by repeated rolling due to the imperfection of rolling time.

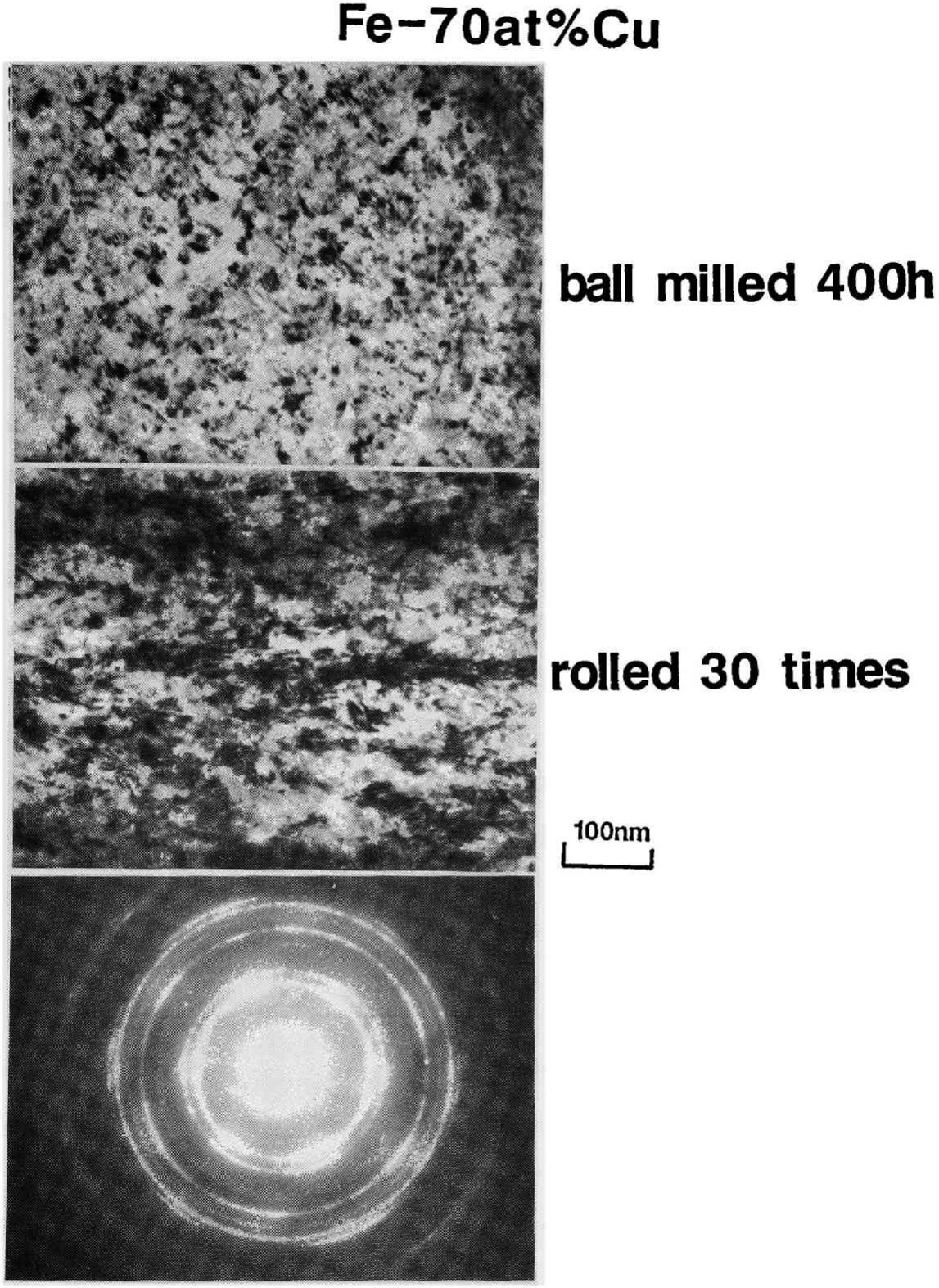

Fig.5.8 TEM images of Fe-70at%Cu alloy powder produced by ball milling and repeated rolling.

References

[1] M.Atzmon, K.M.Unruh and W.L.Johnson; J.Appl.Phys. 58 (1985) 3865.

[2] B.Huang, N.Tokizane, K.N.Ishihara, P.H.Shingu and S.Nasu; J.Non-Cryst.Solids 117/118 (1990) 688.

Chapter 6

Thermodynamical analysis

6.1 Introduction

In the previous chapters, non-equilibrium phase formation was reported in Ag-Cu and Fe-Cu alloy systems with positive heat of mixing. In such alloy systems, the mixture of pure metals before MA is in the most thermodynamically stable state and non-equilibrium phases formation means the elevation of free energy. The elevation of free energy by MA was reported in the case of amorphization by mechanical grinding (MG) of intermetallic compounds[1] and by mechanical alloying of the mixture of intermetallic compounds[2]. In the present chapter, the free energy of these systems was estimated from thermodynamical data and the non-equilibrium phases formation in these system was thermodynamically discussed by estimating the increase of interfacial energy.

6.2 Results and Discussion

Figure 6.1 shows the evaluated free energy[3][4] of Ag-Cu and Fe-Cu system respectively. The mixture of elemental powders corresponds to the broken line connected with both of free energies of pure materials. The free energy of super-saturated solid solution is higher than that of the mixture of elemental powders. Hence, the super-saturated solid solution formation by MA means the elevation of free energy. Such elevation, as mentioned in introduction, was also confirmed in MG of intermetallic compounds and has been interpreted due to the

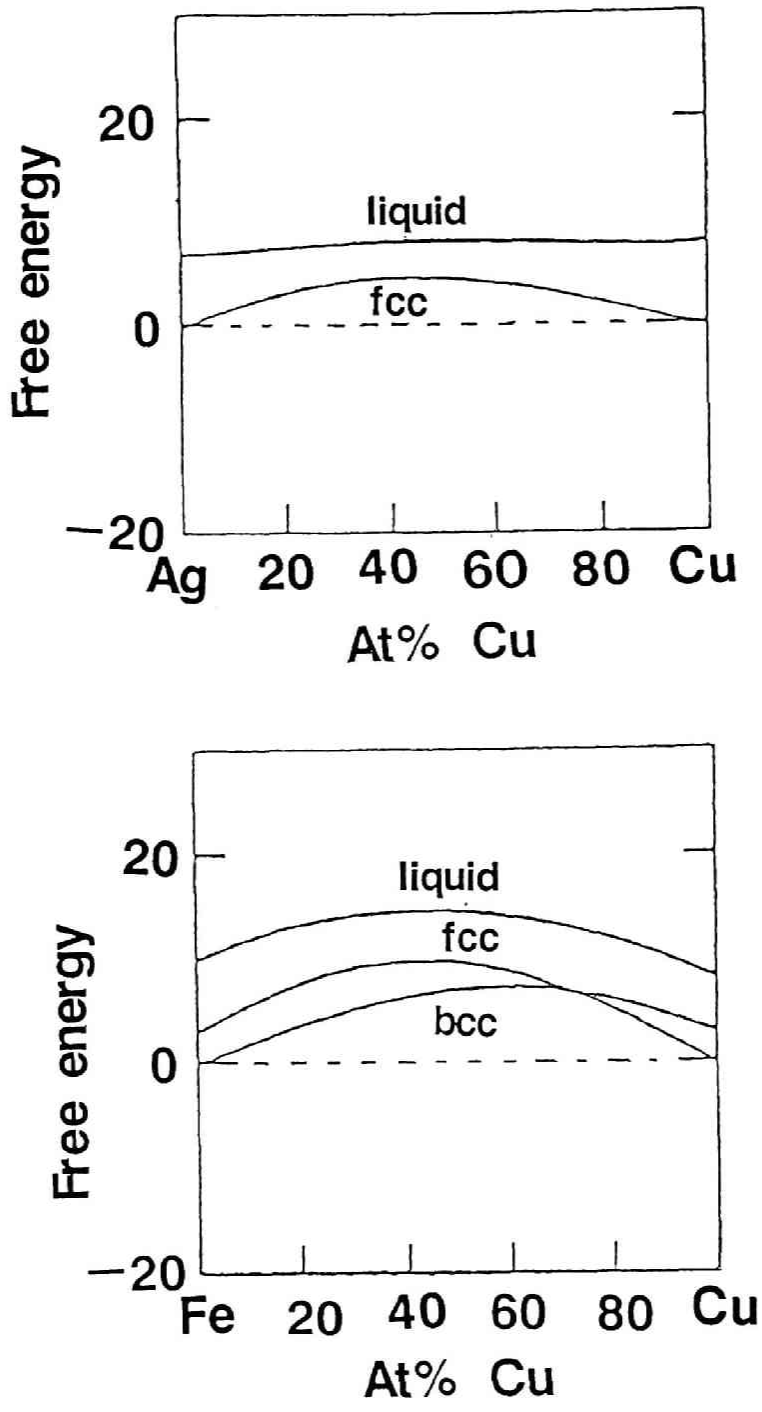

Fig.6.1 Free energy-composition diagrams for Ag-Cu and Fe-Cu systems calculated from the thermodynamical data[3][4].

stored energy as excessively introduced defects or the compositional fluctuation of intermetallic compounds. But in case of MA in the alloy systems with positive heat of mixing, either interpretations is unable to be applied. As shown in Fig.2.12 in chapter 2, the stored energy by MA was maximum about 10kJ/mol. But the stored enthalpy into pure metal by heavy deformation was known to be about only several hundreds J/mol. The fluctuation of composition induces little rise of free energy as is evident from the free energy curves in Fig.6.1.

When the fundamental process of MA, ball milling or repeated rolling, is considered again, it is the kneading process to produce the homogeneous and fine structure. In such structure, the large interfacial energies might be stored. The increase of interfacial energy is considered due to the increase of surface area of both A-A, B-B and A-B interface.

In the alloy system A-B, the energy stored by interfacial energy, H, can be estimated as additivities of multiplied interfacial energy and the corresponding interfacial area about each interface A-A, B-B and A-B.

$$\Delta H = \gamma_{AA} S_{AA} + \gamma_{BB} S_{BB} + \gamma_{AB} S_{AB} \quad \text{---------- (1)}$$

Now γ and S mean the interfacial energy per unit interfacial area and area of the corresponding interface, respectively. Miedema successfully estimated this solid-solid interfacial energy[5][6] with two additive contributions, lattice mismatch and chemical terms.

$$\gamma = \gamma^{\text{mismatch}} + \gamma^{\text{chem}} \quad \text{---------- (2)}$$

One contribution, γ^{mismatch}, is related to the mismatch on the

interfaces between the two metals. For pure metals this term is comparable with large-angle grain boundary. This mismatch term can be written as a function of each surface energy of constituent pure metals, γ^0.

$$\gamma_{AB}^{mismatch} = 0.15 \left(\gamma_A^0 + \gamma_B^0 \right) \quad (3)$$

Another contribution, γ^{chem}, represents the interaction between two metals. This term can be written as a function of molar interfacial enthalpy, $\Delta H^{interface}$ and molar volume, V.

$$\gamma^{chem} = \Delta H_{A \text{ in } B}^{interface} / c_0 V_A^{2/3} \quad (4)$$

c_0 is a constant determined from the morphology of the grain and the average value, 4.5×10^8, was used in this analysis. Surface area per unit volume is inversely proportional to the grain size. As surface area of a molar atomic cell is written as $c_0 \times V^{2/3}$, the surface area of the atomic cluster, S, can be described by using the ratio of atomic distance d to its grain size D.

$$S = c_0 V^{2/3} d / D \quad (5)$$

Each interfacial area can be determined from this surface area, the atomic concentration, c, and constituent element and the surface concentration, c^S of constituent element.

$$S_{AA} = 1/2 \times c_A c_0 V_A^{2/3} d/D \times C_A^S \quad (6)$$

$$S_{BB} = 1/2 \times c_B c_0 V_B^{2/3} d/D \times C_B^S \quad (7)$$

$$S_{AB} = c_A c_0 V_A^{2/3} d/D \times c_B^S \quad (8)$$

Now c^S can be described as follows.

$$c_A^S = c_A V_A^{2/3} / \left(c_A V_A^{2/3} + c_B V_B^{2/3} \right) \quad (9)$$

$$c_B^S = c_B V_B^{2/3} / \left(c_A V_A^{2/3} + c_B V_B^{2/3} \right) \quad (10)$$

From the equations estimated above, enthalpy stored as

interfacial energy can be described as follows.

$$\Delta H = 0.15 \times c_0 [c_A V_A^{2/3} c_A^S \gamma_A^0 + c_B V_B^{2/3} c_B^S \gamma_B^0 + c_A V_A^{2/3} c_B^S (\gamma_A^0 + \gamma_B^0)] d/D + c_A c_B^S \Delta H_{A \text{ in } B}^{\text{interface}} d/D \quad \text{----- (11)}$$

First term corresponding to the interfacial energy due to lattice mismatch can be simply rewritten as eqn.(14) by taking into the eqns. (12) and (13).

$$\Delta H^{vap} = 4.1 \times 10^{-8} \gamma^0 V^{2/3} \quad \text{---------- (13)}$$

$$c_A^S + c_B^S = 1 \quad \text{---------- (14)}$$

$$\Delta H^{mismatch} = 1/6 (c_A \Delta H_A^{vap} + c_B \Delta H_B^{vap}) d/D \quad \text{---------- (15)}$$

ΔH^{vap} means the heat of vaporization of each element.

Another term corresponding to the chemical interaction is just as same as heat of mixing, ΔH_{mix}.

$$\Delta H^{chem} = \Delta H_{mix} d/D \quad \text{---------- (15)}$$

So the stored energy can be described as follows.

$$\Delta H = d/D [1/6 (c_A \Delta H_A^{vap} + c_B \Delta H_B^{vap}) + \Delta H_{mix}] \quad \text{------- (16)}$$

Now, this stored enthaply can be compared with enthalpy of liquid. Enthaply of liquid can be written by using latent heat, L, and heat of mixing, H_{mix}.

$$\Delta H = c_A L_A + c_B L_B + H_{mix} \quad \text{---------- (17)}$$

From these eqn.(16) and (17), it is recognized that H^{chem} increases with decreasing the grain size and then reaches heat of mixing of liquid when mixing was accomplished to an atomic level (d/D=1). On the contrary, latent heat is generally about a 18th of heat of vaporization. So $H^{mismatch}$ also increases with decreasing the grain size but it becomes larger than latent heat when gain size becomes smaller than about one nanometer (d/D is larger than 1/3). In Fig.6.2, stored enthalpy was estimated for Ag-Cu system as a function of the

grain size by using reported thermodynamical data[4].

ΔH_{Ag}^{vap} =217kJ/mol, ΔH_{Cu}^{vap}= 244kJ/mol,

$V_{Ag}^{2/3}$= $4.72\times10^{-4}m^2$, $V_{Cu}^{2/3}$ = $3.7\times10^{-4}m^2$

ΔH_m= $[15.7-2.4(c_{Cu}-c_{Ag})]c_{Cu}c_{Ag}$.

As shown in Fig.6.2, the interfacial energy is inversely proportional to the grain size and almost reaches enthapy of liquid when grain size becomes 1nm. In case the mixing in an atomic level is accomplished, the stored interfacial energy becomes about 45kJ/mol. In Fig.6.3, the stored interfacial energy was estimated by using the grain size evaluated from XRD patterns in chapter 2 and was compared with total heat output measured by DSC. The calculated value was smaller than both of the measured one and the relative enthalpy of fcc phase. However, this interfacial energy is stored locally around grain boundary.There are many reports that solid state reaction during MA occurs around the grain boundary [7]. Around the grain boundary, many defects are locally stored by collision between powders and balls, which rises the diffusivity of atom, and interfacial energy is also locally stored, which gives the driving force for non-equilibrium phase formation. Up to now, there was no report that refining in sub-nanometer order level was achieved by MA. So it may well be mentioned that MA is the process to produce undercooled liquid (amorphous) state by refining the elemental powders. In Ag-Cu system, heat of mixing was much smaller than a 6th heat of vaporization, so the mismatch interfacial term was much larger than chemical interfacial term and chemical term was negligible small. But as

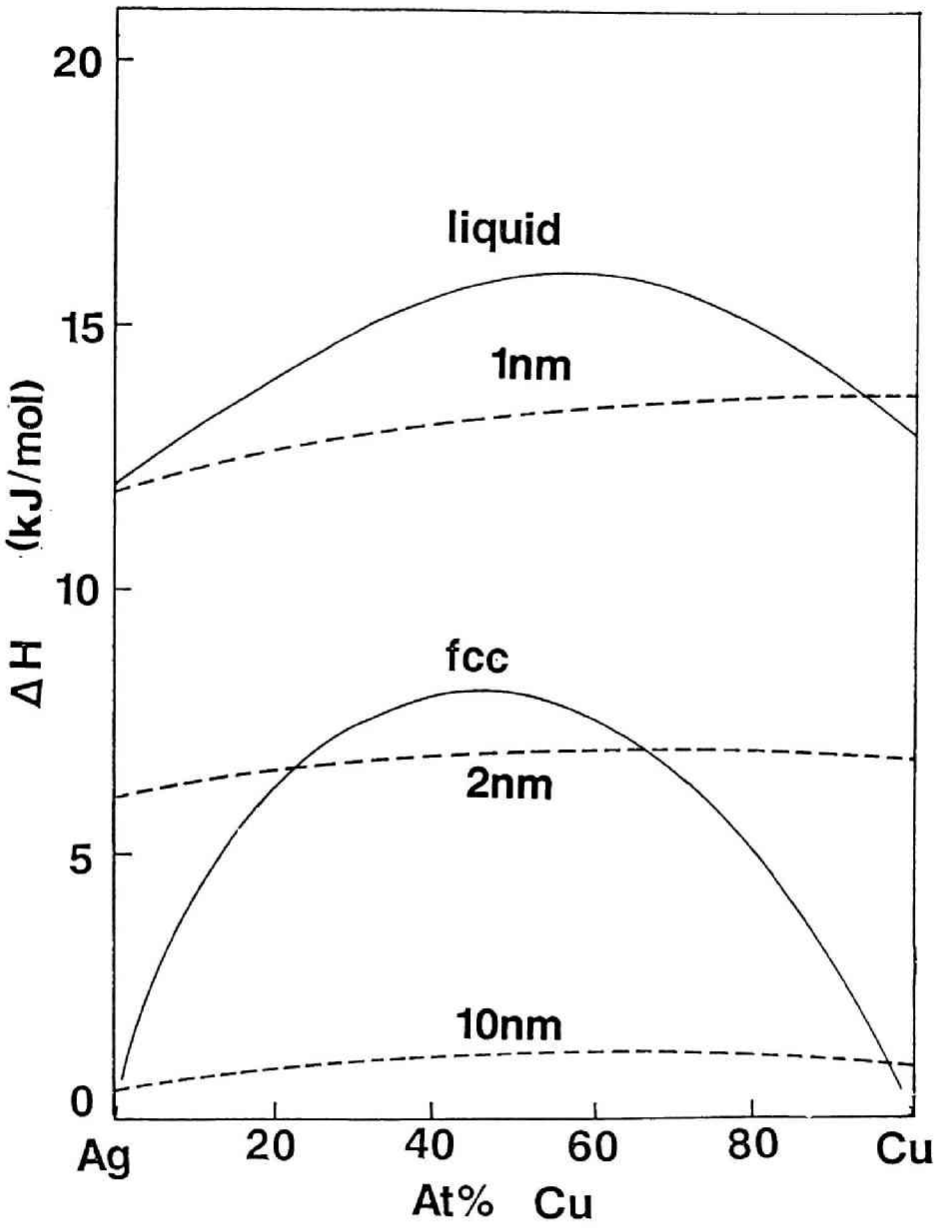

Fig.6.2 Changes of stored interfacial energy estimated by using Miedema model as a function of the dispersed grain size for Ag-Cu system.

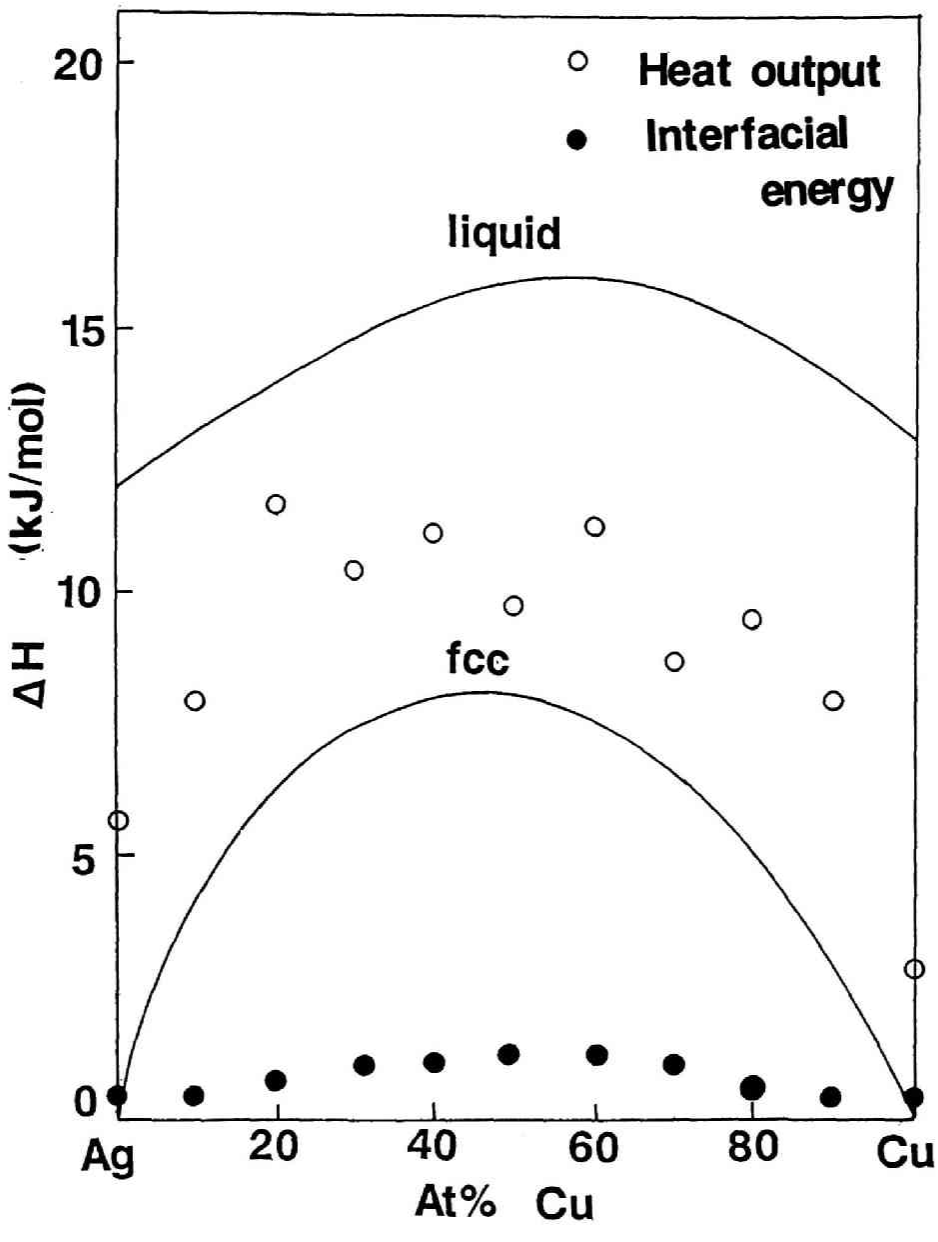

Fig.6.3 Stored energy measured by DSC (open circle) and evaluated interfacial energy (solid circle) from the grain size estimated in Fig.2.9 for the Ag-Cu system.

in the alloy system with relatively large positive heat of mixing, the effect of chemical term is neglectable. Compared with enthalpy of liquid, as mentioned above, mismatch term can be about three times larger than latent heat, but maximum value of chemical term is heat of mixing. So interfacial energy is likely to be smaller than that of non-equilibrium state especially in the central composition range because chemical term is smaller than heat of mixing. For example, in Ag-Fe system with positive heat of mixing, 100kJ/mol, little solubilities can be obtained in the central composition range[8], while heat of vaporization is almost the same as that in Ag-Cu system. On the contrary, in Cu-Ta system with larger heat of vaporization (ΔH_{Ta}^{vap} = 560kJ/mol) than that in Ag-Cu system, amorphous alloy was formed by MA [9], while heat of mixing is almost the same as that in Ag-Cu system.

How fine dispersion of the elemental powders can be accomplished by MA is also significant. In the ternary Fe-Ag-Cu system, 5nm order refining was accomplished in the equiatomic composition range. In such composition range, the stored interfacial energy might larger than on the any other compositions and non-equilibrium on the considerably near amorphous state was formed.

Recently, how large energy can be stored by MA has come to be a problem. However, from the point of above mentioned concept, the absolute value does not exist in common for every alloy systems. The stored energy was related to heat of vaporization of each element, heat of mixing and the interfacial area. so the maximum value of stored energy differs

from each alloy system. The mechanically alloyed alloy system and how fine the dispersion can be achieved decide the stored energy.

6.3 Conclusion

Formation of non-equilibrium phase in Ag-Cu and Fe-Cu system by MA was thermodynamically discussed. By calculating the free energy, the elevated free energy was maximum about 10kJ/mol which was confirmed to be due to the stored energy as interfacial energy. It was confirmed that MA is the process to produce nanocrystalline structure, which increases the free energy of the system up to amorphous state by the increase of interfacial energy.

References

[1] R.B.Schwarz and C.C.Koch; Appl.Phys.Lett. 49 (1986) 146.

[2] P.Y.Lee and C.C.Koch; J.Mater.Sci. 23 (1988) 2837.

[3] J.L.Murray; Met.Trans. A15 (1984) 262.

[4] L.Kaufman; CALPHAD 2 2 (1978) 117.

[5] A.R.Miedema and F.J.A. de Broeder; Z.Metallkde. 70 H1 (1979) 14.

[6] F.R.de Boer, R.Boom, W.C.M.Mattens, A.R.Miedema and A.K.Niessen; 'Cohesion in Metals' vol.1, ed. by F.R.de Boer and D.G.Pettifor, Elsevier Sience Publisher, North-Holland, (1989)

[7] L.Schultz; Phil.Mag.B 61 4 (1990) 453.

[8] J.Kuyama, H.Inui, S.Imaoka, S.Nasu, K.N.Ishihara and P.H.Shingu; Jpn.J.Appl.Phys.2 6 (1991) L854.

[9] T.Fukunaga, K,Nakamura, K.Suzuki and U.Mizutani; J.Non-Cryst.Solids 117/118 (1990) 700.

Chapter 7

Summary

Mechanical alloying, which is a greatly different processing technique from rapid quenching, has been proved to be just as effective as rapid quenching. In this work, formation of non-equilibrium phases by MA was examined in the alloy system with positive heat of mixing. The properties of the produced non-equilibrium phases were examined and the possibility of non-equilibrium phase formation was thermodynamically discussed. The main results confirmed are summarized as follows.

1. In the Ag-Cu system, super-saturated solid solution was prepared by MA in entire composition range. The prepared solid solution had nanocrystalline structure with the grain size of 10nm and the structure was confirmed to be stable until decomposition took place. At the initial stage of decomposition, the grain size of precipitated phases remained at 10nm size.
2. In the Fe-Cu system, up to 30at%Cu bcc and above 40at%Cu fcc super-saturated solid solution was obtained by MA. The composition range where complete solid solution was formed by MA was wider than that by other rapid quenching techniques. Produced solid solution exhibited similar properties as those produced by rapid quenching.
3. In the ternary Fe-Ag-Cu system, super-saturated solid solution was obtained in the wide composition range except the Cu poor composition range. Formation of amorphous was not confirmed by TEM observation.

Changes in the properties such as the increase of magnetization due to Ag addition were recognized.

4. Formation of super-saturated solid solution in Ag-Cu and Fe-Cu was confirmed by repeated rolling method as well as ball milling. MA was confirmed to be a process which produces very fine structure through repeated kneading, making it possible to induce the fast diffusion of atoms.
5. From the results on super-saturated solid solution formation, the free energy was confirmed to increase by MA. The interfacial energy was stored in the system by the refining of the structure by MA, which enabled the non-equilibrium phase formation in the alloy system with positive heat of mixing.